Development of early predictors of cerebral ischaemia after severe aneurysmal subarachnoid haemorrhage

Thesis submitted for Master of Science by Research

Dr Payashi Sakina Garry MA (Cantab) MB BChir FRCA

Nuffield Department of Clinical Neurosciences

University of Oxford

St Edmund Hall College Michaelmas Term 2015

For Joseph and Hannah

Studying the role of nitric oxide signalling in the development of cerebral ischaemia after severe aneurysmal subarachnoid haemorrhage

Dr Payashi Sakina Garry MA (Cantab) MB BChir FRCA

St Edmund Hall, University of Oxford

Submitted for degree of MSc by research, Michaelmas Term 2015

Aneurysmal subarachnoid haemorrhage (SAH) is a severe disease often leading to profound disability and death. There has been increasing interest in nitric oxide (NO) signalling after brain injury, as it appears to influence many of the cellular metabolic pathways that eventually result in apoptosis and neuronal dysfunction.

Many animal studies have shown exogenous cerebral NO donation appears to confer neuroprotective effects. It has shown to particularly affect many of the pathophysiological processes that occur after SAH.

The work presented here describes two studies. The first study correlates changes in quantitative electroencephalography (qEEG) with the infusion of a cerebral NO donor, sodium nitrite after severe (World Federation of Neurosurgeon's grades 3, 4 and 5) SAH. There is a need for better cerebral function assessment tools in this patient cohort as the usefulness of neurological examination is limited.

The second study investigates magnetic resonance imaging (MRI) methods of evaluating acute tissue blood flow changes that occur after severe SAH, namely vessel encoded pseudo-continuous arterial spin labelling (VEPCASL).

The results from the first study demonstrate that qEEG changes in response to an NO donor correlate with the subsequent development of delayed cerebral ischaemia (DCI) and poor clinical outcomes. The results from the second study show that VEPCASL can be used to obtain measures of regional cerebral blood flow changes that occur over time in the acute stages of severe SAH.

This thesis demonstrates that bedside EEG monitoring is an extremely useful tool to give additional information regarding neuronal health after severe SAH. We have offered a new insight into the mechanisms behind therapeutic repletion of NO, aiding its development as a potential new therapy. We have also shown that VEPCASL MRI is a useful tool in assessing cerebral perfusion in the acute stages of injury.

Acknowledgements

I would like to thank my supervisor, Professor Kyle Pattinson for his ongoing unwavering support, belief and encouragement at every stage of this work. His insights and suggestions have been invaluable, and without his support none of this would have been possible. I would also like to thank Dr Jon Westbrook for his clinical support during this project, as recruitment of patients from Neuro-Intensive Care would have been impossible without his input. In a similar vein, I would like to thank all the Neuro-Intensive Care Unit Intensivists for their help and encouragement during data collection – Dr Hilary Madder, Dr Mhairi Speirs, Dr Christopher Kearns, Dr Simon Raby, Dr Orlando Warner and Dr David Shlugman.

I would like to thank Dr Matthew Rowland for his help at all stages of this project, from ethical applications to transferring intensive care patients to and from the MRI scanner (although not for his ability to tread on and disconnect infusion lines). Particular thanks must also be given to Dr Martyn Ezra who has been invaluable for intellectual insights and computing assistance!

I am extremely grateful to Dr Anja Hayen for all her help during data collection on NICU and for keeping me calm and sane when it all appeared to be going wrong. I would also like to thank her for her assistance in helping me get to grips with the intricacies of Spike. I am also extremely grateful to Dr Mari Herigstad for her ongoing advice, encouragement and help with physiological data processing. I would also like to thank the other members of our research group – Dr Olivia Faull, Dr Andrea Dennis and Eleanor Evans for their encouragement and support.

I would like to give special thanks to Dr Catherine Warnaby and Professor James Sleigh for their helpful suggestions with regards to the analysis of the EEG data. I would also like to thank Dr Caroline Hartley for her help with EEGlab.

I would like to thank Dr Daniel Lunn in the University Statistics department for his help with R and linear mixed effects modelling. I would also like to thank Dr Thomas Okell for his invaluable assistance with the analysis of the arterial spin labelling data, and Dr Mark Jenkinson for his help with image registration. I would like to give

thanks to Dr Rufus Corkill for his rapid clinical interpretation of the acute MRI scans, and to the AVIC team for their unwavering support – Juliet Semple, Melanie Jones, Peter Manley and Carol Davey.

This work would not have been possible without the financial support of the NIHR Oxford Biomedical Research centre and the Oxford University Clinical Academic Graduate School.

I would like to thank my parents Maa and Gaga, my mother in law Sonia and my step-father in law Michael. I would also like to thank the rest of my extended family for their ongoing love and support.

Finally I would like to thank my children, Joseph and Hannah, for being my inspiration and my best achievement. Last but not least I would like to thank my husband David, my best friend, my main motivator and my greatest support.

Do. Or do not. There is no try.

Yoda

Table of contents

Declaration 12

Manuscripts arising from this thesis 13

List of figures 14

List of tables 15

Abbreviations 16

1 Introduction and overview of thesis 18

1.1 Introduction 19

1.2 Thesis overview 22

2 Nitric oxide signalling in health and disease 24

Abstract 25

2.1 Nitric oxide 26

2.2 Nitric oxide synthase 27

2.2.1 Endothelial nitric oxide synthase 27

2.2.2 Neuronal nitric oxide synthase 28

2.2.3 Inducible nitric oxide synthase 28

2.3 Role of nitric oxide in cerebral blood flow regulation 28

2.3.1 Autoregulation 29

2.3.2 Neurovascular coupling 30

2.4 Nitric oxide signalling during physiological stresses 32

2.4.1 Hypoxia 32

2.4.2 Hypercapnia 33

2.5 The role of nitric oxide in the cerebral response to injury 34

2.5.1 Nitric oxide depletion 35

2.5.2 Endothelial nitric oxide synthase dysfunction 37

2.5.3 Ischaemia/reperfusion injury 38

2.5.4 Inducible nitric oxide synthase 39

2.6 Manipulation of nitric oxide signalling using animal models 42

2.6.1 Inhaled nitric oxide 42

2.6.2 Nitric oxide donors 42

2.7 Conclusion 44

3 Experimental Methods 45

Abstract 46

3.1 Introduction 47

3.2 Current methods 47

3.2.1 CT 47

3.2.2 Trancranial Doppler 48

3.2.3 NIRS and PET 48

3.3 Rationale behind investigation choice 49

3.4 EEG 50

3.4.1 Introduction 50

3.4.2 Principles of spectral analysis 52

3.4.3 EEG after SAH 53

3.4.4 Limitations 54

3.5 Magnetic Resonance Imaging 55

3.5.1 Introduction 55

3.5.2 Arterial Spin Labelling 56

3.5.3 Limitations of MRI 59

3.6 Neurocognitive Testing 60

3.7 Conclusion 61

3.8 Aims of the work presented in this thesis 62

4 Electroencephalography may aid prediction of delayed ischaemia after severe SAH when used with a cerebral NO donor 63

Abstract 64

4.1 Introduction 65

4.1.1 Mechanisms behind action of NO donors 66

4.1.2 Using EEG to measure the neuronal response 67

4.1.3 Aims of the study 67

4.2 Materials and Methods 68

4.2.1 Subjects 68

4.2.2 Study design 70

4.2.3 Quantitative electroencephalography analysis 71

4.2.4 Physiological data analysis 73
4.3 Results 74
4.3.1 Demographics, treatment and outcome 74
4.3.2 Quantitative EEG results 77
4.3.2.1 Multilevel model 77
4.3.2.2 Bayesian model 82
4.3.3 Physiological data 87
4.3.4 Neurocognitive data 90
4.4 Discussion 91
4.4.1 Main findings 91
4.4.2 Explanation of results 92
4.4.3 Limitations of study 94
4.5 Conclusion 96

5 Using arterial spin labelling to estimate cerebral blood flow after severe subarachnoid haemorrhage 97
Abstract 98
5.1 Introduction 99
5.2 Materials and Methods 102
5.2.1 Subjects 102
5.2.2 Study design 103
5.3 MRI scanning parameters 105
5.3.1 TOF 105
5.3.2 VEPCASL 105
5.3.3 T1 structural 106
5.3.4 Fieldmaps 106
5.4 Analysis 106
5.4.1 ASL analysis 106
5.5 Results 110
5.5.1 Clinical results 110
5.5.2 ASL results 112
5.6 Discussion 120
5.6.1 Summary of findings 120
5.6.2 Background to findings 120

5.6.3 Using ASL to quantify GM CBF 121
5.6.4 Discussion of main findings 122
5.6.5 Limitations of study 123
5.7 Conclusion 125

6 General discussion and conclusions 126
Abstract 127
6.1 Main findings 128
6.1.1 EEG findings 129
6.1.2 MRI findings 130
6.2 Methodological considerations 131
6.2.1 Consent 131
6.2.2 Data acquisition challenges 132
6.2.2.1 EEG 132
6.2.2.2 MRI 133
6.2.3 Data analysis challenges 134
6.3 Potential for the development of future therapies 135
6.4 Conclusions 137

Bibliography 138

Appendix A – The role of the nitric oxide pathway in brain injury and its treatment – from bench to bedside

Declaration

I certify that this thesis entitled “Studying the role of nitric oxide signalling in the development of cerebral ischaemia after severe subarachnoid haemorrhage” was performed while I was a full-time postgraduate student at St Edmund Hall, the University of Oxford. I declare that this thesis is of my own composition, and the research contained within is my own original work under the supervision of Dr Kyle Pattinson. No portion of this work has been submitted in support of an application for any other degree.

Manuscripts arising from this thesis

Peer reviewed publications

Garry PS, Ezra M, Rowland MJ, Westbrook J, Pattinson KTS. (2015). The role of the nitric oxide pathway in brain injury and its treatment – from bench to bedside. *Experimental Neurology* 263, 235-243. Pubmed ID: 25447937

Manuscripts in preparation

Garry PS, Rowland MJ, Ezra M, Herigstad M, Hayen A, Sleigh JW, Westbrook J, Warnaby CE, Pattinson KTS. EEG response to sodium nitrite may predict delayed cerebral ischaemia after severe subarachnoid haemorrhage.

List of figures

Figure 2.1	Right shift of autoregulation curve in eNOS knockout mice	30
Figure 2.2	Effects of NO signalling on cellular signalling pathways	32
Figure 2.3	Cerebral neuroprotective and neurotoxic mechanisms of NO	40
Figure 2.4	Mechanisms underlying hypoxic nitrite reduction	43
Figure 3.1	Relationship of CBF to EEG signal	52
Figure 3.2	Principles of ASL	57
Figure 3.3	Vascular territory maps demonstrating VEPCASL	59
Figure 4.1	Percentage change in ADR and mean ADR values	81
Figure 4.2	Diagnostic plots of linear mixed model	82
Figure 4.3	Topical representation of power changes	85
Figure 4.4	Spectrograms from two patients	86
Figure 4.5	Percentage change of baseline ADR over time	87
Figure 5.1	Steps taken during ASL analysis	109
Figure 5.2	Structural scans of patients demonstrating abnormalities	113
Figure 5.3	Whole brain GM CBF at scan 1	114
Figure 5.4	Total perfusion maps showing delayed blood arrival	115
Figure 5.5	Relative vessel contributions in acute scans	117
Figure 5.6	Motion artefact causing incorrect allocation of vessels	118
Figure 5.7	VEPCASL perfusion maps	119

List of tables

Table 1.1	WFNS scoring scale	20
Table 4.1	Patient characteristics	75
Table 4.2	Sedation and vasopressor levels for each patient	76
Table 4.3	Output data from multilevel model	78
Table 4.4	Between group contrasts	79
Table 4.3	Mean physiological values pre vs. during sodium nitrite infusion	89
Table 5.1	Patient characteristics and demographics	102
Table 5.2	Day of scan post aneurysm rupture	110
Table 5.3	Mean arterial pressure, $PETCO_2$ and vasopressor levels	111

Abbreviations

ABP	Arterial blood pressure
ADR	Alpha/delta ratio
ASL	Arterial spin labelling
BOLD	Blood oxygen level dependent
CBF	Cerebral blood flow
CNS	Central nervous system
CPP	Cerebral perfusion pressure
CT	Computerised tomography
DCI	Delayed cerebral ischaemia
EBI	Early brain injury
ECG	Electrocardiogram
EDRF	Endothelium derived relaxing factor
EEG	Electroencephalography
eNOS	Endothelial nitric oxide synthase
EVD	External ventricular drain
FLIRT	FMRIB's linear image registration tool
FMRIB	Oxford centre for functional MRI of the brain
FNIRT	FMRIB's non-linear image registration tool
FSL	FMRIB's software library
GCS	Glasgow coma score
GM CBF	Grey matter cerebral blood flow
iNOS	inducible nitric oxide synthase
ICP	Intracranial pressure
MCA	Middle cerebral artery

MRI	Magnetic resonance imaging
NICU	Neuro-intensive care
NIRS	Near infra-red spectroscopy
NO	Nitric oxide
nNOS	Neuronal nitric oxide synthase
NOS	Nitric oxide synthase
PET	Positron emission tomography
$PETCO_2$	End tidal carbon dioxide
qEEG	Quantitative electroencephalography
RSN	Resting state network
SAH	Subarachnoid haemorrhage
SNR	Signal to noise ratio
SpO_2	Oxygen saturations
TCD	Transcranial Doppler
VEPCASL	Vessel encoded pseudo-continuous arterial spin labelling
WFNS	World Federation of Neurosurgeons

Chapter 1

Introduction and overview of thesis

Chapter 1

1.1 Introduction

Aneurysmal SAH is a rare but serious condition, accounting for only 5% of strokes but disproportionately affecting a younger population, with half of patients being under 55 years (1). It is often fatal, which means that the loss of productive life years approaches that of ischaemic stroke or intracerebral haemorrhage (2). 85% of cases are due to a ruptured cerebral aneurysm, usually located in the circle of Willis. Intracranial aneurysms develop over the course of life, and the majority will not rupture.

There are several modifiable risk factors for SAH including hypertension, smoking and excessive alcohol intake. Genetic predisposition and syndromes such as polycystic kidney disease also increase the likelihood of SAH. Sudden headache is the most common symptom. Systemic effects include hypertension, hypoxia and ischaemic electrocardiographic (ECG) changes that can mimic acute infarction.

There are several scales used to assess severity of SAH. The Fisher scale is a method of grouping computerised tomography (CT) scans into four groups according to the amount of blood (group 1 = no blood, group 4 = intracerebral or intraventricular blood). This scale is useful as it appears to be predictive of subsequent arterial vasospasm (3). The Hunt and Hess scale is based on clinical symptoms and signs and is used as a predictor of survival (4).

The World Federation of Neurosurgeons (WFNS) grading system uses the Glasgow Coma Scale (GCS) and presence of focal neurological deficits to grade the severity,

with 1 being the least severe and 5 being the most severe. It is the most widely used grading system in the UK, therefore is used for the work described in this thesis. For the purpose of the studies described WFNS grades 1-2 are classed as 'good' grade and WFNS 3, 4 and 5 are classed as 'poor' grade. Table 1.1 illustrates the WFNS scoring system.

Table 1.1: WFNS scoring scale

Grade	GCS	Clinical Status
1	15	No motor deficit
2	13-14	No motor deficit
3	13-14	Motor deficit
4	7-12	Motor deficit present or absent
5	3-6	Motor deficit present or absent

Endovascular occlusion of the aneurysm has become the treatment of choice to prevent re-bleeding (5). Complications include early brain injury (EBI), which describes the immediate injury after SAH and occurs in the first 72 hours, and delayed cerebral ischaemia (DCI), which can occur in about 30% of patients unpredictably 3-14 days post primary haemorrhage (6). Traditionally much of the research on minimizing secondary brain injury following SAH has focused on the DCI period. However, the events occurring during EBI are now being considered as significantly contributing to outcome (7), and the focus of many studies is shifting to this phase.

EBI represents the primary injury caused by the haemorrhage, and its direct results over the first 72 hours post haemorrhage. These include the consequences from the mechanical impact of the haemorrhage, which include raised intracranial pressure (ICP) and decreased cerebral blood flow (CBF). These lead to decreased cerebral

perfusion pressure (CPP), resulting in global ischaemia. There is also loss of vascular integrity leading to brain oedema and further contributing to raised ICP (8).

There are also significant molecular alterations, including disruption to the NO signalling pathway, resulting in cell apoptosis (8). Apoptosis is now considered to be a major factor in the development of secondary brain injury after SAH, and is implicated in the later development of arterial vasospasm and DCI (9). When cerebral injury is global, as is the case with SAH, the degree of apoptosis can be more devastating than the injury itself (10).

Apoptosis is thought to contribute significantly to blood brain barrier (BBB) disruption and subsequent cerebral oedema (7). BBB disruption is thought to account for the many neurocognitive deficits that are seen after SAH. Amongst the survivors of SAH, up to 50% experience some form of cognitive dysfunction in the long term (11). Some of these patients have not suffered from any obvious complications with regards to the primary haemorrhage or in the postoperative course, including DCI. This makes it likely that these subtle cognitive deficits are due to EBI (7).

The events occurring during the EBI phase are likely to contribute to the mechanisms underlying the development of DCI. DCI is a clinical syndrome of focal neurological or cognitive deficits that occurs unpredictably in approximately 30% of patients 3-14 days after the initial haemorrhage. DCI remains the most important cause of morbidity and mortality in patients that survive initial aneurysm rupture and treatment (12).

The idea of extravasated blood from aneurysmal rupture leading to cerebral artery vasoconstriction and tissue infarction has been widely held for several years, based on angiographic evidence from SAH patients (13). However, the exact contribution of angiographic vasospasm to subsequent delayed ischaemia remains unclear, due to several factors. The temporal relationship between angiographic evidence of vessel spasm and DCI is weak (14), and patients can develop infarction in a vascular territory unaffected by arterial constriction (15). In addition, treatment of angiographic vasospasm does not lead to improved clinical outcomes (16).

It is therefore likely that mechanisms other than arterial vasoconstriction account for DCI. Both microthrombosis and cortical spreading depolarisations (CSDs) play an important role in the development of this condition and, both are affected by changes in the NO signalling pathway (17, 18). NO depletion is known to occur acutely post aneurysm rupture (19) and NO repletion in animal models has shown to reduce vasospasm and infarct sizes after ischaemic stroke (20). However, these results have yet to be translated to the patient population.

1.2 Thesis overview

In this thesis our main aims were to assess the mechanisms behind the neuroprotective effects of NO repletion after aneurysmal SAH. In Chapter 2 we discuss the physiology and pathophysiology behind cerebral NO signalling in health and disease, and review the current evidence for NO repletion. In Chapter 3 we discuss the assessment methods that we have investigated in this study to evaluate if they confer any additional information about the neuronal health of the brain after acute injury, and whether these methods could be used to assess the response to an intervention.

We explain the rationale behind our choice of imaging modalities that we feel are best placed to answer our research questions.

Chapter 4 describes our main study which uses quantitative EEG as a tool to assess the response to a cerebral NO donor, sodium nitrite, and the correlation with the development of DCI and subsequent outcome. We have found that sodium nitrite induces specific EEG changes that are consistent with improved neuronal health, and that this response is dependent on the subsequent development of DCI. In Chapter 5 we discuss a pilot study investigating the usefulness of vessel specific arterial spin labelling in quantifying tissue perfusion after severe SAH. We discuss some of the challenges posed by acquiring and analysing data from this patient population, and the interesting preliminary results that have arisen from this dataset. We also briefly discuss its utility as a screening tool to identify regions of the brain that are at risk of infarction due to decreased tissue perfusion in the first few days after aneurysm rupture.

The studies presented in this thesis highlight two novel methods for assessing neuronal wellbeing after severe subarachnoid haemorrhage, and raises the possibility of the utility of these methods for evaluation of new therapies. We have also gained some insights into the mechanism behind therapeutic repletion of cerebral NO after brain injury. The results presented indicate that additional larger studies are needed to validate these results and further the development of new therapies for this life-changing condition.

Chapter 2

Nitric oxide signalling in health and disease

Abstract

This chapter will introduce the concept of nitric oxide (NO) as a key signalling molecule in the regulation of cerebral blood flow. Evidence from animal studies will be reviewed to show that NO signalling plays a major role in the regulation of resting cerebral blood flow and the response to physiological challenges. A particular focus is put on the disruption to NO signalling that occurs after brain injury, especially subarachnoid haemorrhage, traumatic brain injury, ischaemic stroke and after cardiac arrest. There is increasing evidence that NO depletion in ischaemic brain tissue plays a pivotal role in the development of subsequent morbidity and mortality through microcirculatory disturbance and disordered blood flow regulation. NO is synthesized by the enzyme nitric oxide synthase (NOS) of which three isoforms exist. NO derived from endothelial nitric oxide synthase (eNOS) appears to have neuroprotective properties. However, nitric oxide derived from inducible nitric oxide synthase (iNOS) may have neurotoxic effects. Increasing cerebral NO, either directly or via a donor, appears to replicate the protective effects of eNOS derived NO in both the adult and immature brain. The promising results from animal studies regarding the use of NO donors as a targeted pharmacotherapy for secondary brain injury will be reviewed, and the potential for translation of these results to humans will be discussed.

2.1 Nitric oxide

In 1980 Furchgott and Zawadzki identified endothelium-dependent relaxation, the phenomenon whereby acetylcholine only induces relaxation of blood vessels if the endothelium is intact (21). Further studies showed that this relaxation was dependent on a specific substance, later termed endothelium-derived relaxing factor (EDRF) (22). EDRF was subsequently identified as nitric oxide (NO), a small, highly diffusible reactive molecule that is spontaneously and rapidly oxidized to nitrite and nitrate (23).

As well as its vascular smooth muscle relaxation properties, it also inhibits platelet aggregation (24). Additional actions include prevention of leucocyte migration and adhesion, and reduction of smooth muscle proliferation. These actions are all mediated via cyclic guanosine monophosphate (cGMP) (25).

In the central nervous system (CNS) it has effects as a neurotransmitter and neuromodulator, mediating neuronal signalling via activation of NMDA receptors (26). It is a key regulator of cerebral blood flow and inflammation, two major factors in the development of brain injury (27). The effects of NO are highly variable depending on the site of its generation, interactions with other signalling molecules, mode of synthesis and the local redox conditions (28).

This chapter will focus on the role of NO signalling in the regulation of cerebral blood flow, and how this becomes disrupted in disease states. The potential for NO to be both neurotoxic and neuroprotective will be discussed, and the exciting potential for

NO donors to translate as targeted neurotherapy for secondary brain injury will be examined.

2.2 Nitric oxide synthase

The nitric oxide synthases (NOS) were first identified and described in 1989. They catalyse the reaction of L-arginine to L-citrulline and NO in the presence of oxygen and specific co-factors, including (6R)-5, 6,7, 8-tetrahydrobiopterin (BH_4) and haem (29, 30). Three distinct isoforms of NOS have been identified which are the products of different genes. They each have different sites of action, catalytic properties, methods of regulation and inhibitor sensitivity (30).

The first isoform discovered, neuronal NOS (nNOS), also known as NOS-I predominates in neuronal tissue. The second isoform, inducible NOS (iNOS) or NOS-II, is inducible in a wide range of cells and tissues. The third isoform, endothelial NOS (eNOS) or NOS-III is the isoform found in vascular endothelial tissues. The isoforms can also be distinguished by their expression – constitutive (eNOS and nNOS) versus inducible (iNOS), or calcium dependence (eNOS and nNOS) versus independence (iNOS).

2.2.1 Endothelial nitric oxide synthase (eNOS)

eNOS is constitutively expressed in the vascular endothelium, platelets and cardiac myocytes, and is calcium dependent. eNOS derived NO plays a role in vasodilatation, inhibition of platelet aggregation and leucocyte adhesion and increases cerebral blood flow, being closely involved in cerebral autoregulation (31). In the patient population,

polymorphisms in the eNOS gene are associated with the incidence of angiographic vasospasm after subarachnoid haemorrhage (32).

2.2.2 Neuronal nitric oxide synthase (nNOS)

nNOS is expressed in perivascular structures that are co-localised with nerve terminals (33). NO derived from nNOS has many actions, one of which is as an important regulator of cerebral blood flow. It is responsible for early reperfusion following neuronal insult (34), and may therefore contribute to ischaemia/reperfusion injury (35). It therefore appears to have both protective and toxic actions in the brain.

2.2.3 Inducible nitric oxide synthase (iNOS)

iNOS becomes active in macrophages, glial cells and tumour cells in response to pro-inflammatory cytokines or endotoxin (36) and unlike eNOS and nNOS it is not expressed unless induced. It can produce a large amount (100-1000 times greater) of NO in relation to eNOS and nNOS (37), due to its independence from calcium dependent mechanisms for activation. After induction, iNOS continuously produces NO until the enzyme is degraded (38).

2.3 Role of nitric oxide in cerebral blood flow regulation

The brain accounts for 20% of the body's energy consumption despite only accounting for 2% of its mass. One of the major roles of cerebral blood flow (CBF) is to supply oxygen to the brain tissues as neuronal activation requires large amounts of energy to regulate the ion fluxes that occur on depolarisation. Therefore, it is essential that this is tightly regulated.

The NO signalling pathway plays a major role in the regulation of CBF at rest and during physiological and pathological stresses. Understanding the mechanisms behind the regulation of these processes may therefore give useful insights into the CBF changes that occur during cerebral injury.

Two main mechanisms underlie the regulation of CBF at rest, autoregulation and neurovascular coupling. eNOS-NO plays a key role in autoregulation, whereas nNOS derived NO appears crucial for neurovascular coupling.

2.3.1 Autoregulation

Autoregulation is the mechanism by which a consistent supply of blood to the brain tissues in the face of changing cerebral perfusion pressure (CPP) is maintained. eNOS derived NO is essential for extending the lower limit of autoregulation. This is demonstrated by a right shift of the autoregulation curve in eNOS knockout mice at low perfusion pressures (31) (see figure 2.1). Elevation of CBF near the lower limit of autoregulation and an increase in the hypotensive portion of the autoregulatory curve is also NO dependent (39) During pathological processes where CBF is reduced, such as subarachnoid haemorrhage or ischaemic stroke, NO depletion could therefore further exacerbate decreased flow conditions and increase the likelihood of permanent neuronal damage.

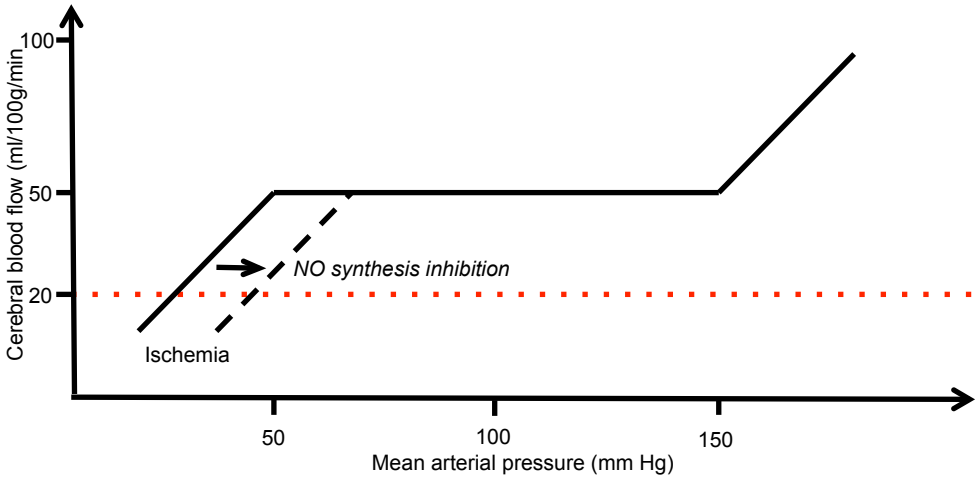


Figure 2.1 Cerebral autoregulation maintains an adequate and stable cerebral blood flow in the face of changes in mean arterial pressure (flat portion of the curve). The brain becomes vulnerable to ischemia when cerebral blood flow falls below 20 ml/100g/min (red dashed line). NOS inhibition results in right shift of the hypotensive portion of the autoregulatory curve, resulting in the brain becoming susceptible to ischemia at higher perfusion pressures. Therefore NO signalling is essential in maintaining adequate cerebral blood flow under conditions of fluctuating mean arterial pressure.

2.3.2 Neurovascular coupling

Neurovascular coupling is the process by which increased neuronal activity is linked to the local regulation of CBF. This ensures that the supply of oxygen is always greater than the demand, and is also known as functional hyperaemia. It is achieved via an integrated action of neurons, glial cells and blood vessels that form a 'neurovascular unit' (40). Several signalling pathways exist to mediate flow/metabolism coupling in this unit, and these interact on multiple levels to ensure a coordinated blood flow response.

Disruption to neurovascular coupling is a common process that underlies many brain disease states (41). Studies where nNOS is knocked out or inhibited have shown a decrease in neuronal activity related blood flow by up to 90% in the cerebellum (42), that is reversible in the presence of an exogenously administered NO donor (43). nNOS inhibition in rats causes significant attenuation of the cerebral blood flow response to forepaw stimulation, which is disproportionate to the degree of attenuation of somatosensory evoked potentials (44), indicating disruption to neurovascular coupling.

Metabolic pathways activated by glutamate also play a key role in neurovascular coupling via activation of neuronal NMDA receptors (40). This causes an influx of calcium that activates NOS, resulting in increased blood flow. Glutamate also stimulates prostaglandin and epoxyeicosatrienoic acid (EET) synthesis in astrocytes via arachidonic acid (AA) pathways (45). This pathway can cause both vasoconstriction and vasodilatation (46). Under conditions of NO depletion vasoconstriction is favoured via predominance of 20-hydroxyeicosatetraenoic acid (20-HETE) and decreased production of vasodilatory expoxyeicosatrienoic acids (EETs). These pathways are illustrated in figure 2.2.

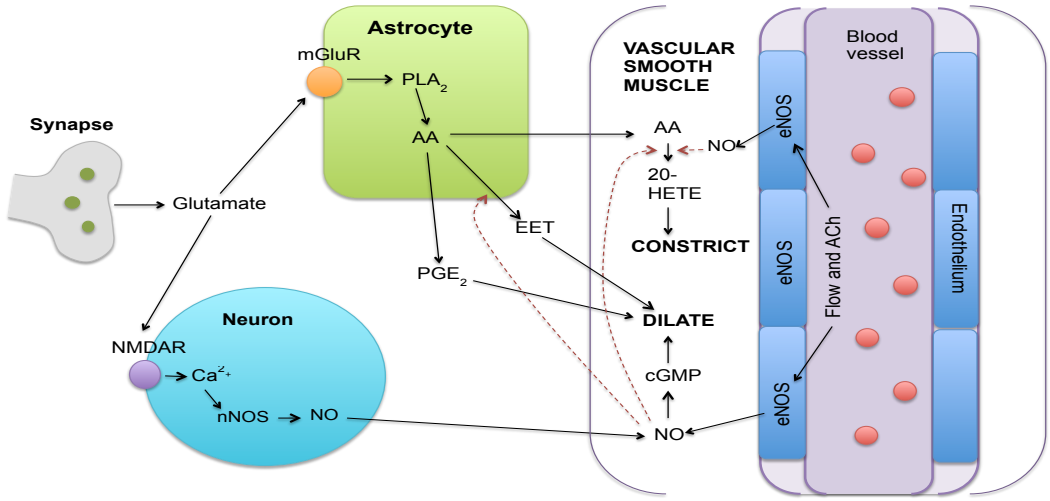


Figure 2.2 Adapted with permission from Attwell et al *Nature* 468(7321): 232-43
NO inhibits (dashed lines) the production of the vasoconstricting 20-HETE as well as the vasodilating EET. Endothelial nitric oxide synthase (eNOS) can be activated by flow-induced shear stress or by acetylcholine (ACh). This may be one mechanism whereby it may improve blood flow to the brain. NO = nitric oxide NMDAR = NMDA receptor PLA_2= phospholipase A_2 nNOS = neuronal nitric oxide synthase AA = arachidonic acid mGLUr = metabotropic glutamate receptor PGE_2= prostaglandin E_2.

2.4 NO signalling during physiological stresses

Hypoxia and hypercapnia are used as examples of physiological stresses as alterations in tissue partial pressures of oxygen and carbon dioxide are extremely common in critical illness following a brain insult (47). The NO signalling pathway plays a central role in the cerebral blood flow response to these alterations. In addition it is known that NO pathway dysfunction occurs after brain tissue ischemia, causing dysregulation of these normal physiological responses.

2.4.1 Hypoxia

Decreased arterial oxygen supply (hypoxia) increases the baseline level of CBF in humans (48). NO plays a role in both signalling this event and the CBF response (49).

Nonselective NOS inhibition abolishes the increased CBF response to hypoxia in rats (50). The evidence for this in humans is more indirect, but it has been demonstrated that exposure to hypoxia during adaptation to high altitudes increases NO levels and high-altitude dwellers such as Tibetans have increased circulating NO levels (51).

2.4.2 Hypercapnia

The modulation of cerebral vascular tone in response to changes in arterial partial pressure of carbon dioxide is known as chemoregulation, and this process may be viewed as one of the main regulators of cerebral vascular tone.

The cerebral vasodilatory response to hypercapnia is inhibited by L-arginine analogues, which act by blocking the NO synthesis pathway, and by NOS inhibitors (52, 53). Cerebral vasodilatation in response to hypercapnia is reduced after experimental traumatic brain injury in a rodent model and exogenous NO acts to reverse this (54), helping to restore the normal physiological response.

A study on human cell cultures showed an increase in NO production in response to increased CO_2 levels (55). However, it is likely that the in vivo response differs from the in vitro response, due to multiple interactions of the NO pathway with other intracellular signalling pathways within the neurovascular unit.

In summary, it can therefore be seen that in the face of a focal brain injury, NO depletion leads to disruption to the normal physiological response to alterations in oxygen and carbon dioxide, which further exacerbates neuronal damage. Restoration

of the normal adaptive response via replenishing cerebral NO levels may be efficacious at reducing secondary brain injury.

There is therefore a need for further investigation into the NO signalling pathway in a 'whole brain' model in humans, to precisely elucidate the specific mechanisms underlying the observed blood flow effects. Healthy volunteer studies examining the role for NO in the CBF responses to hypoxia and hypercapnia would enable clarification of the role of NO signalling during global disruptions to cerebral physiology, while studies in patients with cerebral injury would enable the effects of NO signalling during the evolution of focal brain pathology to be quantified.

2.5 The role of nitric oxide in the cerebral response to injury

Secondary brain injury is an indirect result of the initial insult, resulting from processes initiated by the primary injury, occurring hours or days later. It plays a large role in morbidity and mortality, and unlike the primary injury steps can be taken to mitigate some of its effects.

The NO signalling pathway influences the evolution of secondary brain injury in multiple ways, dependent on site, mechanism and timing of NO synthesis and concentration. NO has effects both on the vasculature and on a cellular level, and interacts with many other signalling pathways. This makes it difficult to translate results from animal models where conditions are tightly controlled to the patient population where the evolution of injury occurs unpredictably.

2.5.1 Nitric oxide depletion

Relative NO depletion appears to occur in the early stages of cerebral injury regardless of the aetiology, e.g. after traumatic brain injury (TBI), subarachnoid haemorrhage (SAH), post cardiac arrest and ischemic stroke (56-58). This occurs simultaneously with a reduction in blood flow (59). L-arginine, which enhances NO production, increases CBF (60, 61). This indicates that disruption to NO signalling is part of a common pathophysiological pathway that leads to the development of secondary brain injury regardless of the mechanism of insult. NO depletion appears to be central in particular to many of the abnormal processes that occur after SAH.

SAH is usually caused by rupture of a cerebral aneurysm located in the circle of Willis (2). Decrease in cerebrospinal fluid (CSF) NO metabolites are seen within 10 minutes of SAH and this is associated with vasoconstriction (19). This is thought to be secondary to destruction of NOS function by haemoglobin (62-64). Decreased NO bioavailability is also caused by cerebral NO reacting with superoxide anions to produce peroxynitrite (ONOO) (65). Peroxynitrite formation may cause damage to mitochondria, the vascular endothelium and smooth muscle cells (66). In patients with SAH, increased CSF levels of the endogenous NOS synthase inhibitor asymmetric dimethylarginine (ADMA) were observed, and higher levels predicted poorer long term outcome (67).

However, another study showed a rise in CSF NO metabolites 24 hours after SAH and the higher the level the worse the outcome (68). The discrepancies in the evidence may be explained by the complexity surrounding the biochemical pathways relevant to the generation and elimination of NO and ADMA. An increase in NO metabolites

is only an indirect measure of NO levels (the short half life of NO making it difficult to measure directly), and gives no information regarding the source or activity of the NO generated.

SAH is associated with microvascular constriction, resulting in microthrombus formation (17) and microinfarctions (69). There is an associated global decrease in cerebral NO levels and a corresponding increase in cerebral P-selectin levels (17). P-selectin is a endothelial cell adhesion molecule that promotes platelet aggregation and fibrin deposition (70). Inhibition of NO synthesis results in increased P-selectin expression (71), therefore NO depletion favours microthromobsis formation.

Cortical spreading depression (CSD) consists of a wave of electroencephalogram (EEG) silence moving across the cortical surface (72). CSDs play a role in both early brain injury (73) and in delayed cerebral ischemia after SAH (74), as well as traumatic brain injury and stroke (75). In healthy brain tissue, spreading depolarisation is associated with vasodilatation. However, in damaged brain tissue an inverse blood brain flow response occurs which results in vasoconstriction and tissue ischemia (76). Reduced levels of NO renders the brain more susceptible to CSDs. Basal levels of NO determine the threshold of CSDs (18) and NO also acts to restore impaired cerebrovascular reactivity after CSD (77).

Therefore it can be seen that NO signalling plays a crucial role in the blood flow changes that occur after subarachnoid haemorrhage. NO depletion plays a major role in early brain injury, microthrombus formation and cortical spreading depression.

Targeting this pathway may enable partial restoration of physiological blood flow, helping to prevent secondary neuronal injury.

2.5.2 Endothelial nitric oxide synthase dysfunction

Impairment of eNOS activity is also implicated in many cellular mechanisms of neuronal injury (78) and is seen after SAH, TBI and ischemic stroke. Innate eNOS activity determines susceptibility to injury, with possession of isoforms with greater activity conferring protection to secondary neuronal insult.

One of the major causes of morbidity and mortality following SAH is delayed cerebral ischemia (DCI). This occurs in about 30% of patients (13, 79) typically between day 3 and 12 following SAH (79). Recently it has been discovered that the NO signalling pathway plays a significant role in the pathogenesis of DCI (80). Genetic variation in the eNOS gene in humans influences the risk of DCI after SAH, as possession of an isoform that results in lower eNOS activity results in greater risk (81, 82).

Functional uncoupling of eNOS from its co-factor BH_4 also occurs after cerebral insult. eNOS uncoupling occurs under ischemic conditions, causing superoxide to be generated instead of NO (83, 84). Superoxide reacts with NO to form peroxynitrite, which is in itself a neurotoxin, decreasing levels of bioactive NO (85, 86). This reduction in NO bioavailability contributes further to secondary brain injury (87, 88).

eNOS uncoupling contributes to injury after SAH (89) and simvastatin acts to re-couple eNOS after SAH (90) in an experimental blood injection model of SAH in

rodents. This implies that recoupling of eNOS may be a promising therapeutic target. However, a large multicentre randomised phase 3 trial failed to detect any benefit in the use of simvastatin for long or short-term outcome in patients with aneurysmal SAH (91). It is unclear why this was the case but it is likely that pathological aneurysm rupture triggers pathways that are not activated by a blood injection animal model, therefore statins may not be acting in the same fashion as in experimental models.

Another possibility is that eNOS uncoupling has metabolic and cellular effects that affect other cellular signalling pathways, and the physiological differences between rodents and humans render results from animal studies difficult to interpret. For example, eNOS knockout appeared to confer neuroprotection in one study, indicating that the detrimental effects of eNOS uncoupling may outweigh the benefits of eNOS activity in this particular model (92).

2.5.3 Ischaemia/reperfusion injury

This is a pathophysiological process responsible for organ injury in a variety of conditions such as myocardial infarction, organ transplantation and cardiac arrest. NO plays a pivotal role in the development of this condition, with NO donor agent administration reducing ischemia/reperfusion (I/R) injury in animal models (93). A systematic review of NO donor administration during animal stroke models demonstrated an overall improvement in cerebral blood flow and a decrease in infarction volume (94). However, whether these results translate into the patient population with cerebral I/R injury (e.g. ischemic stroke, cardiac arrest) has not yet been tested (95) and represents an important area of future research.

Cardiac arrest and subsequent recovery results in complete interruption followed by restoration of blood supply, and therefore may provide the best clinical model of ischemia/reperfusion. Inhaled NO and intravenous sodium nitrite (a NO donor) have been shown to confer neuroprotection in mice and rats (96, 97), and this appears to be mediated by S-nitrosation of proteins rather than the canonical cyclic GMP signalling pathways (97). eNOS mediated mechanisms are responsible for the neuroprotective effects of therapeutic hypothermia after cardiac arrest, and inhaled NO conferred neuroprotection in eNOS knockout mice, replicating the beneficial effects of hypothermia (98). Therefore, there is preliminary evidence for NO donors as a potential neurotherapeutic agent after cardiac arrest.

2.5.4 Inducible nitric oxide synthase

It has been thought that NO derived from iNOS is responsible for some of the neurotoxic actions of NO post brain injury. One proposed mechanism by which this occurs is via the reaction of iNOS generated NO with superoxide generated from uncoupled eNOS to form peroxynitrite. The putative mechanism behind this is illustrated in figure 2.3.

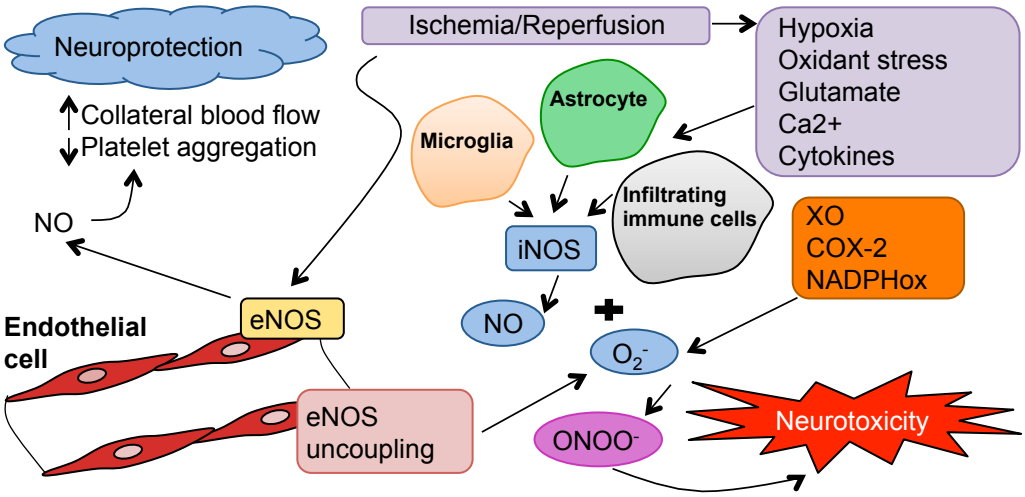


Figure 2.3 Adapted with permission from Pacher P et al. *Physiol Rev* 2007; 87:31 Brain ischemia and reperfusion leads to stimulation of endothelial NOS (eNOS), resulting in brief increases in endothelial NO generation, associated with neuroprotective actions. Ischemic energy depletion and oxidant production triggers the release of glutamate, which results in stimulated activity inducible NOS (iNOS) in astrocytes, microglia and infiltrating inflammatory cells. iNOS activation also occurs in response to the release of inflammatory cytokines such as TNFα and IFNβ, and cellular signalling pathways responsible for the response to hypoxia. During the same period of time, superoxide production is enhanced due to uncoupling of eNOS, mitochondrial dysfunction, and the stimulated activity of NADPH oxidase, xanthine oxidase (XO), and cyclooxygnease-2 (COX-2). Formation of peroxynitrite is then favoured, damaging lipids, proteins and DNA that contributes significantly to neurotoxicity.

However, this is an oversimplified view, and it is more likely that iNOS derived NO, like eNOS-NO, has several roles to play and that the balance between neurotoxicity and neuroprotection is dependent on many factors. As iNOS derived NO has multiple actions, results from animal studies may be focusing on its effects on cerebral blood flow (which is an easily measurable outcome) without accounting for the cellular and metabolic effects (which are more difficult to quantify).

NO derived from iNOS appears to contribute to neurotoxicity after ischemic stroke, as animal knockout models have smaller infarcts than their wild type counterparts (99). An increase in NO above basal levels secondary to iNOS occurs 12-24 hours after MCA occlusion and contributes to neurotoxicity, with iNOS inhibition leading to reduced infarct volume (100).

There is also evidence that NO produced by iNOS contributes to neurotoxicity following TBI. iNOS expression is significantly induced by brain injury, with peak concentrations occurring around 1-2 days after TBI (101, 102). Patients with higher levels went on to have a worse outcome (103). A recent phase II clinical trial (NOSTRA) in TBI patients using the NOS inhibitor 4-amino-(6R,S)-5,6,7,8-tetrahydro-L-biopterin (VAS203), which preferentially inhibits iNOS (104), showed significantly improved extended Glasgow Outcome Scores compared to placebo (105).

However, the evidence on the role of iNOS after TBI is conflicting. Attenuation of CBF at 72 hours after TBI was demonstrated in iNOS knockout mice (106), which also correlated with long-term functional outcome (107, 108). Inhibition of iNOS appeared to lead to exacerbation of deficits in cognitive performance and increased neuron loss (107). However, these studies are confined to rodent models of controlled cortical impact injury, and the CBF results may be linked to pathological vasodilatation linked to inflammation. This may explain the apparent contradictory results shown, and emphasises that simply measuring cerebral blood flow does not give the entire picture with regards to the effects of NO in the brain after injury.

Overall, the balance of evidence is in favour of iNOS activity being harmful in the patient population, and therefore inhibition of destructive cascades mediated via iNOS may have promise as a potential future therapy.

2.6 Manipulation of nitric oxide signalling using animal models

Despite the controversies surrounding NO dysfunction after brain injury, there is animal evidence that increasing cerebral NO levels either directly using inhaled NO or indirectly using NO donors has neuroprotective effects. Exogenous NO appears to replicate the actions of eNOS derived NO, without contributing to neurotoxicity. NO donors may be neuroprotective by preventing NO depletion, helping to normalize capillary blood flow and improve oxygen delivery to the tissue (109).

2.6.1 Inhaled NO

There have been several rodent studies showing that increasing cerebral NO levels directly using inhaled NO gas results in reduced infarct sizes and improved neurological function after experimental TBI and middle cerebral artery occlusion (110-112).

2.6.2 NO donors

Cardiovascular instability when using classic NO donors such as glyceryl trinitrite (GTN) and sodium nitroprusside precludes their use in critically ill unstable patients, and makes results of drug trials difficult to interpret as local effects are negated by systemic blood pressure effects.

However, sodium nitrite is emerging as a feasible, safe NO donor with minimal effects on the systemic vasculature in patients after SAH (113, 114). It has also been used safely in cardiac arrest survivors (97). This is because cerebral tissue is able to convert endogenous nitrite to NO without the need for oxygen as a substrate (115), meaning that when the tissues are hypoxic (such as after cerebral injury) nitrite is only converted to NO locally. The mechanisms underlying this are illustrated in Figure 2.4.

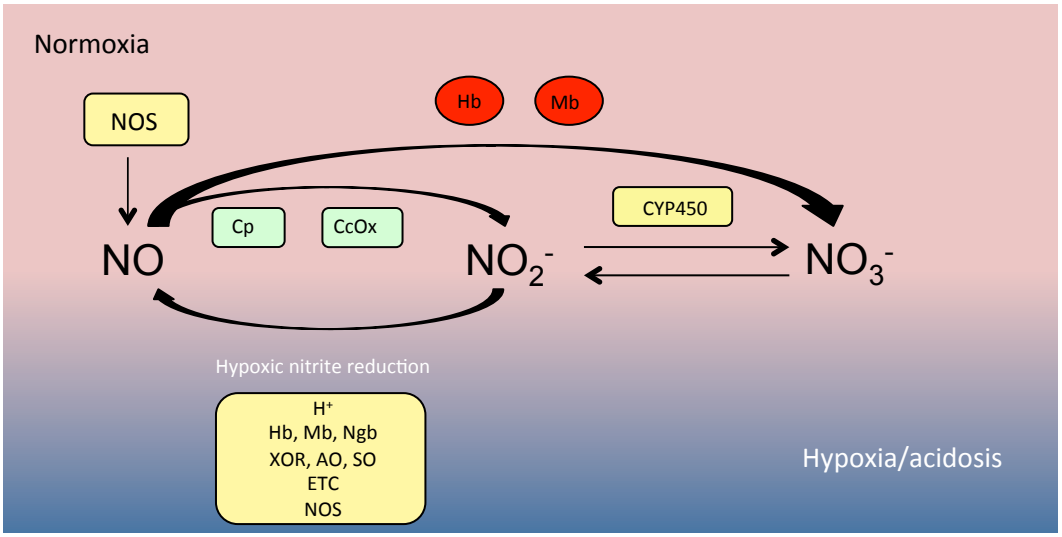


Figure 2.4 Adapted with permission from Shiva S. *Redox Biol* 2013; 1(1): 40-44
In normoxia NOS is functional and generates NO, which is oxidised by haemoglobin (Hb) and myoglobin (Mb) to nitrate (NO_3^-) and by cytochrome c oxidase (ccox) and ceruloplasmin (Cp) to nitrite (NO_2^-). Nitrate is also derived from the diet as well as the normoxic oxidation of nitrite by cytochrome P450 enzymes (CYP450). In hypoxia, nitrite is reduced to bioactive NO by a number of mammalian nitrite reductase enzymes including Hb, Mb, neuroglobin (Ngb), xanthine oxidoreductase (XOR), aldehyde oxidase (AO), sulphite oxidase (SO), components of the mitochondrial electron transport chain (ETC) and NOS.

The results from animal studies have been promising, with prevention and reversal of cerebral vasospasm after experimental SAH (20, 116). However, these are based on autologous blood clot injection models, and as discussed previously pathological

aneurysm rupture is likely to activate multiple cellular signalling pathways that may not be replicated in these experimental models. Therefore large-scale clinical trials are needed to translate these results to patients.

2.7 Conclusion

In this chapter, we have shown that NO is an important mediator in the regulation of CBF in the resting state, acting as a key modulator on the pathways responsible for maintaining resting CBF and perfusion under physiological stresses such as fluctuations of blood pressure, hypoxia and hypercapnia. Disruption to NO synthesis and metabolism underlies many of the pathophysiological processes that occur after brain injury, and appears to occur regardless of the mode of injury. The available evidence suggests that NO derived from eNOS is neuroprotective after acquired brain injury whereas NO synthesised by iNOS contributes to further harm, and that this difference is due to differences in timing, spatial location and concentration of NO generated by each isoform. This evidence has led to investigation of drugs that influence NO signalling as potential therapeutic agents. In particular, NO donors have been shown to be neuroprotective and efficacious in reducing secondary brain injury in animals, potentially by replicating some of the effects of endogenous NO derived from eNOS. Future research should focus on translating the promising results from animal studies to the patient population. Better understanding of the role of the NO signalling pathway after cerebral injury may lead to exciting new pharmacotherapies to prevent the development of secondary brain damage.

Chapter 3

Experimental Methods

Abstract

In this chapter the current tools available to assess the degree of neuronal injury after severe subarachnoid haemorrhage (SAH) will be discussed. The limitations of these methods will be discussed. We will then go on to discuss two relatively new methods of assessing cerebral injury after SAH - electroencephalography (EEG) and magnetic resonance imaging (MRI). The principles underlying these methods will be discussed and the current evidence available regarding using these methods to measure brain injury after SAH will be studied. Their uses and limitations in the neurocritical care setting will be explored, and our rationale behind choosing these methods to answer our research questions will be explained. In particular, the use of EEG to allow evaluation of the possible cellular and vascular actions behind exogenous cerebral NO repletion will be explored. The utility of arterial spin labelling (ASL) MRI to determine cerebral blood flow will also be discussed, and the use of EEG and MRI as potential tools for the evaluation of new treatments will be explained.

3.1 Introduction

There is a need for the development of diagnostic methods that enable early, accurate detection of DCI after SAH. These would also ideally allow a window of opportunity to initiate therapies prior to the establishment of clinically detectable symptoms, in particular during the EBI period. This is of special importance after severe SAH, where patients are sedated and therefore it is very difficult to detect any deterioration in neurology from clinical examination alone. Exposing these already critically unwell patients to additional risk in the form of ionizing radiation and contrast agents is not ideal and is best avoided if possible.

Currently, the methods available for monitoring of neuronal tissue health after SAH each have their own set of limitations and risks. The development of a non-invasive, bedside test that does not involve the use of ionizing radiation or injection of contrast, and that provides real time accurate information about the state of the brain would have the potential to greatly improve clinical care and reduce the morbidity and mortality burden from this severe disease.

3.2 Current methods

3.2.1 CT

Non contrast computerised tomography (CT) is widely available, quick and relatively easy to obtain. This uses a series of X-rays of the head taken from many different directions to compose images comprising of a series of cross sections of the brain. It requires exposure to ionizing radiation but has greatly improved the diagnosis of acute SAH (117). However, its utility in detection of developing ischaemia after initial diagnosis is limited, as it relatively insensitive at detecting active infarction. Changes

usually only become visible many hours after they have occurred, missing the window for any therapeutic intervention (118). CT perfusion imaging has shown more promise at diagnosing ongoing tissue ischaemia (119) but still requires exposure to radiation and injection of intravenous contrast.

3.2.2 TCD

Transcranial Doppler ultrasonography (TCD), is a non invasive and widely available technique that has been widely used in the past to screen for angiographic cerebral vasospasm, (previously thought to be linked to the development of DCI (13)). However, its use is limited to the middle cerebral artery (MCA), and while it is highly accurate at detecting MCA vasospasm, false positive results are common (120). In addition, there is increasing evidence that cerebral arterial vasospasm is not directly linked to the development of subsequent neurological deficits (14, 120). Therefore, the concept of monitoring for DCI is shifting from modalities used to detect angiographic vasospasm to techniques focusing on tissue perfusion.

3.2.3 NIRS and PET

Positron emission tomography (PET) maps perfusion and physiological activity via the systemic injection of exogenous radioactive compounds. It has been used to assess the impact of various interventions on tissue oxygen delivery (121) in patients with SAH that have developed DCI. However, it is currently limited as a useful clinical tool by expense and restriction to major research centres only.

Near Infra-Red Spectroscopy (NIRS) uses infra-red light to penetrate the skull and provide a measure of cortical oxygen saturation. It has been used to assess real-time

cerebral autoregulation changes in patients after SAH (122) and is potentially more accurate than TCD at detecting blood flow changes (123). It also enables quantification of brain tissue oxygen saturations, which may give an indication of evolving changes in neuronal and astrocyte metabolism. However, further validation studies of this technique are needed before the clinical significance of the new information gained from this method can be determined.

3.3 Rationale behind choice of investigations

Many of the modalities discussed above require exposure of the patient to risks such as radiation or contrast agents. Others give accurate information about the macrovasculature, but little insight into the tissue changes that are occurring. We have already seen that cellular signalling disruption and microcapillary disturbance are likely to play a major contribution to the evolution of EBI, therefore these methods are not suitable for investigation of the above.

EEG has been used for many years as a non-invasive test of neuronal activity. However, recently there has been more interest in its use in the critical care setting as a potential predictive marker of cerebral ischaemia. We hypothesized that EEG would be a sensitive way to assess any changes of neuronal activity induced by cerebral NO repletion, based on previous studies in ischaemic stroke and SAH (124). The main advantages that led us to chose this modality was its relative simplicity to set up at the bedside, removing the need to transfer a critically unwell patient, its non invasive nature and the relatively low risk associated with carrying out a recording.

Arterial spin labelling MRI is recently emerging as an accurate method of quantifying cerebral tissue perfusion. As we are interested in investigating changes happening at a cellular level we chose to investigate this sequence as a means of evaluating blood flow changes that occur in the acute stages of the bleed.

3.4 Electroencephalography

3.4.1 Introduction

Electroencephalography (EEG) is a non-invasive bedside method to record the activity of the brain from electrodes placed on the scalp. The EEG is a measurement of currents that are generated during synaptic excitations of the dendrites of pyramidal neurons located in the cerebral cortex. These are detected via multiple electrodes applied to the patient's scalp. The signal is greatly attenuated by the many layers between the scalp and the cerebral cortex. Therefore each electrode is connected to one input of a differential amplifier and a common reference electrode is connected to the other input. After amplification of the difference the signal is filtered, digitized and recorded.

Electrode locations are typically specified by the International 10-20 system, which is an internationally recognized method to describe the location of scalp electrodes. The lobe and hemisphere location are denoted by a letter and number respectively. F, T, C, P and O stand for frontal, temporal, central, parietal and occipital lobes. The naison, which is the depressed area between the eyes, and the inion, the lowest point of the skull at the back of the head are used to aid positioning, with electrode locations along regular points of a line joining the two.

The EEG signal is also affected by noise, either from within the brain (internal noise) or over the scalp (system noise or external noise), meaning that only large populations of active neurons can generate enough potential to be recordable by scalp electrodes. The recording is usually filtered, with low-pass filters being used to remove high frequency artifacts such as signal from muscle and high-pass filters being used to remove slow frequency artifacts such as movement. Notch filters are also often used to remove 50 Hz noise from electrical power lines.

The acquired signal can be used for the investigation of many clinical problems, such as epilepsy and seizure origin location, monitoring alertness, coma and brain death, and locating areas of damage following head injury, stroke and tumours. In healthy adults, the amplitude and frequencies of EEG signals change from one state to another, such as from wakefulness to sleep.

There are five major brain waves distinguished by their different frequencies. These are called alpha (α), beta (β), gamma (γ), delta (δ) and theta (θ). Delta waves are in the range of 0.5-4 Hz and are primarily associated with deep sleep. Theta waves are in the range of 4-7.5 Hz and appear as consciousness becomes drowsiness. Alpha waves predominate in the posterior aspect of the brain and lie within the 8-13 Hz frequency range. They are thought to indicate a relaxed awareness without attention or concentration. Beta waves are typically in the 14-26 Hz range although in some literature there is no upper boundary, and represent active thinking, attention and focus on the outside world. The frequencies above 30 Hz correspond to the gamma range and modulate perception and consciousness, disappearing under anaesthesia.

EEG monitoring may therefore allow early detection of focal ischaemia by providing continuous information about cerebral function (125). There are typical changes that occur in the EEG signal as tissue perfusion falls, illustrated by Figure 3.1. EEG changes due to ion pump failure occur when CBF falls below 25-30 ml/100g/min. As infarction only occurs when CBF falls to below 18ml/100g/min this provides a window of opportunity for therapeutic intervention to prevent permanent brain damage (126).

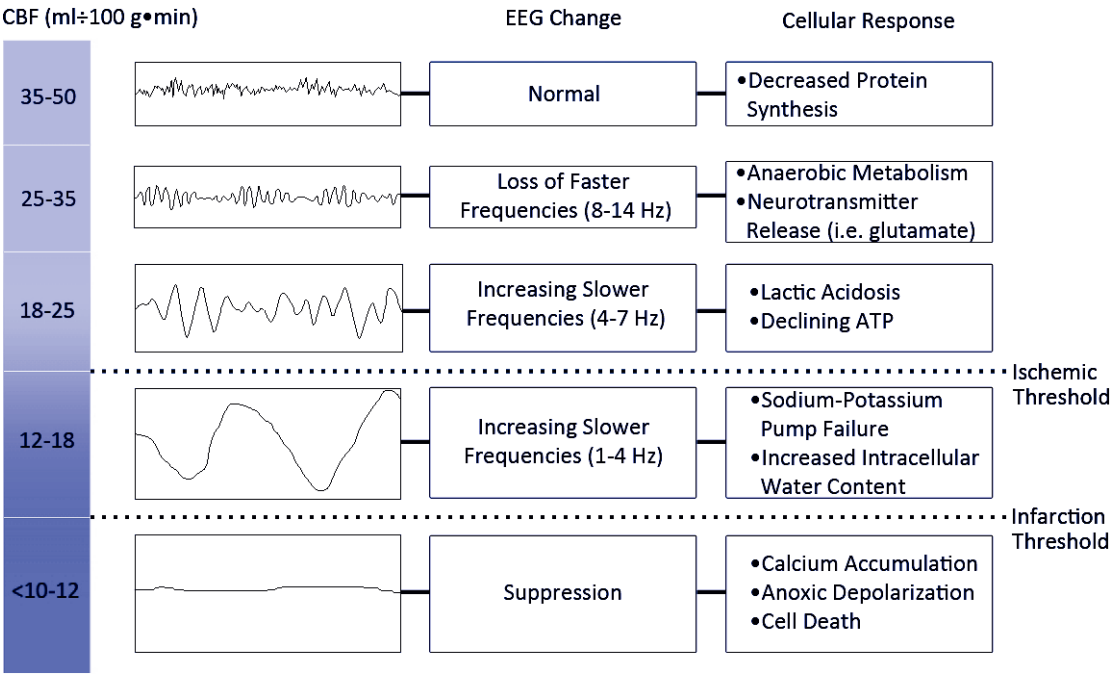


Figure 3.1 The relationship of cerebral blood flow to electroencephalogram (EEG) and pathophysiology (adapted with permission from Foreman and Claassen Critical Care 2012, 16:216 http://ccforum.com/content/16/2/216) ATP = adenosine triphosphate

3.4.2 Principles of Spectral Analysis

Digital EEG can be transformed into power spectra by fast Fourier transformation (FFT), which enables long periods of EEG to be compressed into quantitative EEG (qEEG) parameters. This allows raw EEG to be quantified in terms of amplitude, power, frequency and rhythmicity to generate numerical values that may be used as

ratios, percentages or as graphical representations. Time compressed spectral arrays incorporate both power and frequency spectrum data to create an image that uses colour to represent power at different frequencies over time – a 'spectrogram'. Currently, fast Fourier transformation appears the most suitable for quantifying the EEG after cerebral ischaemic insult (127).

However, conventional Fourier analysis is somewhat limited in its ability to estimate a signal's spectral properties. This is because each Fourier coefficient is not necessarily always a reliable representation of the corresponding component frequency, potentially giving a biased estimate of the true spectral content. The multitaper method reduces estimation bias by obtaining multiple independent estimates from the same sample, and as each taper is orthogonal to all other tapers, the windowed signals provide statistically independent estimates of the underlying spectrum (128).

Several qEEG parameters have been used clinically and have their own strengths for a given clinical situation. These include relative alpha power, total power and the alpha/delta ratio. These will now be discussed further in the context of SAH.

3.4.3 EEG after SAH

SAH results in a large number of abnormalities on EEG. EEG abnormalities may occur even prior to the onset of DCI, with certain patterns being predictive of later ischaemia (129). QEEG for the detection of ischaemia after SAH has been examined in a total of 89 patients over 4 studies since 1991. Total power (125) and the

variability of relative alpha power (130) appeared to be the most predictive of subsequent ischaemia in good grade, non-comatose patients.

However, a study in poor grade, comatose patients showed that the ratio of alpha power to delta power (the alpha/delta ratio or ADR) after stimulation demonstrated the strongest association with DCI, with a decrease in ADR of 24% in patients with ischaemia (131). Another study not restricted to poor grade patients found that a decrease in the composite alpha index (which was derived from the mean alpha power multiplied by the standard deviation) occurred more than 24 hours prior to neurodeterioration (132). A more recent study found that a decrease in alpha power represented a marker for DCI in SAH patients, although this study was also not restricted to poor grade patients (133).

3.4.4 Limitations

In spite of this potential to detect ischaemia, continuous EEG is limited in its usefulness in the acute setting, as to achieve the goal of real-time detection of critical brain events access to continuous expert review of the raw EEG would be required, which would be time consuming, expensive and is not currently available.

Another major limitation of EEG monitoring is that its interpretation is ultimately subjective. Quantification of power spectra partially overcomes this, but there is no one parameter that has been identified as being potentially predictive, and all require several days' worth of continuous EEG recording and vigorous artifact rejection. Therefore, there is a need for the development of a tool to enable EEG to be used at the bedside in neuro-intensive care in an objective, clinically useful way. The

alpha/delta ratio appears to be the most robust parameter to investigate when investigating patients with a severe SAH.

3.5 Magnetic Resonance Imaging

3.5.1 Introduction

Magnetic Resonance Imaging, or MRI uses magnetic fields to form images of the body. It relies on an external magnetic field (B0) that aligns protons found in water in the body, and then the application of perpendicular radiofrequency (RF) pulses that tip the magnetization away from the external field. Once this is removed the protons in the nuclei realign themselves parallel to the main magnetic field. This return to equilibrium is known as relaxation. During relaxation, the nuclei lose energy by emitting their own RF signal. This signal is measured by a conductive field coil placed around the object being imaged (in this case the head). This measurement is then reconstructed to obtain 3 dimensional grey scale MR images.

The intensity of a tissue type (e.g. grey matter vs. white matter) depends on 3 things:

1. The density of protons in that tissue
2. The longitudinal relaxation time (T1) i.e. the time needed for the displaced nuclei to realign themselves with B0
3. The transverse relaxation time (T2) i.e. the time needed for the relaxation RF signal to decay

During the acquisition of MR images, the perpendicular RF pulse is repeated at a fixed rate, known as the repetition time or TR. The relaxation RF signals can be measured at various intervals during the TR, and the time between the application of

the perpendicular pulse and the signal detection is known as the echo time, or TE. The MR image can be 'weighted' towards highlighting different tissue types by making adjustments to these parameters. More complicated sequences may be applied that enable detection of blood flow changes, which will be discussed further below.

The main advantages are of MRI is that it is non-invasive and does not use ionizing radiation. However, due to the high magnetic field it is unsuitable for certain patient populations, such as those with a pacemaker or with ferrous or electronic objects in their body.

3.5.2 Arterial Spin Labelling

Several blood flow changes occur after aneurysmal rupture. These blood flow changes can be immediate, or delayed by several hours or days. Quantification of the CBF changes that do occur may be useful in the detection of DCI in comatose patients, who may not exhibit any clinical or CT signs as discussed above.

Arterial Spin labelling (ASL) uses arterial blood water as tracer by inverting the magnetization of the blood outside the slice of interest using radiofrequency (RF) pulses. After a delay to allow the labelled blood to flow into the brain tissue, images are acquired that contain signal from both the static water and the labelled water. Separate control images are also acquired, and the signal difference between control and labelled images enables estimation of the tissue perfusion, using a biophysical model (see Figure 3.2) (134).

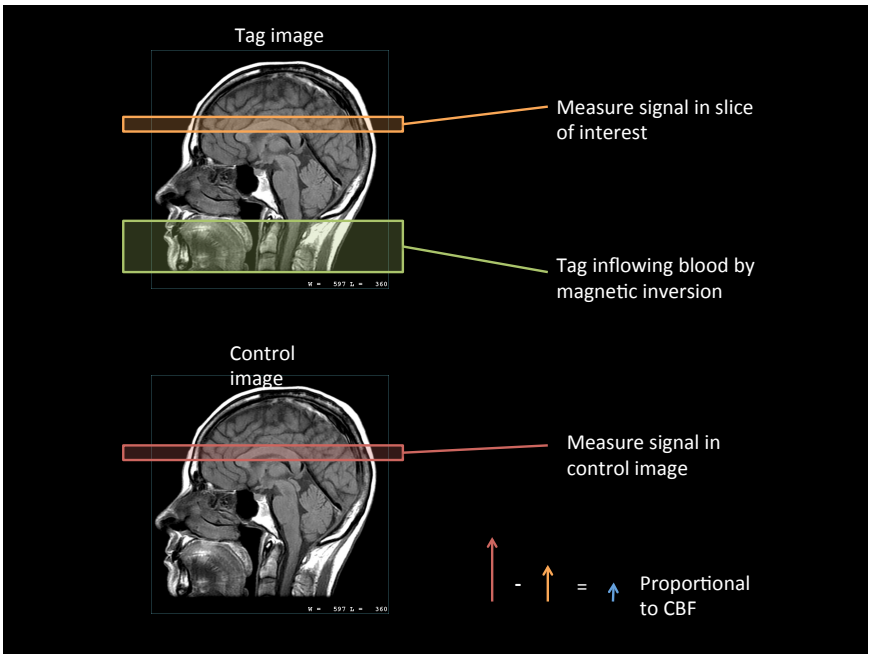


Figure 3.2 Principles of ASL. The difference in magnetization between control and tag conditions is proportional to regional cerebral blood flow.

ASL labelling approaches can be grouped into three types: continuous labelling, pulsed labelling and velocity selective labelling. Velocity selective ASL is not currently in use for clinical studies. Pseudocontinuous ASL (PCASL) results in better labelling efficiency than continuous ASL, and the signal to noise ratio (SNR) is higher than of pulsed ASL (PASL) therefore this is the labelling scheme that is recommended for clinical imaging (135), where the images obtained are often structurally abnormal and pose analysis challenges.

As discussed above, current techniques for measuring changes in brain tissue perfusion require ionizing radiation, or the injection of contrast, exposing already critically unwell patients to the risk of a contrast reaction. This is a particular issue when repeated measures over time are required in a cohort of patients. There is also a risk of ischaemic stroke (136). Therefore, ASL is gaining popularity for cerebral

perfusion imaging as a non invasive method of quantifying blood flow without the need for contrast or exposure to ionizing radiation.

However, apparently normal cerebral perfusion is occasionally a result of excellent collateral blood flow, rather than preserved flow through the circle of Willis. It is currently difficult to determine this through PCASL alone. Therefore, several ASL techniques have been developed that are capable of generating perfusion maps identifying the vessel origins of the observed blood flow. Wong et al (137) described a vessel encoded PCASL (VEPCASL) approach, which combines the high SNR of PCASL with the ability to tag individual arteries at the same time. This enables assessment of the perfusion territories of the main arteries supplying blood to the brain (left and right carotid arteries (LICA and RICA) and left and right vertebral arteries (LVA and RVA) (134, 137). Figure 3.3 demonstrates a perfusion map that may be obtained from a patient, enabling visualization of the different vascular contributions to blood flow.

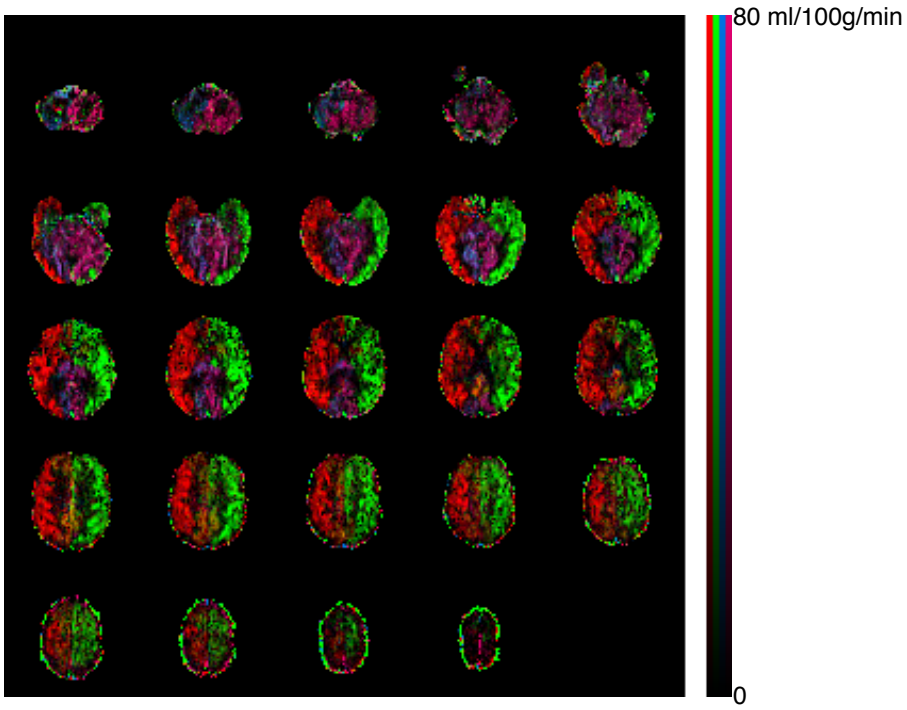


Figure 3.3 Vascular territory maps showing blood flow after aneurysmal subarachnoid haemorrhage, scan from a patient recruited to MRI study red = right internal carotid artery (RICA) green = left internal carotid artery (LICA) blue = right verterbral artery (RVA) pink = left vertebral artery (LVA)

3.5.3 Limitations of MRI

Although MRI represents an exciting imaging modality it has several limitations to acquisition and analysis. As previously mentioned, the scanner is large and expensive, and necessitates transfer of the patient. This can present several challenges when the patient is intubated, fully sedated and ventilated. There is a risk associated with any transfer and this has to be weighed up against the potential benefits from the extra information gained. Patients are often on multiple drug infusions given by pumps that are not MR compatible, necessitating transfer of infusions to longer lines, putting the patient at risk of interruption of vasopressors and other essential drugs. The ventilators are also often not MR compatible, also requiring disconnection of the respiratory circuit and putting the patient at risk of hypoxia.

The signals obtained from functional imaging are often very small, especially when using imaging techniques such as ASL. This is because the signal from blood water is relatively small when compared to that from tissue water. This necessitates the use of high field strength scanners (at least 3 Tesla) and makes this technique very susceptible to motion artifacts. This is not an issue in the acute stages of severe SAH as the patients are sedated and paralysed, but can present major problems in patients with neurocognitive impairment at their follow up scan, if they are unable to follow instructions to lie still. The perfusion maps generated by the ASL analysis tool are susceptible to confounding by either abnormally fast or abnormally slow blood flow in the Circle of Willis. This is likely to occur in this cohort of patients, with disordered blood flow secondary to aneurysmal rupture therefore data has to be carefully inspected and interpreted with caution.

3.6 Neurocognitive testing

Neurocognitive assessment forms an important part of patient follow up, as it is often neurocognitive deficits that cause patients the most distress in the long term. However, outcomes are extremely variable after severe SAH due to the serious nature of the disease, therefore many patients are not suitable for extensive neurocognitive testing as they will be unable to perform many of the tasks.

The Oxford Cognitive Screen (OCS) (http://www.psy.ox.ac.uk/research/oxford-cognitve-neuropsychology-centre/oxford-cognitive-screening/tests) is a short and efficient cognitive screening tool that enables assessment of patients despite of the presence of aphasia or neglect. This makes it ideally suited for use in this patient cohort. It can be performed at the bedside and offers a snapshot of the patient's

performance across the following domains: attention (visuospatial & task switching), memory (orientation, recall, recognition and episodic), language (picture pointing, reading and picture naming), praxis (imitation and sequencing) and number (writing and calculation).

3.7 Conclusion

Neurological deterioration after SAH accounts for a large degree of the disease burden, with events occurring during the EBI phase paving the way for the development of DCI. It is almost impossible to predict which patients will develop DCI at presentation using current methods, and the detection of ischaemia is even more difficult in the more severe cases, where the patient is usually comatose and clinical examination is very limited. Intervention during the EBI phase may be key to protecting against subsequent development of DCI, and there is a need for the development of non-invasive tools to enable close monitoring of cerebral function. EEG is sensitive to changes in neuronal firing as a surrogate marker for tissue health, but raw EEG is time consuming to analyse. Calculation of qEEG parameters is more practicable in a clinical setting. Measuring the EEG response to an intervention such as a drug infusion may enable more rapid identification of patients that have severe disruption to neurovascular signalling and therefore may be more likely to develop ischaemia. Other non-invasive methods of measuring cerebral blood flow includes ASL MRI, which enables quantification of regional tissue perfusion changes. This may yield useful information regarding the acute blood flow changes that occur after aneurysm rupture, and be of use in identification of tissue at risk

3.8 Aims of the work presented in this thesis

The work presented in this thesis aims to use a combination of current knowledge regarding nitric oxide signalling after brain injury, and qEEG changes in response to ischaemia to investigate nitric oxide signalling in the brain after SAH. We intend to use a cerebral nitric oxide donor, sodium nitrite, as a physiological 'probe' to quantify the EEG changes that occur when cerebral nitric oxide levels are increased. We hypothesise that these changes bear relation to the development of subsequent ischaemia and clinical outcome, to provide information about potential therapeutic intervention and provide a method of risk stratification.

We also aim to assess the feasibility of using MRI in this patient population to quantify cerebral blood flow changes. We hypothesise that ASL may aid identification of regions of tissue that are at risk of ischaemia, and provide insights into the possible blood flow alterations underlying EBI. High grade SAH patients have a high blood load and structurally abnormal brains and we aim to evaluate the implications this has for the current analysis methods available.

The work presented in this thesis contributes to furthering the understanding of neurovascular signalling disruption and potential methods for assessing this. There is currently an area of unmet clinical need, where it is difficult to judge and predict which patients subsequently deteriorate. There is also a paucity of therapies available to prevent the development of DCI, and the work presented here aims to further the development of a potential novel therapy based on the NO signalling pathway, as well as suggest possible methods for assessing the mechanisms of action and efficacy of any future interventions.

Chapter 4

EEG may aid prediction of delayed ischaemia after severe subarachnoid haemorrhage when used with a cerebral NO donor

Abstract

We have already discussed that impaired nitric oxide (NO) pathway mechanisms may play a role in the pathogenesis of brain injury after SAH and that quantitative electroencephalography parameters such as reduced alpha/delta frequency ratio have been shown to be sensitive markers of neuronal health. The aim of the study presented in this chapter was to investigate whether the qEEG response to a cerebral NO donor (sodium nitrite) correlated with the subsequent development of delayed cerebral ischaemia (DCI) after severe subarachnoid haemorrhage. Patients underwent one-hour control EEG recording followed by IV sodium nitrite 10 mcg/kg/min and continued EEG recording for one hour. The alpha/delta ratio was measured at 5 separate time points before and during infusion. The alpha/delta ratio increased significantly (p=<0.0000) in response to sodium nitrite in patients that did not develop DCI, whereas there was a significant decrease (p=0.006) in those that subsequently developed DCI. Therefore it appears that giving an NO donor after severe SAH influences markers of neuronal health differently depending on the patient's susceptibility to the later development of DCI. Increasing cerebral NO may activate cellular pathways that prevent apoptosis. However, with a more severe injury, the vasculature may be so damaged as to become unresponsive. We will discuss the potential implications for these results for the development of novel monitoring and potentially treatment tools further in this chapter.

4.1 Introduction

As discussed in Chapter 1, subarachnoid haemorrhage (SAH) is usually caused by rupture of a cerebral aneurysm located in the circle of Willis (2). It disproportionately affects a younger population, with half of patients being under 55 years (1). It is often fatal, which means that the loss of productive life years approaches that of ischaemic stroke or intracerebral haemorrhage (2).

The main complications after SAH include early brain injury (EBI), which describes the immediate injury after SAH and occurs in the first 72 hours, and delayed cerebral ischaemia (DCI), which can occur in about 30% of patients unpredictably 3-14 days post primary haemorrhage (6). Much of the focus of SAH research to date has been to investigate DCI. This is because DCI remains the most important cause of morbidity and mortality in patients that survive initial aneurysm rupture and treatment (12). Traditionally it has been thought that cerebral artery vasoconstriction ('vasospasm') leads to the clinical syndrome of delayed infarction. However, as seen in Chapter 1 there is only a weak temporal relationship between vessel spasm and DCI (14), and patients can develop infarction in a vascular territory unaffected by arterial constriction (15).

Therefore, it is likely that changes occurring at a cellular level much earlier in the disease process account for much of the damage associated with DCI (6, 16). A better understanding and measurement of the processes associated with EBI potentially offers a window of opportunity for intervention to prevent further cerebral damage (8). This is important, as during the first few days following SAH it is currently impossible to predict which patients will subsequently deteriorate.

4.1.1 Mechanisms behind the action of NO donors

Significant molecular alterations occur during the EBI phase, leading to cellular injury and eventual apoptosis (8). Disruption to the nitric oxide (NO) signalling pathway has been proposed to promote secondary injury through mechanisms such as impaired cerebral blood flow, inflammation, microthrombus formation and generation of reactive oxygen species (8, 138). NO depletion plays a key role in these processes (139). Animal models suggest the brain after SAH is relatively NO deplete, secondary to endothelial nitric oxide synthase (eNOS) dysfunction and scavenging by haemoglobin (19).

Exogenous NO donors have been shown to play a protective role by decreasing infarct sizes in animal studies (20, 110, 140), thus giving a scientific foundation to therapeutic repletion of NO. The safety profile of intravenous sodium nitrite has been well established in humans suffering SAH (114), demonstrating low toxicity and minimal effects on systemic blood pressure (113). Furthermore one study in human cardiac-arrest survivors also demonstrated the neuroprotective action of NO donors (97).

It is also possible that in the most severely injured patients the vascular dilatory effects of NO act to vasodilate in areas where neurovascular coupling is relatively intact (i.e. in areas that are less severely injured), effectively diverting blood flow away from the most ischaemic areas, and creating a 'steal' phenomenon. This process may counteract some of the beneficial cellular effects of NO. The response to an NO donor may therefore act as a 'physiological probe of brain function'.

4.1.2 Using EEG to measure neuronal response

Quantitative electroencephalography (qEEG) uses power spectral analysis to obtain measures of the different components of the EEG, sensitively detecting disturbed neuronal activity during the development of ischaemia (141). SAH results in a variety of abnormalities in qEEG parameters all associated with ischaemia. Specifically these are decreases in the alpha/delta ratio (ADR) and a decrease in relative alpha power variability (125, 130, 131, 133). These patterns have been shown to predict subsequent ischaemia in this patient group with high specificity (124).

4.1.3 Aims of the study

The aim of this study was to use sodium nitrite in combination with qEEG as a physiological probe of neuronal function to investigate the role of NO signalling after severe SAH. We hypothesised the qEEG response to a sodium nitrite infusion would consist of restoration of alpha waves and a decrease in the power of slower frequencies such as delta waves, resulting in an increase in the alpha/delta ratio. In those with greater EBI and therefore worse neurovascular signalling disruption and higher levels of free radicals, there may be a stronger qEEG response to exogenous NO. Alternatively the ability to respond to a NO donor may be overwhelmed or even compounded by a 'steal' phenomenon, potentially causing a worsening of neuronal health. The balance of these processes potentially relates to the severity of EBI.

Therefore, the combined use of EEG and a NO donor may show usefulness as a tool to help predict which patients may go on to develop DCI and experience poor outcomes.

4.2 Materials and Methods

4.2.1 Subjects

14 patients (mean age 52.8 range 41-69; 11 female) with spontaneous SAH successfully treated with endovascular coiling were recruited over a total study period of 13 months. All patients admitted to the NICU at the John Radcliffe Hospital were eligible for inclusion in the study.

Three patients died, two from complications following severe delayed cerebral ischaemia and one from cardiovascular instability. Support was withdrawn only after CT diagnosis of widespread infarction. There was no rebleeding. Three patients developed sepsis secondary to chest infection, which were treated with intravenous antibiotics.

Patients aged 18-80 years admitted to the Neurosciences Intensive Care Unit (NICU) at the John Radcliffe Hospital, Oxford after having suffered severe aneurysmal SAH (WFNS grade 3, 4 or 5 at time of presentation) were eligible for inclusion in the study. There were no specific selection criteria apart from grade of SAH, and the absence of any exclusion criteria (see below). No patient showed angiographic evidence of DCI or cerebral arterial vasoconstriction as seen at endovascular coiling performed prior to the study.

Written informed consent was obtained from the next of kin of all participants, and from participants if they regained capacity to consent. The study was approved by the South Central – Oxford C NHS Health Research Authority Ethics Committee 12/SC/0366. Exclusion criteria included contraindications to sodium nitrite,

specifically severe cardiovascular compromise and pre-existing methaemoglobinaemia. Next of kin provided information regarding smoking, medication, hypertension and family history.

All patients underwent standard clinical care that was not influenced by inclusion in this study. This included therapeutic sedation with a combination of propofol, fentanyl, and midazolam with neuromuscular blockade using atracurium administered as required. Computed Tomography (CT) scans were performed in the event of lack of wakening in sedated patients or worsening of neurological signs in awake patients, as per unit policy. Patients that did not demonstrate neurological deterioration did not undergo scanning in the acute period, however they did later receive follow up MRI imaging at 6 months as per local protocol which confirmed lack of new infarction.

DCI was diagnosed based upon consensus guidelines (142). In those patients who remained intubated and sedated this was by CT. Two patients (numbers 2 and 4) had treatment withdrawn and subsequently died after CT evidence of widespread infarction secondary to DCI. The investigators responsible for this study were not responsible for the clinical care of these patients.

Treatment of suspected cerebral arterial vasoconstriction and/or DCI (‘vasospasm’) was via a standardized protocol involving hypertension (maintenance of mean arterial pressure >85mmHg), maintenance of euvolaemia and maintenance of a haemoglobin >8g/dL.

4.2.2 Study design

Following definitive endovascular aneurysm treatment, each patient underwent a two hour period of continuous EEG monitoring (Porti 7 system, Twente Medical Systems International) on one occasion as soon as was practically possible after endovascular securing of the aneurysm.

An infusion of sodium nitrite at 10 mcg/kg/min was commenced at the start of the second hour of recording, and continued for one hour. The dosing schedule was based upon previous studies using sodium nitrite (143, 144), and was decided upon to reach a compromise between ensuring adequate delivery of cerebral NO and minimisation of any cardiovascular effects. Sedative drug levels, muscle relaxants and vasopressors were documented and changes in infusion rates were minimised for the duration of the recording.

We used a simplified EEG montage (130) that aimed for compromise between stable maintenance of recording and full coverage of all vascular territories. Consequently, 7-13 unipolar EEG electrodes (depending on the presence of external ventricular drains and intracranial pressure (ICP) monitors) at the following positions defined according to the international 10-20 system: Cz, Fz, Pz, Fp1, Fp2, F3, F4, P3, P4, T3, T4, O1, O2. EEG data were digitized at a sampling rate of 2048 Hz, with a high pass filter of 0.5 Hz and a low pass filter of 30 Hz.

The patients also underwent simultaneous transcranial Doppler (TCD) monitoring. Insonation of the MCA M1 segment was performed unilaterally on the side with the

best window using colour-coded duplex ultrasound (EZ-Dop, DWL; 2Mz probe). One patient (10) did not have an adequate TCD window therefore this was not recorded.

The patient's end tidal carbon dioxide ($PETCO_2$), end-tidal O_2, arterial blood pressure (ABP) and SpO_2 were recorded continuously and collected on a Power-1401 data acquisition interface (Cambridge Electronic Design). Twelve patients had an intracranial pressure monitor inserted, but due to technical issues we were unable to record the ICP waveform for two patients (1 and 13). Arterial CO_2 values were collected once during the duration of the recording as part of routine clinical care.

Each surviving patient was followed up at three to six months post-rupture. Telephone follow up was performed for patients who were unable to attend hospital due to their clinical status. Our primary outcome measure was the presence or absence of delayed ischaemia. Additionally, long term outcome was assessed by modified Rankin scale at 3 months, via structured standardized questions in person or by telephone. The modified Rankin scale, is a commonly used grading system that measures the degree of disability or dependence in the daily activities of people who have suffered a neurological insult. Good outcome is defined as a score of 0-2, whereas poor outcome is defined as ≥ 3 (145).

4.2.3 Quantitative EEG analysis

Pre-processing was carried out using custom written MATLAB (MathWorks Inc.) code and the EEGLAB v13.4.3b analysis toolbox (146). Datasets were re-referenced to the average of bilateral mastoid reference electrodes and band pass filtered from 0.5 to 15 Hz using a linear finite impulse response (FIR) filter. Each EEG recording was

visually inspected and artifacts were manually removed. Channels showing evidence of excessive amounts of noise were removed from each recording.

Spectral analysis was carried out using FieldTrip (147), a MATLAB software toolbox for EEG analysis. Data was windowed into 30-second segments that overlapped by 50%. Time-frequency analysis was performed using a multi-taper spectral estimation using discrete prolate spheroidal (Slepian) sequences with 14 tapers, and fast Fourier transform algorithm for each electrode channel. Five 60-second epochs were selected randomly from the first (baseline) and last thirty minutes of the recording (during infusion). The epochs were separated by at least 60 seconds to avoid autocorrelation. The corresponding frequency distribution in each epoch was identified, which enabled determination of power values in the following frequency bands: delta 1-4 Hz, alpha 8-12 Hz and total low frequency power 1-15 Hz.

Statistical analysis was carried out using R (R Foundation for Statistical Computing) (148) and the analysis package nlme (R package version 3.1-120) (149). Our data was comprised of repeated measurements of the alpha/delta power ratio, five measures taken before drug infusion (‘baseline’ or 0) and five taken during the infusion (‘nitrite’ or 1) on fourteen patients.

Age, severity of subarachnoid haemorrhage (SAH) as measured by the World Federation of Neurosurgeons (WFNS) grade and drug sedation levels are all potential confounds of these measures. Therefore, our model needed to account for possible effects of these variables on the ADR response to the drug.

In order to use the ADR as a response, it was necessary to obtain normality and homoscedasticity by transforming ADR by taking its square-root. The model reported in the results fitted $\sqrt{ADR}$ as response, distinguished between the baseline measures and measures taken during the nitrite infusion with an indicator variable (0 or 1) and used patient ID (1-14) to identify repeated measures.

A qqnorm (normalised quantile-quantile plot) was used to identify any outliers and these were subsequently eliminated from the model. Goodness of fit was assessed via Shapiro-Wilk normality tests on fixed and random effect residuals, and calculation of R^2 for the model.

4.2.4 Physiological data analysis

Waveform analysis was performed using custom written MATLAB code, enabling calculation of average pre and during infusion values for TCD middle cerebral artery velocity (MCAV) ABP, $PETCO_2$, end-tidal O_2 and ICP.

4.3 Results

4.3.1 Demographics, treatment and outcome

All patients were modified Fisher grade 4 (thick SAH with intra ventricular haemorrhage (IVH)), WFNS grade 3-5 on initial presentation. All patients were intubated and sedated on the NICU. It was necessary to intubate and sedate the WFNS grade 3 patients either due to a subsequent drop in their Glasgow Coma Score (GCS) secondary to seizures or subsequent episodes of vomiting. Detailed information on patient demographic and complications are given in Table 4.1. Levels of sedative drugs/vasopressor levels can be found in Table 4.2.

Table 4.1: Patient characteristics

Patient	Age (yrs)/sex	WFNS grade	Aneurysm location	DCI (y/n)	Day post bleed of DCI diagnosis	Study day post bleed	mRS at 3 months
1	55/F	5	L PComm	N	n/a	2	1
2	53/F	5	A1/A2	Y	10	4	6
3	52/F	4	AComm	N	n/a	2	0
4	48/F	5	MCA	Y	5	2	6
5	50/F	3	A1/A2	Y	16	3	5
6	44/M	5	AComm	N	n/a	4	2
7	58/F	3	R MCA	Y	7	2	6
8	54/F	4	R PComm	N	n/a	2	2
9	56/F	3	R PComm	N	n/a	2	1
10	41/F	3	L PComm	N	n/a	2	1
11	47/F	4	L A2	Y	9	2	2
12	49/F	3	R Vertebral	Y	8	2	4
13	63/M	4	AComm	N	n/a	3	2
14	69/M	5	AComm	Y	5	3	4

WFNS = World Federation of Neurosurgeons; L = left; R = right; F = female; M = male; AComm = anterior communicating artery; MCA = middle cerebral artery; PComm = posterior communicating artery; A1/A2 = A1 and A2 segment of anterior communicating artery; DCI = delayed cerebral ischaemia; mRS = modified Rankin scale

Modified Rankin scale

0 = no symptoms at all; 1 = no significant disability despite symptoms, able to carry out all usual duties and activities; 2 = slight disability, unable to carry out all previous activities, but able to look after own affairs without assistance; 3 = moderate disability, requiring some help, but able to walk without assistance; 4 = moderately severe disability, unable to walk without assistance and unable to attend to own bodily needs without assistance; 5 = severe disability, bedridden, incontinent and requiring constant nursing care and attention; 6 = dead

Table 4.2 - Sedation and vasopressor levels for each patient

Patient	Propofol (mg/hr)		Fentanyl (mcg/kg/hr)		Midazolam (mg/hr)		Atracurium (mg/hr)		Noradrenaline (mcg/kg/min)	
	Pre	During	Pre	During	Pre	During	Pre	During	Pre	During
1	0	0	200	200	10	10	0	0	0.34	0.34
2	0	0	300	300	20	20	50	50	0.38	0.38
3	200	200	150	150	0	0	0	0	0	0
4	0	0	250	250	10	10	0	0	0.16	0.16
5	180	200	0	0	0	0	0	0	0.17	0.20
6	100	100	150	150	0	0	0	0	0.15	0.15
7	100	100	200	200	0	0	0	0	0	0
8	0	0	100	100	0	0	0	0	0.14	0.14
9	220	230	200	250	0	0	0	0	0.25	0.25
10	0	0	150	150	0	0	0	0	0.03	0.03
11	150	150	100	100	0	0	0	0	0.15	0.16
12	180	180	200	200	0	0	0	0	0.20	0.20
13	150	200	200	200	0	0	0	0	0	0
14	200	200	150	150	0	0	0	0	0.13	0.13

mg/hr = milligrams per hour; mcg/kg/hr = micrograms per kilogram per hour; mcg/kg/min = micrograms per kilogram per minute

Data was collected between 2-4 days (mean 2.5) following primary SAH. Due to cardiovascular instability and unknown behaviour of sodium nitrite in this population at that time it was not possible to collect data sooner than day 4 in patients 2 and 6. Seven (50%) of the study patients developed DCI as defined by the presence of infarction on CT within 6 weeks after SAH that was not present on the CT scan between 24 and 48 hours after aneurysm occlusion, and that was not attributable to other causes such as surgical clipping or endovascular treatment (142). This is in

keeping with a higher incidence of DCI reported in previous studies of high-grade (WFNS grade 3-5) SAH patients (150).

All patients were diagnosed with hydrocephalus and were treated with external ventricular drainage immediately on admission to the neurosurgical centre. All patients were treated with endovascular embolization.

4.3.2 qEEG results

Visual inspection of raw EEG data did not reveal any ictal or pre-ictal activity in any of the recruited patients. Datasets were also examined for evidence of burst suppression.

4.3.2.1 Multilevel model

There was a strong correlation between $\sqrt{ADR_{nitrite}}$ and $\sqrt{ADR_{baseline}}$ with a R^2 value of 0.664, so a multilevel model was mandatory in order to account for this.

The effects of subsequent development of DCI, propofol and midazolam on the baseline ADR were taken into account. There was no significant effect of age, WFNS grade or propofol levels on the ADR (age mean effect = 0.972, SEM = 0.1343, p value = 0.8344, propofol mean effect = 0.0003, SEM = 0.0002, p value = 0.1158, WFNS mean effect = -0.012, SEM = 0.028, p value = 0.6856) i.e. there was no evidence of an effect of these variables on the response variable (ADR during nitrite infusion).

The nitrite effect on the patients that subsequently developed DCI was significantly different from the drug effect on the non-DCI patients. This had an R-squared of 0.80, indicating that approximately 80% of the variability was accounted for by this model.

Table 4.3 - Output data from model

	Value	Std.Error	DF	t-value	p-value
(Intercept)	0.309	0.532	121	0.581	0.56
DCI	0.038	0.036	9	1.046	0.32
Drug	0.049	0.005	121	8.902	<0.0001**
Propofol	0.0003	0.0002	121	1.584	0.12
midazolam	0.004	0.004	9	0.992	0.35
log(Age)	-0.029	0.134	9	-0.215	0.83
WFNS.grade	-0.012	0.028	9	-0.418	0.67
DCI:Drug	-0.064	0.007	121	-8.614	<0.0001**

Intercept = the effect on the ADR response in the absence of drug or DCI (ie baseline in the patients who did not develop DCI)
DCI = the effect of development of DCI on the baseline ADR response (ie the effect of development of DCI in the absence of the drug)
Drug = the effect of sodium nitrite on the baseline ADR response
DCI:Drug = interaction term showing the effect of subsequent development of DCI on the ADR during the drug infusion
** = significant at 5% level

In order to satisfy the normality and homoscedasticity requirements for valid fitting of a linear model, a transformation of the original response variable y to a suitable response variable, say z, had to be carried out. Suppose further that, to return to the original variable, the inverse transformation is $y = f(z)$. By Taylor expansion about the mean μ_z it can be shown that, to order n^{-1} where n is the sample size,

$$\mu_y \simeq f(\mu_z), \qquad \sigma_y \simeq \sigma_z f'(\mu_z),$$

where f' is the first derivative of f.

We therefore applied a back transformation to the results obtained above to enable calculation of the absolute ADR values and standard errors resulting from this model. Mean baseline ADR in the patients that did not get DCI was 0.033 (SEM = 0.008). In these patients, sodium nitrite led to an increase in ADR (mean ADR = 0.055, SEM = 0.010, p value = <0.000). In those patients who subsequently developed DCI, mean baseline ADR was 0.056, SEM = 0.010. In these patients sodium nitrite led to a decrease in ADR (mean ADR = 0.0050, SEM = 0.009, p value = 0.006).

To obtain the between group contrasts, the model was 're-levelled' to account for all combinations of DCI and drug. This involved adjusting the baseline (intercept) for the absence (0) or presence (1) of nitrite, and the absence (0) or presence (1) of subsequent DCI.

Table 4.4 – between group contrasts

Group	DCI0: Baseline	DCI 0: Nitrite	DCI 1: Baseline	DCI 1: Nitrite
DCI 0:Baseline		<0.0001**	0.072	0.186
DCI 0:Nitrite	<0.0001**		0.918	0.703
DCI 1:Baseline	0.072	0.918		0.006**
DCI 1:Nitrite	0.186	0.703	0.006**	

DCI 0 = no DCI, DCI 1 = DCI,
Values are p values for each contrast. ** = significant at 5% level

There was no difference between the mean baseline ADR in the non-DCI group (0.033) compared to the DCI group (0.056), (p value = 0.0718). There was also no

significant difference in the ADR during the drug infusion between the two groups (p value = 0.7026).

These results are illustrated in Figure 4.1 below.

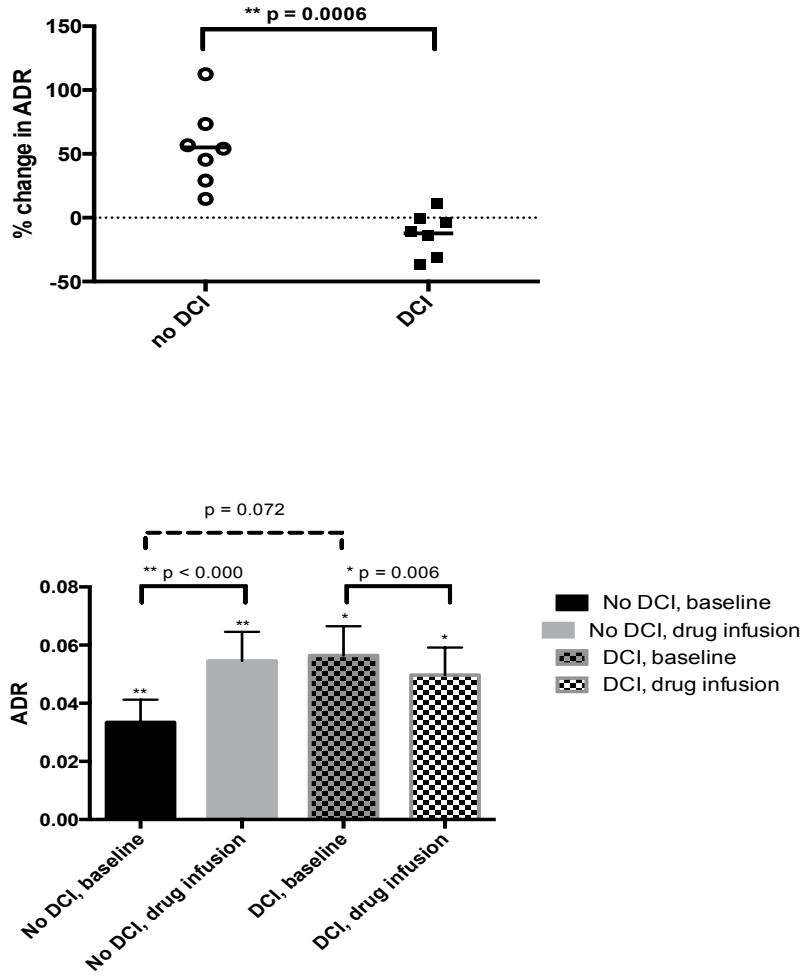


Figure 4.1 Top graph shows a scatter plot showing the percentage change in ADR for each patient, grouped by the presence or absence of subsequent DCI. The mean for each group is represented by the horizontal bar. It can be seen that there is greater variability in the response to the drug in the group that did not develop DCI, suggesting that there may be a spectrum of neuronal damage that is unmasked by the drug, raising the possibility that there may be differing degrees of neuronal disruption after severe SAH.

Bottom graph demonstrates the mean ADR values for each condition. It can be seen that there is a significant increase in the ADR in the patients that did not develop DCI, and a significant decrease in the ADR of the patients that did develop DCI. The difference in the mean baseline ADRs of the no DCI vs. DCI groups was not significant, although there was a trend to a higher baseline ADR in the DCI group. Error bars represent the SEM.

A Shapiro-Wilk normality test of the fixed and random effects residuals resulted in p values of 0.5569 and 0.9765 respectively. A qqnorm plot of the model residuals and standardised residuals vs. fitted residuals for the model are shown in Figure 4.2.

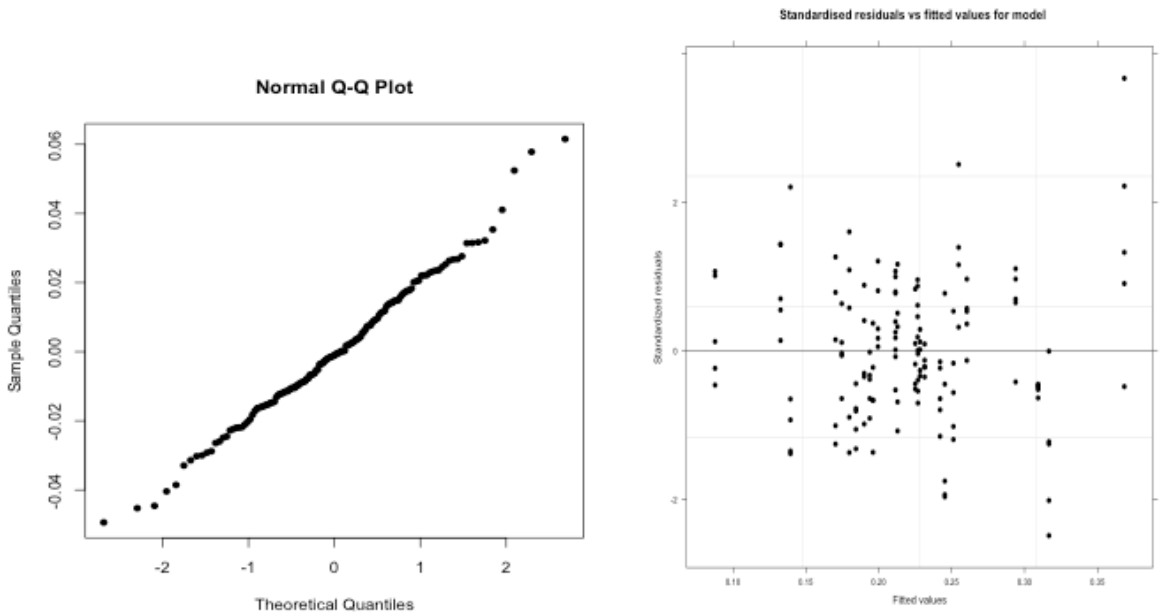


Figure 4.2 Diagnostic plot to show the normality of the residuals in the linear mixed-effects model (left panel) and plot to show that variation in residuals for the fitted model are unbiased and homoscedastic i.e. the model is a good fit for the data (right panel).

4.3.2.2 Bayesian model

As can be seen from the tables above, there is a trend towards a higher baseline ADR in the patients that developed DCI versus those that did not (p = 0.072). This raises the possibility that the baseline ADR was predictive of the ADR response to the drug,

and that if the starting ADR was taken into account as an explanatory variable, this could possibly reduce or negate the drug effect seen and account for the observed results. Therefore, we remodelled the data to account for this.

In order to fit the baseline ADR as an explanatory random variable, it was necessary to use Bayesian model fitting. This is because the baseline ADR is a random variable in itself, with a highly significant effect on the ADR response variable as shown above. The linear regression multilevel modelling used above does not give an assessment of the magnitude of the effect whereas the Bayesian model does.

Therefore using the "JAGS" library in R, a full model with all covariates was fitted, with 30,000 MCMC iterations of which the first 10,000 were used as a burn-in and discarded in the summary statistics.

The model is:

$$\sqrt{ADR_{nitrite}} = b_0 + b_1\sqrt{ADR_{baseline}} + b_2 DCI + b_3 Propofol + b_4 midazolam + b_5 \log(Age) + b_6 WFNS.grade + b_7 DCI{:}\sqrt{ADR_{baseline}}$$

	estimate	sd.err	2.5%	25%	50%	75%	97.5%
b0	0.043	0.179	-0.305	-0.077	0.043	0.162	0.396
b1	1.221	0.149	0.933	1.129	1.220	1.315	1.502
b2	0.029	0.055	-0.077	-0.009	0.028	0.065	0.137
b3	0.000	0.000	0.000	0.000	0.000	0.000	0.000
b4	0.001	0.001	-0.001	0.000	0.001	0.002	0.004
b5	-0.015	0.047	-0.109	-0.047	-0.016	0.016	0.077
b6	0.005	0.008	-0.011	-0.001	0.005	0.010	0.020
b7	-0.476	0.241	-0.959	-0.637	-0.476	-0.309	-0.017
sigma	0.029	0.005	0.019	0.026	0.030	0.033	0.040
sigma0	0.026	0.007	0.016	0.022	0.025	0.030	0.040

`sigma` is the estimated standard error of the underlying normal distribution of the response; `sigma0` is the estimated standard error of $\sqrt{ADR_{baseline}}$.

Dropping the terms where the 95% credible interval contains zero we reduced the model to:

$$\sqrt{ADR_{nitrite}} = b_0 + b_1\sqrt{ADR_{baseline}} + b_2 DCI + b_7 DCI{:}\sqrt{ADR_{baseline}}$$

	estimate	sd.err	2.5%	25%	50%	75%	97.5%
b0	0.004	0.026	-0.042	-0.013	0.004	0.020	0.052
b1	1.273	0.137	1.026	1.190	1.279	1.362	1.514
b2	0.050	0.041	-0.029	0.023	0.050	0.078	0.132
b7	-0.558	0.184	-0.927	-0.680	-0.556	-0.435	-0.195
sigma	0.029	0.005	0.018	0.025	0.029	0.032	0.039
sigma0	0.026	0.007	0.016	0.022	0.025	0.029	0.039

The `b1` coefficient shows that nitrite ADR depends significantly on baseline ADR, which is to be expected. However, the DCI: $\sqrt{ADR_{baseline}}$ interaction term gives the correction to the dependence on baseline-ADR and has the effect of modifying the coefficient from 1.273 down to $1.273 - 0.558 = 0.715$. This is a significant ($p < 0.0001$) reduction to 56% of its previous value and shows the effect of DCI on the nitrite ADR score.

In terms of baseline - nitrite difference, for no DCI:

$$\sqrt{ADR_{nitrite}} - \sqrt{ADR_{baseline}} = 0.004 + 0.273\sqrt{ADR_{baseline}}$$

whilst for the patients that subsequently developed DCI:

$$\begin{aligned}\sqrt{ADR_{nitrite}} - \sqrt{ADR_{baseline}} &= 0.004 + 0.050 + (0.273 - 0.558)\sqrt{ADR_{baseline}} \\ &= 0.054 - 0.285\sqrt{ADR_{baseline}}\end{aligned}$$

Therefore this model shows that in the no DCI group, the baseline ADR increases by $0.273\sqrt{ADR_{baseline}}$ in response to sodium nitrite, whereas in the DCI group the baseline ADR decreases by $0.054 - 0.285\sqrt{ADR_{baseline}}$ in response to sodium nitrite, confirming the results of the multilevel model.

Figure 4.3 shows topographical representations of the change in ADR in response to the infusion of sodium nitrite in each patient.

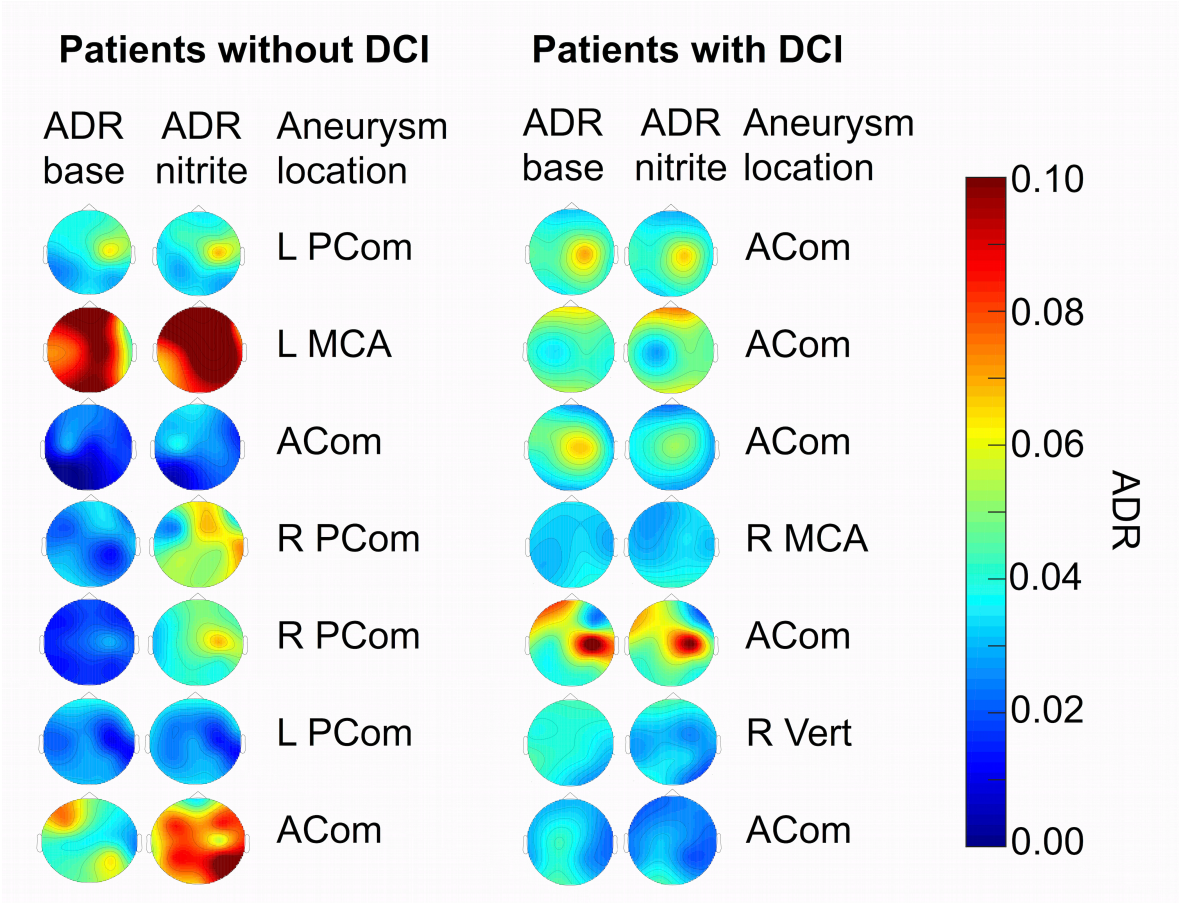


Figure 4.3 Topographical representation of power changes before and during infusion of sodium nitrite in each patient. Location of aneurysm is shown beside each patient. Abbreviations: L, left; R, right; PCom, posterior communicating artery; MCA, middle cerebral artery; ACom, anterior communicating artery; Vert, vertebral artery; ADR, alpha/delta ratio

Spectrograms showing power analysis of the entire recording for two patients are shown in Figure 4.4. These demonstrate how the power spectrum changes over the course of the recording. Figure 4.5 demonstrates the percentage change from baseline ADR over time for the two groups.

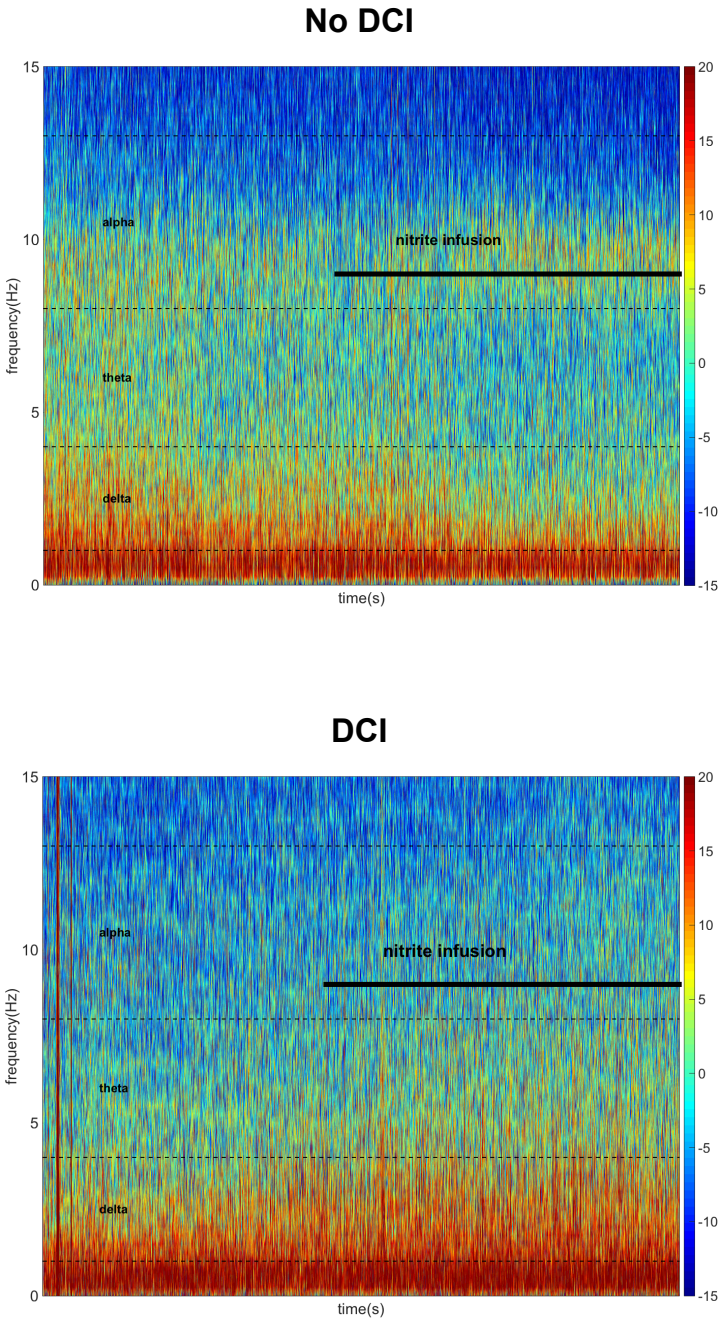


Figure 4.4 Top panel shows single channel spectrogram from a patient who did not subsequently develop DCI. Bottom panel shows single channel spectrogram from a patient who developed DCI

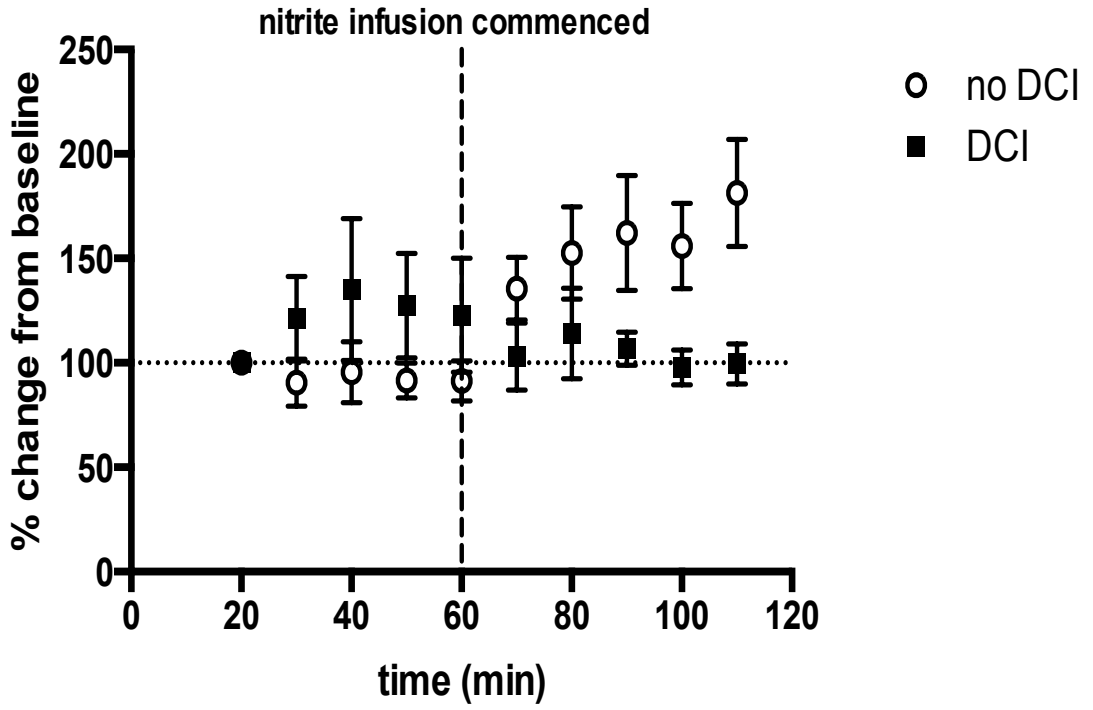


Figure 4.5 Percentage change from baseline ADR over time, calculated by dividing the ADR at each timepoint by the baseline for the patients who subsequently did not develop DCI compared to those who did develop DCI. Hollow circles represent the patients that did not develop DCI and filled squares represent the patients that did develop DCI. Error bars represent the standard error of the mean. A dashed line represents the start of the sodium nitrite infusion.

The ADR increases after commencement of the infusion in the no DCI group, and does not change in the DCI group. The baseline over the initial 60 minutes remains stable for both groups. There is greater variability in the response to nitrite in the no DCI group, suggesting a spectrum in the response to increasing cerebral NO levels.

4.3.3 Physiological data

Arterial blood pressure data was collected on all 14 patients. There was a significant decrease ($p = 0.026$, paired student's t test) in the MAP of the patients in response to sodium nitrite, from a mean MAP of 87 mmHg to 84 mmHg.

PETCO2 was collected on 13 patients. Two patients did not have an intracranial pressure monitor inserted, reflecting current differences in clinical practice in our unit, and technical issues prevented ICP recording from the other two patients. There were no significant changes in TCD MCAV, ICP, or PETCO2 values as a result of sodium nitrite infusion (see Table 4.3). The variability in the physiological measurements did not appear to be greatly affected during the sodium nitrite infusion, as the standard deviation remained relatively constant.

Table 4.5 - Mean physiological values pre vs. during sodium nitrite infusion

Patient	MAP (mm Hg) mean (sd) Pre	During p = 0.02	CO_2 (kPa) mean (sd) Pre	During p = 0.98	Arterial CO_2 values (kPa)	MCAV TCD (cm/s) mean (sd) Pre	During p = 0.96	ICP (mm Hg) mean (sd) Pre	During p = 0.53
1	73 (3)	67 (1)	4.2 (0.4)	4.8 (0.1)	5.86	62 (10)	85 (3)	n/r	n/r
2	80 (3)	77 (2)	3.8 (0.1)	3.7 (0.1)	5.59	51 (6)	46 (2)	n/r	n/r
3	75 (2)	73 (1)	3.9 (0.1)	4.0 (0.0)	5.20	91 (2)	88 (2)	3.3 (0.7)	2.7 (0.7)
4	75 (2)	73 (2)	3.8 (0.1)	3.95 (0.0)	4.87	91 (2)	89 (2)	3.3 (0.7)	2.8 (0.8)
5	93 (3)	91 (6)	4.7 (0.0)	4.7 (0.3)	5.57	50 (3)	52 (6)	7.5 (1.6)	6.4 (3.0)
6	81 (16)	86 (15)	4.9 (0.4)	4.8 (0.2)	5.35	55 (6)	69 (6)	6.6 (1.5)	6.9 (1.0)
7	86 (11)	90 (5)	n/r	n/r	4.72	47 (2)	44 (3)	n/r	n/r
8	78 (1)	75 (2)	5.8 (0.1)	5.7 (0.2)	5.06	108 (3)	103 (3)	20.4 (0.0)	20.5 (0.0)
9	90 (1)	83 (3)	3.9 (0.1)	3.9 (0.1)	4.12	35 (2)	36 (5)	11.4 (0.0)	11.2 (0.0)
10	105 (5)	94 (5)	4.4 (0.5)	4.3 (0.5)	5.46	n/r	n/r	12.5 (2.6)	11.5 (1.9)
11	88 (4)	82 (5)	4.1 (8.5)	4.8 (5.9)	4.93	93 (13)	97 (8)	8.5 (3.4)	5.9 (3.3)
12	79 (3)	75 (2)	3.4 (0.1)	3.5 (0.2)	4.04	43 (3)	45 (3)	8.9 (2.7)	11.7 (3.0)
13	118 (4)	114 (6)	3.4 (0.1)	3.5 (0.2)	5.66	70 (3)	69 (8)	n/r	n/r
14	92 (8)	92 (4)	4.1 (0.6)	3.6 (0.1)	4.75	50 (14)	36 (16)	7.1 (4.3)	5.9 (1.6)

MAP = mean arterial pressure (millimetres of mercury); CO_2 = end tidal carbon dioxide (kilopascals); MCAV = middle cerebral artery velocity; TCD = transcranial Doppler (centimetres per second); ICP = intracranial pressure (millimetres of mercury); n/r = not recorded p values represent the results of 2 tailed t-tests comparing pre vs. during infusion values

4.3.4 Neurocognitive data

Neurocognitive data in the form of the Oxford Cognitive Screen (OCS) described in Chapter 3 was collected in all patients that attended for follow up. These were patients 1, 3, 5, 6, 8, 9, 10 and 11. Only two patients that developed DCI (5 and 11) were able to attend for follow up. This was due to the death of three patients in this group, and poor neurological condition making transfer to Oxford unsuitable for the remaining two patients.

In the DCI group, patient 5 was too profoundly neurologically impaired to perform the OCS. Patient 11 could only perform a limited part of the test due to not having English as their first language, but subjectively their next of kin reported some persisting memory problems.

In the non DCI group, patients 1, 3, 6, 9 and 10 scored full marks on the OCS. Patient 5 showed a deficit in the attention and memory domains compared to age and sex matched healthy controls. Despite this patient 5 scored highly on all other domains, showing evidence of only mild neurocognitive impairment. This corroborated the results from the modified Rankin scale and EEG.

During subjective assessment, all patients reported persisting feelings of fatigue during the follow up interview.

4.4 Discussion

4.4.1 Main findings

This aim of this study was to investigate the importance of the NO signalling pathway in the pathogenesis of early brain injury after SAH. Patients that went on to develop DCI and have a poor outcome showed a significant alpha/delta ratio (ADR) decrease to a 1-hour infusion of sodium nitrite, whereas patients that did not develop DCI showed a significant increase in the ADR. A decrease in ADR is a qEEG measure that has been associated with the subsequent development of cerebral ischaemia after SAH. These data implicate NO pathway disruption as a potential mechanism for the development of neuronal dysfunction that may lead on to cerebral ischaemia in SAH.

It is important to note that the two groups of patients were indistinguishable at presentation in terms of clinical severity (WFNS score), Fisher grade or baseline qEEG parameters. Therefore the change in qEEG response to sodium nitrite infusion signifies that increasing cerebral NO unmasks cerebral neuronal and metabolic dysfunction that is otherwise not detectable by current clinical methods.

The lack of significant change in TCD recordings or ICP suggests that these changes were not due to changes in global cerebral blood flow, but rather were indicative of changes occurring at the neuronal level. This is in keeping with our theory that cerebral NO donors exert their principal mechanism of neuroprotective action on the microvasculature and metabolic cellular signalling pathways, with the effects on the macrovasculature being less important. There was a small drop in mean arterial pressure (MAP) in response to the drug from 87 to 84 mmHg, although statistically significant is very unlikely to be clinically relevant.

The lack of change in the TCD in response to the nitrite infusion in particular was as expected, as nitrite is only reduced to NO under conditions of acidosis or hypoxia (secondary to hypoxic nitrite reduction) (109) therefore we would only expect the vascular vasodilatory actions to occur locally and not have measureable effects on the macrovasculature. The patients that developed DCI were not followed up with repeat TCD or other measurements outside routine clinical care, but this would be an interesting addition to any future studies.

4.4.2 Explanation of results

We propose that these results suggest mechanistic differences in the way the brain responds to increasing cerebral NO, depending on the severity of the injury. The importance of the EBI phase as a key window of therapeutic opportunity must also be emphasised. The development of DCI was associated with poor outcome in this study, but this cannot be predicted in the first few days post injury with clinical measures alone.

Previous studies using continuous EEG in SAH showed that reduced ADR was strongly associated with the development of DCI in high-grade SAH, compared to a small increase for the patients without DCI (131). Other studies in moderate and good-grade SAH have shown that a persistent decrease in alpha power from baseline is a consistent marker for DCI (133). In ischemic stroke it has been demonstrated that slow frequency EEG activity increases as cerebral perfusion falls and the tissues become more ischaemic (124). There is also loss of higher frequencies such as alpha, resulting in a reduced ADR (151).

Astrocyte dysfunction and changes in capillary permeability are extremely important in the development of secondary brain injury (40), with the NO signalling pathway playing a pivotal role in this. One explanation for the decrease in the poor outcome group is that there may be greater disruption to the neurovascular signalling cascade that ensures cerebral blood flow is closely matched to neuronal demand (152).

Increased cerebral NO may selectively vasodilate in areas where there is less tissue damage, diverting blood away from the more ischaemic areas in the more severely injured patients. Emerging evidence suggests that there are changes to capillary morphology and function after SAH. It has been recently shown that the availability of oxygen in the brain is not only dependent on cerebral blood flow but also on the microscopic distribution of the blood (139). If severe capillary dysfunction is present, giving an NO donor is likely to have little effect, as vasodilatation increases shunting through the capillary bed, and may actually cause a 'steal' phenomenon. This also implies loss of local autoregulation, which would increase the risk of subsequent infarction. Delivering NO to areas of the brain with increased levels of free radicals may encourage the production of neurotoxic peroxynitrite, further contributing to cell damage (153).

Another explanation for these results is that those who developed DCI had a more severe initial brain injury (currently undetectable with the methods available), which resulted in greater cerebral NO depletion, as demonstrated by several animal models of SAH (154). It is possible that NO depletion was greater in those who developed DCI and a longer duration of infusion would have demonstrated a move towards a less ischaemic picture (as measured by qEEG). The patients who did not develop DCI

were not as NO deplete and therefore showed the expected improvement in qEEG parameters during the course of the study. The neurocognitive data collected appears to corroborate the EEG changes seen, although a significant floor and ceiling effect of the OCS was demonstrated.

4.4.3 Limitations of the study

Although the recruited participants are representative of patients admitted with SAH, this study has some limitations. Firstly, the number of patients recruited was relatively small. However, previous studies using qEEG as a potential marker of cerebral ischaemia after SAH have shown significant changes with smaller patient numbers (125, 132), therefore we were confident that the changes seen were consistent.

As a study such as this has not been performed before, a formal power calculation was not possible. An important aim of the study was to help inform the statistical design of future studies further investigating EEG patterns in response to nitrite in patients suffering severe SAH. We anticipated a powerful effect on EEG power based on a previous resting EEG study which showed a 24% median decrease in ADR in 9 patients that developed DCI (131). Animal studies have demonstrated that sodium nitrite appears to have a powerful effect on the subsequent development of ischaemia (116). We therefore expected 10-14 patients to demonstrate enough change to allow an effect of the drug to be detected, and decided to aim recruit to the higher number if possible.

The baseline ADR was stable, making it unlikely that natural variability in the EEG power would account for the changes seen over the timecourse of the recording.

However, in acknowledgement of the small numbers of participants, future studies will aim to recruit larger numbers of patients. The investigators were also not blinded, which introduces the risk of potential bias, which we acknowledge, and will eliminate from any further studies.

The study participants only underwent a relatively short duration of EEG monitoring and the sodium nitrite infusion was only given for an hour. We acknowledge that given the pharmacokinetic and pharmacodynamics properties of sodium nitrite it is likely that steady state was not achieved in all patients. Future studies should aim to continue the infusion for a longer period of time, as well as incorporating a study of the EEG changes during the offset of sodium nitrite. We would also recommend that future studies included investigation of the role of NO signalling in those patients with a less severe degree of EBI by including WFNS grade 1 and 2 SAH.

Using a drug to probe brain function via EEG enabled the duration of recording to be considerably shorter than those used in previous studies which recorded continuously for an average of 5 days (range 1-60 days) (155) before consistent changes were observed. This increases the practicability and usefulness of using qEEG as a marker to enable targeted therapy and prognostication. Also, unlike previous studies on SAH using qEEG, this study was restricted to patients with high-grade SAH only.

By comparing pre-infusion to post infusion values in the same patient each patient acted as their own control, minimising the effects of metabolic alterations, ICP changes or effects of sedation. Sedation levels and physiological parameters were recorded and did not change significantly over the course of the recording for each

patient. The level of sedation did not significantly affect the results. However, we acknowledge that sedation will have affected the EEG pattern, and this should be accepted as a limitation of the study, although it is difficult to avoid when studying this cohort of patients.

Due to the limited number of electrodes that it was practicable to use it is difficult to find a consistent pattern of EEG changes related to the aneurysm location. However, fewer EEG electrodes increase the practicability of using this method in an ICU setting.

4.5 Conclusions

In conclusion, we have shown in this pilot study that a one-hour infusion of intravenous sodium nitrite can induce qEEG changes over a relatively short recording period. This implicates NO pathway disruption as a method by which neuronal function is impaired after SAH. The differential EEG response to an NO donor emphasises the importance of early brain injury being a key window of therapeutic opportunity. Patients that did not subsequently develop DCI showed qEEG changes consistent with improved neuronal health, whereas patients that did develop DCI showed changes consistent with the potential development of ischaemia. Therefore this method may represent a potentially useful tool for prognostication, and may have implications for large-scale clinical trials involving sodium nitrite infusions after SAH. The beneficial effects of NO donors may be restricted to a particular subset of patients, or higher doses are required in more severe disease. This represents an avenue for future research, with the potential to develop a patient specific targeted therapy for this often debilitating and life-changing condition.

Chapter 5

Using arterial spin labelling to estimate cerebral blood flow after severe subarachnoid haemorrhage

Abstract

This chapter will focus on the MRI methods that have been trialled to investigate cerebral blood flow changes after subarachnoid haemorrhage. Currently there are no clinically practical methods for repeated quantification of tissue perfusion changes that occur in the acute stages of severe SAH. There is a need for non-invasive yet robust measures of regional cerebral blood flow to enable patients at risk of infarction to be identified, and targeted therapies to be initiated. We hypothesise that analysis of the pattern of cerebral blood flow after SAH and how it changes using VEPCASL MRI may provide insights into the potential mechanisms behind neurovascular bundle disruption and subsequent cell death. This may enable risk stratification and the initiation of specific therapies. However, obtaining MRI images in this patient group is challenging, from both a data acquisition and analysis perspective. These issues and the methods used to overcome them will also be explored in this chapter. We conclude that it is possible to measure vessel specific blood flow in these patients with reasonable accuracy, and that there appears to be elevated blood flow in the acute stage, which warrants further investigation.

5.1 Introduction

Aneurysmal subarachnoid haemorrhage results in disruption to CBF as a result of rupture of a berry aneurysm. An increase in intracranial pressure (ICP) secondary to this further compromises CBF. Compensatory mechanisms such as increasing mean arterial pressure (MAP) aim to restore CBF to normal levels, however the changes in tissue blood flow after aneurysmal SAH are currently poorly understood. Events occurring in the early phase of the disease process may set the scene for the later development of delayed cerebral ischaemia (DCI), which as discussed previously is a leading cause of morbidity and mortality in those that survive SAH (156).

It is therefore important to develop a tool that enables accurate quantification of the cerebral blood flow changes that occur acutely after aneurysm rupture. This may enable new neuroprotective therapies to be trialled and instigated, in an effort to reduce disease burden that results from this condition. Traditionally, neurological deterioration such as the development of aphasia or decreased conscious level has been used to alert physicians to the development of DCI. However, in severe SAH, the patients are often sedated, intubated and ventilated which can often make worsening of the patient's condition extremely difficult to detect by examination alone. It is often too late to instigate protective therapies once an infarct is visible on CT scan.

Tissue cerebral blood flow may be quantified using arterial spin labelling (ASL) MRI. This technique has been described in Chapter 3, and may enable risk stratification and identification of patients that are potentially at risk of developing ischaemia, especially in those in which neurological examination is limited in usefulness. It has a

low signal to noise ratio (SNR) so it is extremely susceptible to motion artifacts. However, severe grade SAH patients are comatose, intubated and paralysed for ventilation, which further adds to the applicability of this method for this patient cohort. Other pitfalls include results being confounded by delayed delivery of blood into the slice of interest secondary to slow flow and other intravascular artifacts such as the presence of arterio-venous malformations (AVMs) (135). However, this method has previously been trailed in good grade (1 and 2) SAH patients, and has shown to give reliable and consistent results (157). In that study, a new technique called vessel encoded pseudo-continuous arterial spin labelling (VEPCASL – see chapter 2) was also performed on one patient. The advantage of this technique is that it not only enables CBF quantification, it also allows calculation of the vessel from which the blood originated.

Determination of the vessel of origin of cerebral tissue perfusion is useful after SAH as it would enable identification of the source of any decreased blood flow, and the presence of any collateral circulation that may partly compensate. It also enables the laterality and arterial source of any blood flow changes to be identified, more accurately enabling potential targets for blood flow restoration techniques such as intra-arterial nimodipine (158). It would also offer further useful insights into the nature of the acute blood flow changes that occur immediately after aneurysmal rupture, potentially allowing for detailed assessment of new treatments.

In this pilot feasibility study, we aimed to use VEPCASL to assess overall and regional CBF in patients in the acute phase post SAH. This group of patients is often unstable from a cardiorespiratory perspective, therefore transfer to and from MRI

presents a major challenge. Our aim was to determine whether this method could be used to gain useful interpretable information from this patient group in a manner that did not compromise patient safety or ongoing clinical care.

We also aimed to serially scan patients to assess the degree of change of the relative contributions of the vessels, to see if this correlated with any change in clinical condition. Specifically, we aimed to determine the blood flow changes that occurred in the vessel where the aneurysm is located, to enable further insights as to the perfusion changes that occur immediately post aneurysm rupture. Failure of autoregulation post SAH is known to occur (159), therefore this may result in increased blood flow and worsening of cerebral oedema, which could result in poorer outcomes. Therefore we hypothesized that it may be possible to use VEPCASL imaging to provide clinically important information that may aid with prognostication and targeting of therapy in this patient group, meeting a current unmet area of clinical need.

5.2 Materials and Methods

5.2.1 Subjects

Six patients with SAH were recruited following securing of the aneurysm by endovascular coiling. Patient demographics and aneurysm location are shown in Table 5.1. All patients were intubated and ventilated. The WFNS grade was the one recorded on admission. Subsequent neurological deterioration resulted in patient 1 being intubated and ventilated. All patients were modified Fisher grade 4 (thick SAH with intraventricular haemorrhage).

Table 5.1: Patient characteristics and demographics

Patient	Age/sex	WFNS grade	Aneurysm location	DCI	mRS at 6 months
1	78F	2	Left P Comm	no	1
2	77F	4	Left P Comm	yes	5
3	62M	4	Left A1/A2	no	2
4	49F	5	L A Comm	no	5
5	70F	5	Basilar tip	no	2
6	76F	4	Right distal carotid	no	4

DCI = delayed cerebral ischaemia; WFNS = World Federation of Neurosurgeons scoring system for subarachnoid haemorrhage; PComm = posterior communicating artery; A1/A2 = junction of the A1 and A2 segments of the anterior cerebral artery; A Comm = Anterior communicating artery; mRS = modified Rankin Scale (see below)
Modified Rankin scale
0 = no symptoms at all; 1 = no significant disability despite symptoms, able to carry out all usual duties and activities; 2 = slight disability, unable to carry out all previous activities, but able to look after own affairs without assistance; 3 = moderate disability, requiring some help, but able to walk without assistance; 4 = moderately severe disability, unable to walk without assistance and unable to attend to own bodily needs without assistance; 5 = severe disability, bedridden, incontinent and requiring constant nursing care and attention; 6 = dead

Patients were recruited following endovascular coiling of their aneurysm. All patients were intubated and ventilated on the neurosciences intensive care unit (NICU), John Radcliffe Hospital, Oxford. Written informed consent was obtained from the next of kin of all participants, and from the study participants if they regained capacity to consent. The study was approved by the South Central – Oxford C NHS Health Research Authority Ethics Committee 12/SC/0366.

Healthy controls with no pre-existing neurovascular diagnoses who were matched for age (+/- 2 years) and sex were also recruited and scanned on one occasion using an identical imaging protocol to provide information regarding regional blood flow in the non-disease state.

Inclusion criteria for patients included World Federation of Neurosurgeons (WFNS) grade 2, 3, 4 or 5 (moderate-severe) SAH, who had uncomplicated endovascular aneurysm treatment, were fully sedated and ventilated at the time of the first scan and had no contraindications to MRI scanning.

5.2.2 Study design

Patients were scanned on up to three occasions in a 3T Siemens Verio MRI scanner (Siemens Healthcare, Erlangen, Germany), once as soon as practically possible following aneurysm treatment, a second occasion 7-10 days later and a follow up scan at approximately 3-6 months post primary haemorrhage. End tidal carbon dioxide ($PETCO_2$), mean arterial pressure (MAP), continuous electrocardiogram (ECG) and oxygen saturations (SpO_2) were also recorded during each scan. Daily clinical assessment of the patient's condition was recorded, and where possible a simplified

neuropsychological evaluation was performed at the follow up appointment (http://www.psy.ox.ac.uk/research/oxford-cognitve-neuropsychology-centre/oxford-cognitive-screening/tests).

The scanner was equipped with a transmit body coil and a 12 –channel receive head coil. Foam inserts were used to minimize head motion and earplugs and headphones were used to limit scanner noise. MAP (+/- 5 mmHg) and $PETCO_2$ (+/- 0.5 kPa) were kept consistent within each acute scanning session via adjustments to vasopressors and ventilation.

Patients were transferred from the NICU with full monitoring, which included invasive arterial blood pressure monitoring (IABP), SpO2, end-tidal CO2 (PetCO2) and ECG (Philips Healthcare, Eindhoven, The Netherlands), accompanied by two anaesthetists trained in critical care transfers and a NICU nurse. All transfers were performed as to the interhospital transfer guideline published by the Association of Anaesthetists of Great Britain and Ireland (AAGBI) (https://www.aagbi.org/sites/default/files/interhospital09.pdf).

All patients continued with standard clinical care that was not influenced by inclusion in this study. CT scans were performed in event of clinical deterioration or worsening clinical signs as part of routine clinical practice. The MRI scanning protocol was approximately 29 minutes in duration and included the following sequences: time-of-flight (TOF) angiography, T1 weighted structural scan, fieldmaps and VEPCASL.

5.3 MRI scanning parameters

5.3.1 Time of Flight Angiography

The location of the labelling plane for the VEPCASL sequence was determined by performing a TOF angiography scan at the base of the brain (repetition time/echo time = 24 ms/ 4.08 ms, number of slices = 22). The total TOF sampling time was 1 min 51 seconds. The resultant image of the vertebral and carotid arteries enabled positioning of the VEPCASL labelling plane approximately halfway between the upper and lower contortions of the vertebral arteries as per Okell et al (134). This ensured that the carotid and vertebral arteries were perpendicular to the labelling plane and therefore optimized the VEPCASL labelling efficiency.

5.3.2 VEPCASL

A multi-inversion time (T1) VEPCASL sequence was used to assess CBF. The sequence consisted of a 1.4 s labelling duration during which arterial blood water in the neck was magnetically labelled, followed by six post-labelling delays (250 ms, every 250 ms up to 1500 ms) and a gradient-echo (GE) echo-planar imaging (EPI) readout (time repetition (TR) =4008 ms, time echo (TE) =14 ms, slice thickness 4.5 mm) to provide whole-brain VEPCASL images. This enabled assessment of the perfusion territories of the main arteries supplying blood to the brain (left and right internal carotid arteries (LICA and RICA) and left and right vertebral arteries (LVA and RVA). Two separate calibration scans that used both the head coil and body coil for signal reception were also acquired. These allowed the VEPCASL data to be corrected for the uneven spatial sensitivity profile of the head coil and facilitated calibration of CBF in absolute units.

5.3.3 T1-weighted structural image

A high-resolution (1.8 x 1.8 x 1.0 mm voxel size) structural image was acquired to enable registration of functional data using FMRIB's Linear Image Registration Tool (FLIRT) and for generation of anatomically derived masks (MPRAGE sequence, TR = 2004 ms, TI = 900 ms, TE = 4.55 ms, flip angle 8°).

5.3.4 Fieldmaps

Fieldmaps were obtained to correct for magnetic field Inhomogeneities (TE 1 = 5.19 ms, TE 2 = 7.65 ms, field of view 240 x 240 mm, voxel size 3 x 3 x 3 mm, 24 slices).

5.4 Analysis

5.4.1 ASL analysis

The VEPCASL raw images were processed as previously described (134) except that a voxelwise tissue calibration was used rather than a global CSF calibration to obtain CBF in absolute units. This was to avoid the confounding effect of blood present in the ventricles of all patients, as described below. Briefly, the pre-processing included motion correction (160) using the calibration image generated using the head coil as a reference.

Pre-existing scripts in MATLAB (Mathworks Inc.) were used to generate vessel territory perfusion maps from the VEPCASL data. The relative CBF of each of the four arteries supplying blood to the circle of Willis was calculated by fitting the general kinetic model (161) including a macrovascular component (162) to each of the multi-TI VEPCASL perfusion images to allow the variation in the contributions of the arteries to be followed over time. FAST (FMRIB's Automated Segmentation

Tool) was used to segment the brain image into different tissue types, to enable CBF quantification in the grey matter using MATLAB code (163).

It was necessary to modify the analysis pipeline specifically for this cohort. Signal calibration is typically performed using cerebrospinal fluid (CSF) as an average reference to enable estimation of the effective equilibrium magnetization of the blood, which is then used to divide the VEPCASL perfusion images (134). However, in this patient cohort the ventricles contain blood, which causes inaccuracies in the calibration. Therefore, a voxelwise based approach to calibration was used to overcome this, which is currently recommended for ASL in clinical practice (135) and this analysis option is now built into the FMRIB Software Library (FSL) ASL analysis tools. This involves using a separately acquired calibration proton density (PD) image to obtain the scaling factor needed to convert the signal intensities of the subtracted ASL images to absolute CBF units on a voxel-by-voxel basis.

We hypothesized that abnormalities in the blood flow velocity in some patients resulted in inaccuracies in placing vessel locations, therefore it was necessary to restrict the amount the analysis was permitted to shift the vessels when searching for a good match to the data. This prevented the analysis switching the vessel locations between scans. The patients were paralysed for the acute scans, so these inaccuracies were not due to patient motion.

To aid creation of grey matter masks fieldmaps were used to improve image registration as the structural scans of some patients were very abnormal, due to the presence of parenchymal haematoma and ventricular blood. Due to the presence of

blood in the ventricles, which had the same contrast as grey matter, it was necessary to mask out the ventricles from the final CBF quantification using a standard MNI152 ventricular mask (164). The standard mask was non linearly registered using FNIRT (FMRIB's non linear image registration tool) (165) to the subject's structural image, followed by linear registration using FLIRT (FMRIB's linear image registration tool) (160) to the ASL calibration image. Areas of haematoma also caused significant dropout in the calibration scans performed, so it was necessary to mask out these areas. The GM mask was then created from this final image.

The steps taken to overcome the analysis challenges posed by acquiring these scans is shown in Figure 5.1 below.

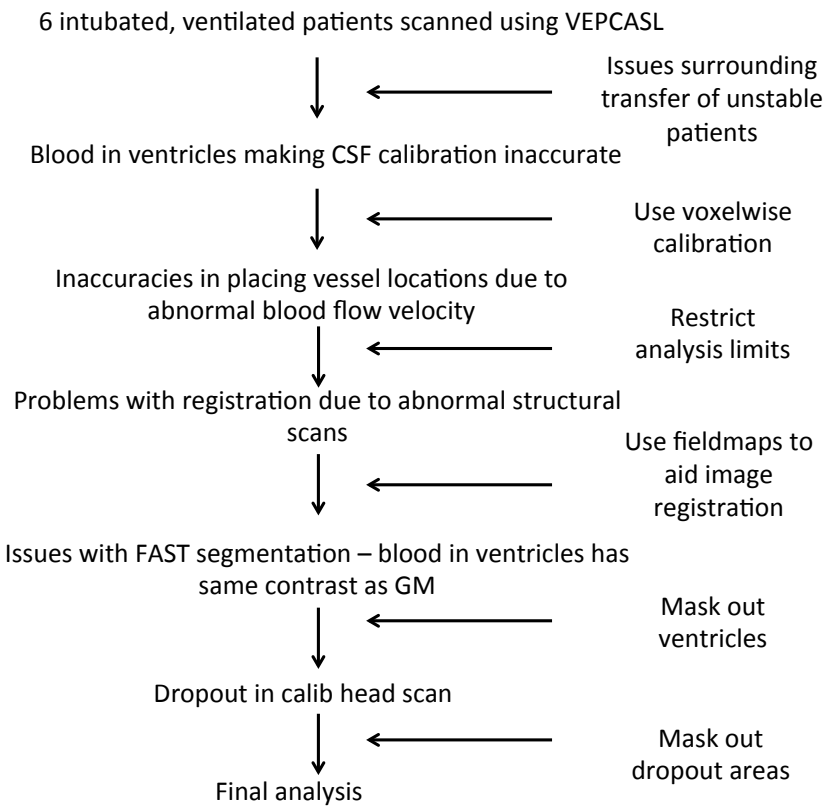


Figure 5.1 Analysis challenges and the methods used to overcome them during analysis of VEPCASL data. Transfer challenges included the presence of multiple drug infusions, cardiorespiratory instability and non MR compatible monitoring equipment. A voxelwise calibration was used to estimate the M0 of blood instead of CSF due to the presence of blood.

5.5 Results

There was some variability in the number of scanning sessions and day on which scanning was performed for each patient. Delays in obtaining scan 1 were secondary to a postponement of endovascular coiling (patient 4) and admission over the weekend so no research scanning time available (patient 5).

Two patients underwent all 3 scans, two patients underwent 2 acute scans and two patients were only scanned on one occasion immediately post endovascular coiling. This was due to patient 3 declining to participate further in the study and clinical deterioration (patient 6). The number and timing of the patient scans is shown in Table 5.2.

Table 5.2 – day post aneurysm rupture that scan was performed

Patient	Scan 1	Scan 2	Scan 3
1	2	7	✖
2	2	10	✖
3	2	✖	✖
4	5	13	6 months
5	5	9	3 months
6	2	✖	✖

5.5.1 Clinical results

All patients had hydrocephalus on admission, treated via external drainage. No patient suffered from rebleeding. No patient died during the course of the study. Patient 2 suffered from delayed cerebral ischaemia (DCI), (as defined by Vergouwen et al (166)), diagnosed via CT scan on day 20. Patient 3 became septic from a chest infection, which was treated with antibiotics.

MAP (+/- 5 mmHg) and $PETCO_2$ (+/- 0.5 kPa) remained consistent within the acute scanning sessions. Four patients were on vasopressors at the acute scan, the type and level of which are shown in table 5.3. Patients remained physiologically stable throughout the transfer process and during the scan. No patient suffered a complication as a direct result of undergoing transfer to MRI, and his or her clinical condition remained stable after the scan.

Table 5.3 – Mean arterial pressure (MAP) and $PETCO_2$ and vasopressor levels during scan 1

Patient	Average MAP (mmHg)	$PETCO_2$	Vasopressor type and level
1	n/r	n/r	Adrenaline 0.3 mcg/kg/min Noradrenaline 0.4 mcg/kg/min
2	78.3	4.8	Noradrenaline 0.14 mcg/kg/min
3	87.5	4.5	Noradrenaline 0.03 mcg/kg/min
4	74.6	4.6	none
5	80.1	4.7	none
6	85.6	4.1	Noradrenaline 0.28 mcg/kg/min

n/r – monitored but not recorded due to patient instability and equipment issues

Three patients (1, 3 and 5) were discharged home following their acute admission. One patient (2) was still an inpatient in a district general hospital at 6 months, having made a very limited neurological recovery. Patient 4 was an inpatient at a specialist neuro-rehabilitation unit at the 6 month follow up mark. Patient 6 required ongoing respiratory support in a specialist centre at 6 months. Neuropsychological testing was

done on patients 1 and 5, as patient 3 declined follow up and patients 2, 4 and 6 were too severely impaired to perform even the most basic neurocognitive test.

Patient 1 scored at or above the 95th centile on all tasks from the Oxford Cognitive Screen, demonstrating no on-going neurocognitive impairment. Patient 5 showed impairment in memory (orientation, recall, recognition and episodic), attention (visuospatial and task switching), number writing and calculation and language (picture naming). Praxis (imitation and sequencing) and language (picture pointing and reading) were unimpaired compared to the control population.

5.5.2 ASL results

The scans obtained were structurally abnormal, due to the high blood load and presence of parenchymal haematoma. There was also a large amount of blood present in the ventricles, demonstrated in Figure 5.2.

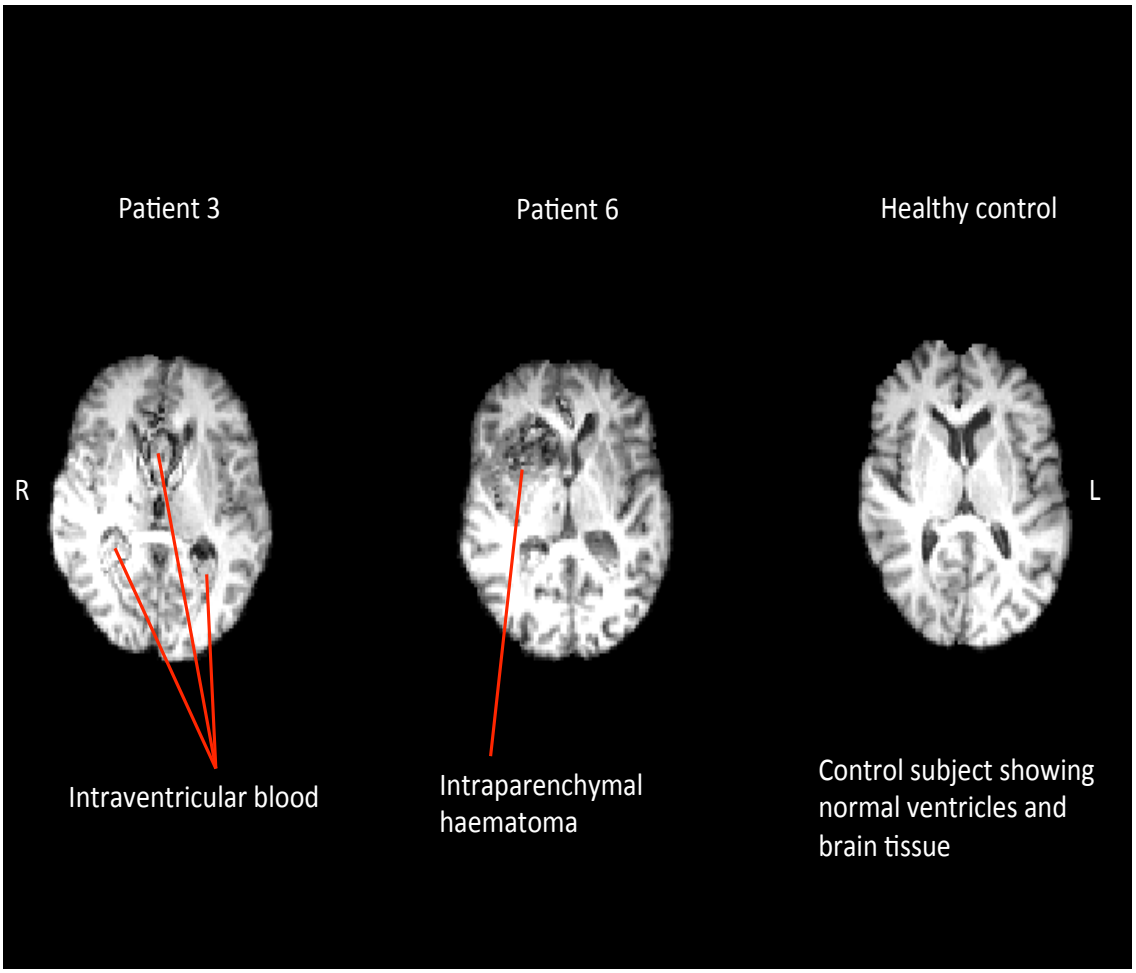


Figure 5.2 T1 structural scans of patients and one healthy control demonstrating abnormalities seen on the first acute scan. All patients had a high intraventricular blood load, which was problematic for the CSF calibration of the ASL analysis, and some patients also had intraparenchymal haematoma, which caused problems with registration. All slices were taken from the same level.

The final analysis revealed that there was a trend towards elevated whole brain GM CBF in the acute phase of SAH in all patients except patient 5, as can be seen in Figure 5.3. Acute grey matter cerebral blood flow appeared to be particularly elevated in the patients that subsequently had a poor neurological recovery as measured by modified Rankin score of > 3 at 6 months (patients 2, 4 and 6). A two tailed Wilcoxon matched-pairs signed rank test showed that this difference was not significant (p =

0.1563, median difference 10.6 ml/100g/min) but this would be difficult to demonstrate with such a small dataset.

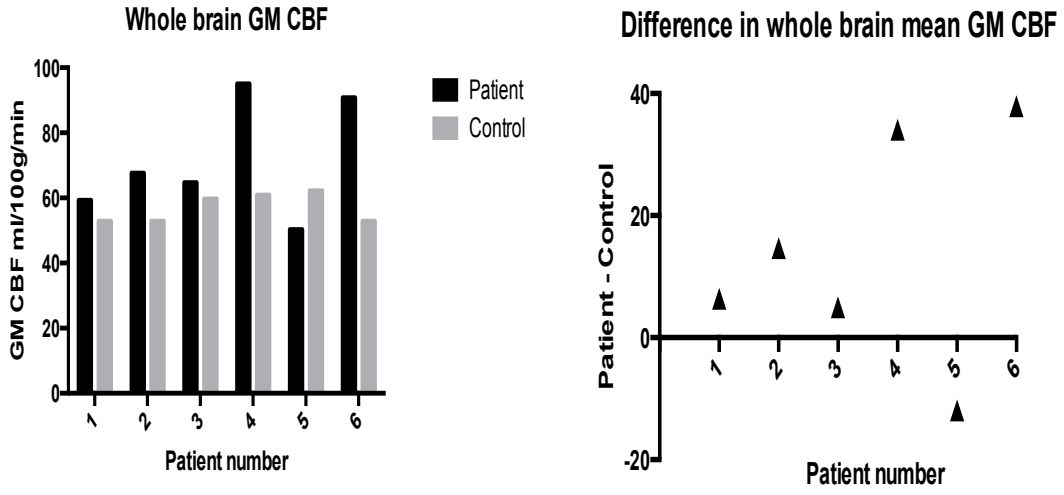


Figure 5.3 Whole brain GM CBF at scan 1. It can be seen that there is elevated blood flow in the patients (black bars) in the first few days after haemorrhage, compared to age and sex matched healthy controls (grey bars). The blood flow was most acutely raised in patients that went on to have a poor neurological outcome, shown in the graph of differences (patients – controls).

On further inspection of the scans from Patient 5 it appears that the arrival of blood was quite delayed (see Figure 5.4) which decreased the sensitivity of the measures derived from the ASL analysis. This demonstrates one of the potential confounds of this method, and may explain why the calculated result is not in keeping with the trend seen in the other patients. Delayed arrival time is already accounted for in the analysis pipeline as the data is averaged over all repetitions to boost the SNR and the kinetic model is fitted to the data across all post labelling delays. However, as we have demonstrated, extremely prolonged blood arrival time that goes beyond the sampled post labelling delays cannot be dealt with. In addition, the longer the delay the greater the signal decay, having an adverse effect on the SNR. It is possible to

analyse CBF using smaller subsets of data and looking at variability across time, however with this dataset this would technically be very challenging and the SNR will be poorer, resulting in a less reliable CBF estimate.

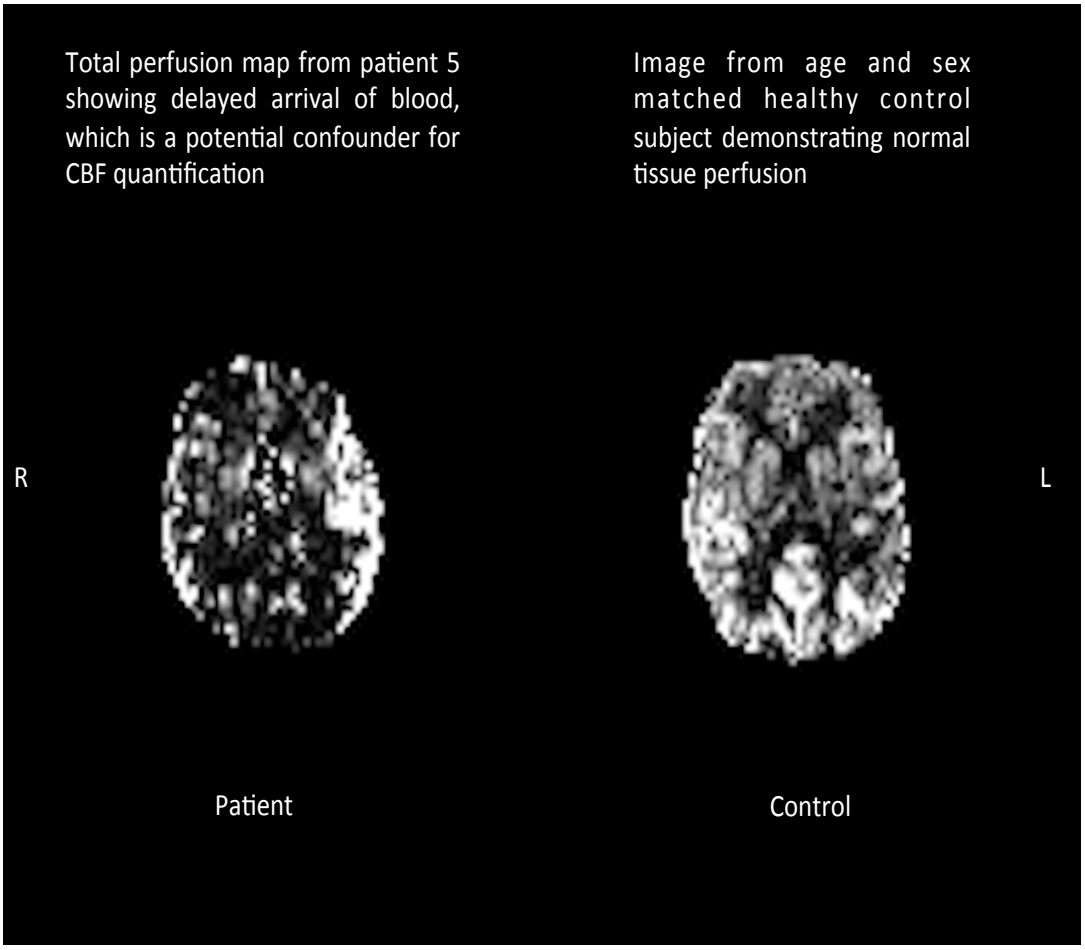


Figure 5.4 Total perfusion maps from a patient and age and sex matched healthy control illustrating differences in blood arrival. Both slices were taken from the same level.

Analysis of the relative vessel contributions of the patients that were scanned serially and correlation with the location of their aneurysm revealed that there appeared to be a reduced contribution of the left posterior circulation (left vertebral artery, LVA) at scan 1 in patients 1 and 2, which had almost resolved by scan 2. However, Patients 4

and 5 demonstrated near normal relative contribution of the artery in which the aneurysm was located (left internal carotid, LICA and basilar tip (posterior circulation, RVA and LVA)) during scans 1 and 2, compared to healthy control subjects. These changes are demonstrated in figure 5.5.

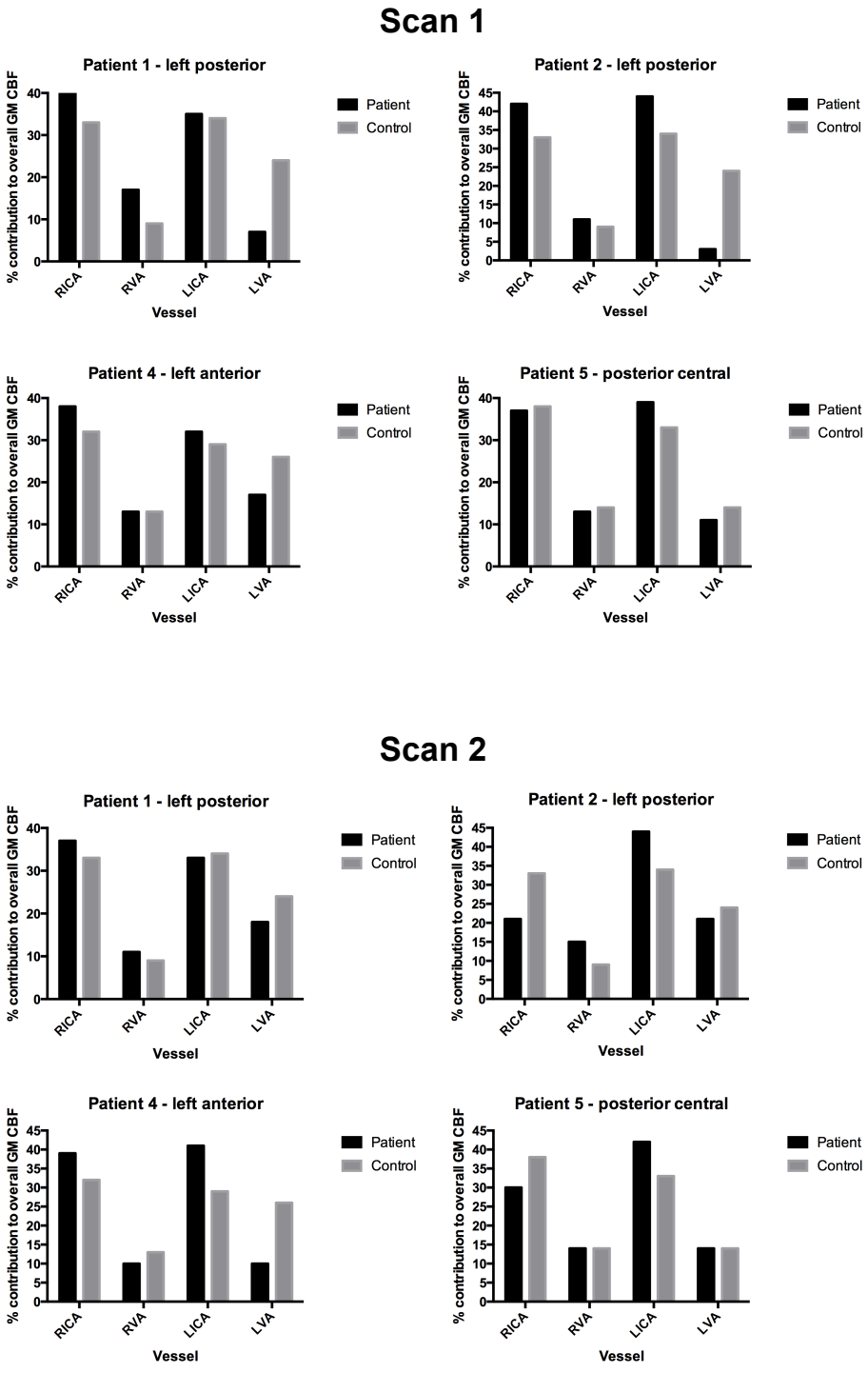


Figure 5.5 Relative vessel contributions in the acute period post severe SAH. It can be seen that the contribution from the posterior circulation (vertebral arteries) is decreased in patients 1 and 2 at scan 1, and approaching restoration towards normality by the time of scan 2. RICA = right internal carotid, LICA = left internal carotid, RVA = right vertebral artery, LVA = left vertebral artery

As discussed above, ASL suffers from low SNR due to the relatively small signal obtained from blood water compared to tissue water. This makes it extremely susceptible to motion artefact, as demonstrated by scan 3 of patient 4, where excessive movement artefact resulted in misassignment of vessels to the perfusion map (figure 5.6). As motion correction is incorporated into the analysis pipeline, further work needs to be done to determine whether this issue can be overcome via modification to the analysis.

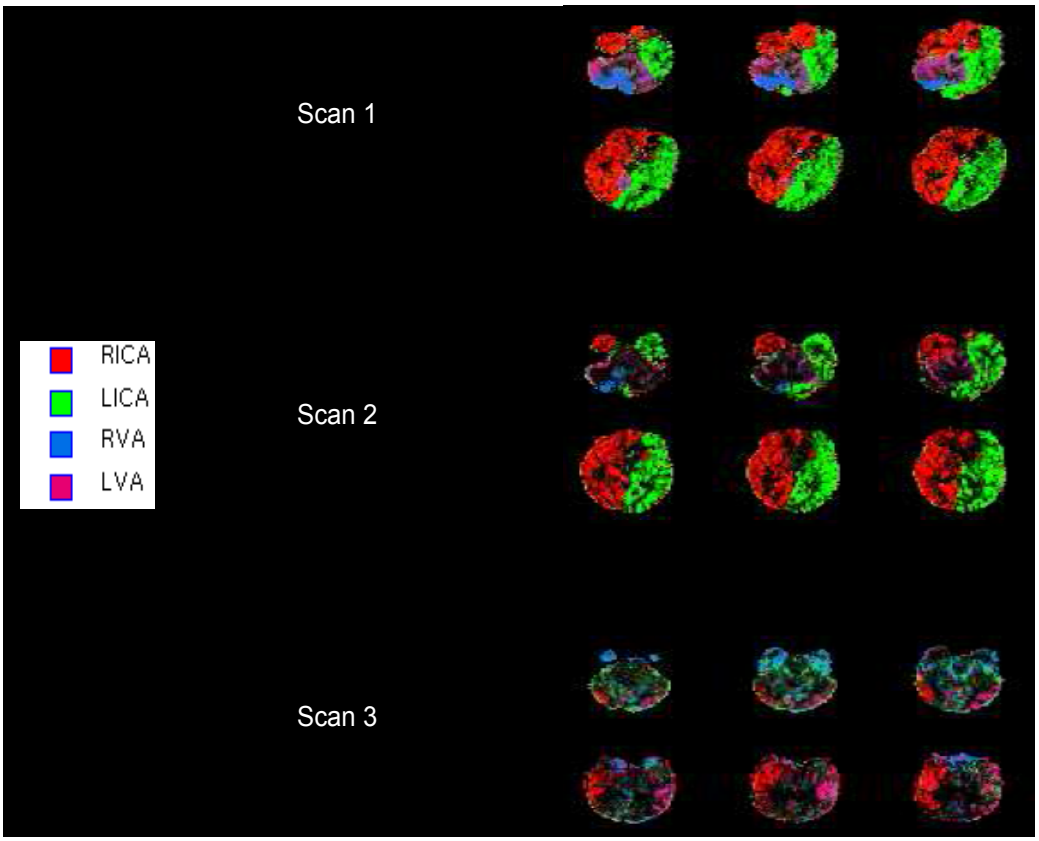


Figure 5.6 Motion artefact causing incorrect allocation of vessels to the relevant vascular territories at scan 3 of patient 4, despite motion correction. This demonstrates a limitation of this technique in neurologically impaired patients. RICA = right internal carotid, LICA = left internal carotid, RVA = right vertebral artery, LVA = left vertebral artery

Figure 5.7 shows VEPCASL perfusion territory maps from representative slices of patient 1 at scan 1 and scan 2. The perfusion map from an age and sex matched healthy control is also included for comparison. The individual vessels are represented in the colour maps. This enables a visuospatial demonstration of the changes demonstrated above. Red represents the right internal carotid (RICA), green represents the left internal carotid (LICA), blue represents the right vertebral artery (RVA) and purple represents the left vertebral artery (LVA).

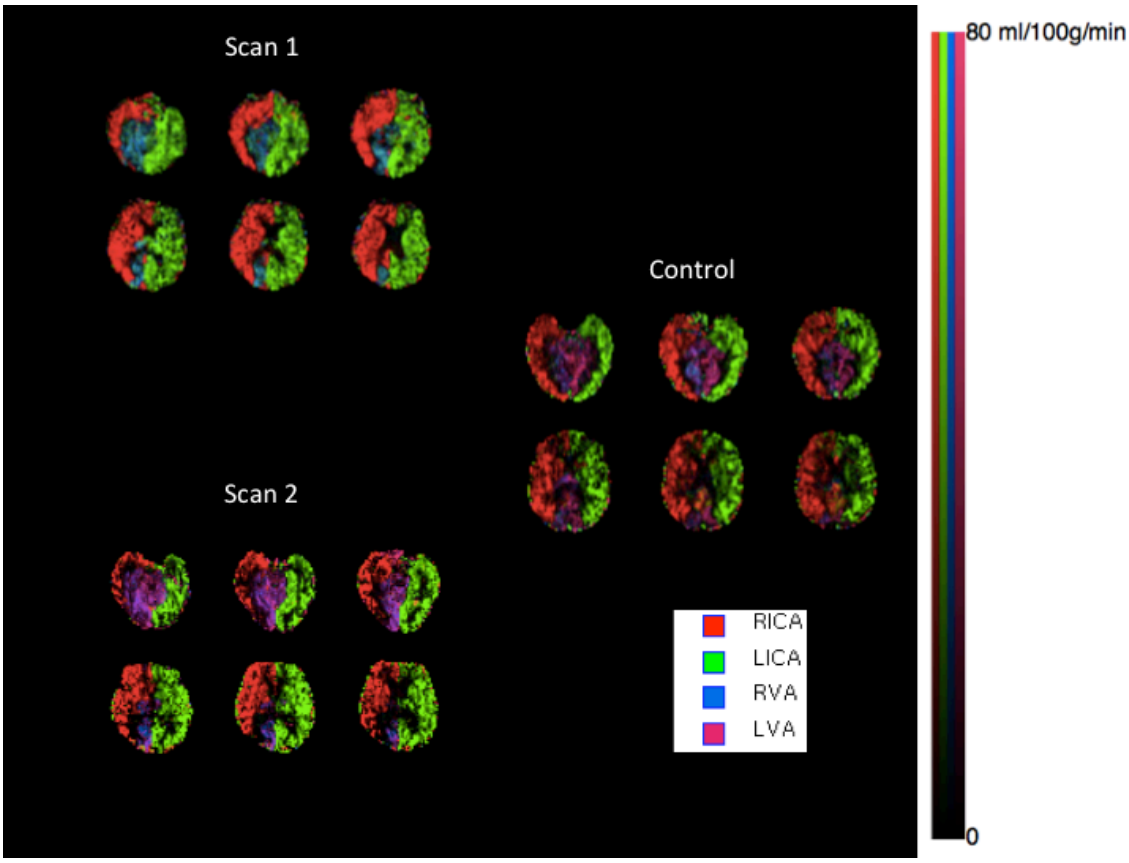


Figure 5.7 VEPCASL perfusion maps from patient 1 (scans 1 and 2), age and sex matched healthy control. It can be seen that most of the posterior portion of the brain is being supplied by the RVA in the patient at the acute scan, indicating a decrease in the flow from the LVA (which is where the aneurysm is situated). This has reversed at scan 2, where now the main posterior blood flow is from the LVA, as per the healthy control subject. RICA = right internal carotid, LICA = left internal carotid, RVA = right vertebral artery, LVA = left vertebral artery

5.6 Discussion

5.6.1 Summary of findings

In this study, we have demonstrated that it is possible to accurately quantify whole brain and regional GM CBF in six patients with severe SAH. This is the first study to our knowledge that has used this technique in this patient cohort. We have shown that despite the challenges posed by acquiring and analysing data in this patient group, it is possible to gain potentially useful clinical information from this method.

There was a trend towards a higher than expected overall GM CBF at the time of the acute scan (day 2-5 post aneurysm rupture). The only patient that did not demonstrate this is patient 5. However inspection of the perfusion scans revealed that the arrival of blood in this patient was delayed (figure 5.4), possibly secondary to slow flow, potentially confounding the ASL result. This highlights one of the limitations of this technique. Despite this, these results warrant further investigation in a larger cohort of patients to determine whether increased cerebral blood flow in the very early stages post aneurysm rupture is a true result and whether this has any impact on eventual outcome.

5.6.2 Background to findings

The disease burden resulting from aneurysmal SAH remains high, with relatively few new therapies having shown to confer morbidity or mortality benefits. One of the main causes of morbidity, as discussed previously, is delayed cerebral infarction (DCI). There are currently few tools available to enable diagnosis of patients at risk of DCI and assessment of the efficacy of novel therapies. In this pilot feasibility study we have attempted to show that VEPCASL MRI can be used to obtain clinically

useful information about the blood flow changes that occur in the acute period following SAH, which could have the potential to identify patients that are vulnerable to DCI, and to assess the effect of new treatments in the future.

This cohort of patients has much to gain from VEPCASL MRI, as all high grade SAH patients are sedated and ventilated, limiting the usefulness of monitoring clinical signs. CT changes occur too late for any rescue therapy to be initiated, therefore this method may represent an important method of risk stratification when it is still feasible to initiate targeted neuroprotective therapy. This cohort of patients is most at risk of DCI due to more severe early brain injury (150, 167) therefore it is important to discover biomarkers that may enable prediction of which patients are at risk of infarction. It presents many advantages over the methods that are currently available to assess patients after SAH.

5.6.3 Using ASL to quantify GM CBF

ASL MRI therefore has several advantages to other methods of assessment of tissue cerebral perfusion described above. This study is the first to our knowledge that demonstrates that it is feasible to acquire reliable serial measurements of regional cerebral perfusion using VEPCASL MRI from this cohort of patients i.e. severe SAH that are intubated and ventilated. Endovascular coils do not result in significant artifacts in these MRI sequences (157). The MRI scan was well tolerated in the acute phase by all 6 patients and no patient suffered a complication as a direct result of transfer.

A study performed in 'good' (grade 1 and 2) SAH demonstrated that PCASL MRI can be used to quantify whole brain tissue perfusion in this patient group. It was also sensitive at detecting an acute decrease in GM CBF on one patient, correlating with worsening clinical symptoms but no drop in GCS (157). This indicates that this method may be more sensitive than current clinical tools available to monitor potential deterioration in these patients.

5.6.4 Discussion of main findings

We found a trend towards elevated whole brain GM CBF in this patient group in the acute stages (ie first 96 hours) of acute aneurysmal SAH. One possible explanation is disruption to cerebral autoregulation that is known to occur acutely after SAH (168). Increased cerebral blood flow in an attempt to perfuse ischaemic tissue may inadvertently cause tissue oedema, resulting in mitochondrial dysfunction, microcapillary disturbance and activation of apoptosis pathways (139). It is interesting to note that the grey matter CBF was highest in the patients that went on to have a poor outcome (as measured by modified Rankin score of >3). This may be an indication of the spectrum of brain injury, with elevated flows being associated with a greater injury.

Another explanation for the increased cerebral blood flow in the early stages may be disruption to the nitric oxide signalling pathway. Activation of inducible nitric oxide synthase (iNOS) may cause pathological vasodilatation, contributing to the formation of toxic metabolites such as peroxynitrite. iNOS activation appears to be detrimental after ischaemic stroke and traumatic brain injury (138), but this has not yet been

shown after SAH. A further study correlating the time course of CSF NO metabolites may enable this to be quantified further.

An analysis of the changes in the regional CBF pattern also yielded interesting results in those patients that were scanned serially (patients 1, 2, 4 and 5). An expected result might be that there would be decreased relative blood supply in the territory supplied by the artery directly affected by aneurysm rupture (due to arterial spasm or direct pressure effects of the blood clot), with compensatory increase in supply from arteries not affected. This was the case in patients 1 and 2 that both had posterior communicating aneurysms on the left and consequently showed decreased relative supply from the LVA at scan 1. This appeared to almost completely resolve at scan 2.

This interesting result warrants further investigation in a larger cohort of patients to determine whether this phenomenon is in any way linked to the development of infarction or outcome, in particular whether changes seen in a particular vascular territory correlate with the areas of eventual infarction.

5.6.5 Limitations of the study

The main aim of this feasibility study was to assess whether it is possible to acquire clinically useful information from this imaging technique in this patient cohort. Therefore the data presented here suffers from several limitations. There were only a small number of patients recruited, due to the logistical challenges in the acquisition of the scans.

Critically ill patients are often on multiple drug infusions and are supported by non-MRI compatible ventilation equipment. They are also often unstable from a respiratory and cardiovascular point of view, presenting problems when in a remote environment such as the MRI scanner. Due to this, any interpretation of results can only be speculative.

ASL MRI suffers from low SNR, therefore it is very susceptible to motion artifact. This was not an issue during the acute scanning period, as the patients were paralysed. However, at follow up many patients after severe SAH will be neurologically impaired and may not be able to keep completely still, causing issues with the data analysis, evidenced in the follow up scan of patient 4, where vessel locations were misplaced due to motion. Current existing motion correction techniques can only partially overcome this, therefore this represents an area for future development.

Delayed blood arrival time in the slice of interest also causes inaccuracies in the CBF quantification, and it is not unlikely that these patients will have abnormal blood flow velocities, as demonstrated by patient 5. Therefore any results obtained must be treated with caution and the perfusion maps should be checked for this.

Other issues with the analysis included issues with image registration to standard space due to the presence of intraparenchymal haematoma. This was improved by the use of gradient fieldmaps, obtained as part of the BOLD sequence. The signal of fully relaxed blood spins is needed to calculate CBF in ml/100g/min from the differing signal intensities obtained by ASL scanning. This is often calculated by estimation from a reference tissue e.g. CSF. However, blood in the CSF of severe SAH patients

rendered this approach inaccurate. Therefore a different approach to quantify CBF was used, by calculating the scaling factor needed from a separately acquired proton density (PD) image on a voxel-by-voxel basis. This enabled the inaccuracies caused by intraventricular blood to be removed.

5.7 Conclusions

In conclusion, in this chapter we have shown that it is possible to obtain robust measurements of CBF in the acute stages of severe SAH, despite the practical challenges that this poses. We have shown some interesting changes that occur in the early on in the disease process, which suggest a loss of autoregulation and perhaps activation of pathological signalling pathways that promote vasodilatation. Cerebral oedema is a result of this elevated flow, resulting in activation of apoptosis pathways and neuronal damage. There also appear to be changes in the relative vessel contributions to tissue perfusion depending on aneurysm location. Further imaging work in the acute setting in this patient population is likely to provide extremely useful insights into the changes that occur in this critical stage of disease evolution. Imaging may also provide a useful tool to assess the response to potential novel therapies.

Chapter 6

General discussion and conclusions

Abstract

The aims of this thesis were to investigate novel methods of assessing cerebral injury after severe subarachnoid haemorrhage, and to investigate the utility of these tools in providing clinically useful information. There is a need for simple yet robust measures of measuring neuronal dysfunction after severe SAH as neurological examination is limited by the fact that these patients are sedated. The study presented in Chapter 4 explored electroencephalography as a beside assessment tool to quantify the degree of responsiveness to a nitric oxide donor, sodium nitrite. One aim was to translate some of the promising work surrounding nitric oxide donors conferring cerebral protection in animals to the patient population. A further aim was to assess whether a combination of electroencephalography and sodium nitrite could provide an insight into neuronal wellbeing immediately after SAH, and whether this correlated with outcomes. Chapter 5 explored non-invasive assessment of cerebral blood flow using arterial spin labelling MRI, to assess whether it is possible to gain information regarding acute changes in tissue perfusion. In this chapter, the implications of this research for future studies in severe subarachnoid haemorrhage, and the scope for potential novel therapies to be devised are discussed.

6.1 Main findings of this thesis

The work in this thesis set out to determine the usefulness of novel tools of cerebral function and perfusion to determine the extent of cerebral injury after severe (WFNS grade 3-5) subarachnoid haemorrhage (SAH). This is currently an area of unmet clinical need, as despite the high morbidity and mortality of this condition it is currently extremely difficult to predict which patients will go on to do well or badly. It is also very difficult to assess any clinical deterioration, such as the development of new neurological deficits when a patient is deeply sedated for ventilation purposes.

Currently there are very few options available for bedside neurological monitoring of this patient group. Intracranial pressure monitoring offers limited information regarding the overall pressure inside the cranial vault, and has little correlation with underlying neuronal ischaemia (169). Transcranial Doppler (TCD) has high sensitivity but low specificity for middle cerebral artery (MCA) vasospasm (120). However there is now mounting evidence that large artery vasospasm is not necessarily predictive of cerebral infarction or eventual clinical outcome (16). Therefore these methods are limited in value.

Early detection and treatment of DCI would theoretically enable preventative measures to be taken against the development of cerebral infarction. It is known that the development of DCI is correlated with increased morbidity and mortality (170), therefore strategies to prevent its development are of utmost importance in improving outcomes. In chapter 1 we discussed that events occurring during the early phase of injury play a crucial role in the subsequent pathophysiology of the disease.

6.1.1 EEG findings

We have shown in the study described in Chapter 4 that electroencephalography (EEG) is a useful bedside monitoring test, and that specific power spectral changes occur as cerebral blood flow falls and the tissues become progressively more ischaemic. Manipulation of the nitric oxide (NO) pathway via cerebral nitric oxide donors has been shown to have beneficial effects in ischaemic stroke and SAH animal models (110, 116). Therefore, we aimed to show that EEG can be used as a surrogate marker of neuronal 'health' after SAH, and that the response to increasing cerebral NO could be quantified by changes in the power spectrum of the EEG. We demonstrated that patients that go on to develop ischaemia and subsequently do worse showed a significant decrease in the ADR (a 'more ischaemic' response) to an infusion of sodium nitrite, whereas those patients who had an EEG response towards a 'less ischaemic' pattern did not develop DCI and had more favourable outcomes.

This raises interesting questions regarding the role of the NO signalling pathway in the development of ischaemia after SAH. A combination of EEG and NO donor may represent a physiological probe that enables quantification of the degree of neuronal injury present, and a method of risk stratification to identify those most at risk of DCI.

These results also offer mechanistic insights into the changes that occur in NO signalling after SAH. Traditionally it has been thought that NO and NO donors exert their beneficial effects via their actions on the macrovasculature and therefore increase blood flow. However, we have showed that EEG power spectral changes occur in the absence of any alteration of flow velocities as measured by MCA TCD.

This indicates that changes may be occurring at a cellular level, possibly by the actions of NO signalling on mitochondrial activation and protein nitrosylation.

Conversely, the decrease in ADR seen in patients that did develop DCI may be secondary to greater cellular disruption and a more severe injury, meaning that exogenous NO does not have intact signalling pathways on which to operate. Alternately, the exogenous NO may be activating harmful pathways mediated by iNOS, exacerbating cellular injury. Therefore this study may indicate a potential method for determining the extent of cerebral injury present at a cellular level in the early stages of the disease process. NO donors continue to show promise as a potential therapy for preventing ischaemic damage after SAH.

6.1.2 MRI findings

In the study described in Chapter 5 we investigated whether it would be possible to non-invasively accurately quantify regional cerebral blood flow after severe SAH using vessel encoded arterial spin labelling (VEPCASL). In this pilot study we scanned six poor grade sedated and ventilated SAH patients, four of them serially in the acute phase. We found evidence to suggest elevated blood flow in the first 2-5 days post aneurysm rupture, implying loss of local autoregulation. It has been shown that loss of autoregulation is an adverse sign after SAH, and is linked to poor outcomes (168). Interestingly, the patients that had the worst outcomes also had the highest blood flow. We also found that there were changes to regional cerebral tissue perfusion in these patients immediately post aneurysm rupture, raising the possibility of development of new therapies aimed at restoration of normal flow.

The direct contributions of each of these studies were discussed in more detail in their respective chapters. We will now go on to discuss the methodological considerations and wider implications for neurocritical care research relating to SAH, and the lessons learnt from these studies. We will also discuss future directions and further studies that lead on naturally from this preliminary work.

6.2 Methodological considerations in neurological critical care research

Research in neurological critical care (NICU) presents multiple challenges. However, this is an extremely important cohort of patients to study, as they represent the extreme spectrum of pathology. It is very difficult to prognosticate in this patient group, and often a significant amount of resources are used only to result in a very poor clinical outcome. Therefore novel methods of assessing cerebral response to various interventions would greatly aid clinical decision making, as well as enabling accurate assessment of new treatment methods.

6.2.1 Consent

Patients lack the capacity to give informed consent, so this has to be done via a consultee process involving the next of kin. This involves detailed discussion with patient ethics committees at the time of designing the study. The next of kin is often not readily available, or in some cases not contactable. This may be overcome by consultation with a member of the clinical team not directly involved with patient care, however this can be difficult to achieve in the necessary time frame.

The critical care unit can often feel overwhelming to those not used to the hospital environment and the patients relatives are often extremely upset at the sudden illness

of their loved one. Patients affected by SAH are often otherwise fit and healthy and in some cases have never been admitted to hospital. Therefore it is necessary to handle any interactions with the next of kin sensitively and compassionately, which can be a challenge when attempting to recruit patients in a time critical manner.

We also discovered many challenges to acquiring and analysing data in NICU patients, which will be discussed further below.

6.2.2 Data acquisition challenges

NICU patients are critically unwell, often having a labile blood pressure, changing oxygen requirements and rapidly altering intracranial pressures. They are also often on multiple drug infusions. These all affect the signal from EEG and MRI.

6.2.2.1 EEG

All patients on NICU are sedated to aid mechanical ventilation in the acute phase of severe SAH. Mechanical ventilation is usually initiated due to low GCS and inability of the patient to protect their own airway. In order for mechanical ventilation to be tolerated, sedation in the form of propofol anaesthesia and opiate analgesia (usually fentanyl or remifentanil) is required. These all affect the EEG signal.

Propofol is a short acting hypnotic drug that is widely used for sedation in neurocritical care. It has several effects on the resting EEG, including increase of slow wave activity and at higher concentrations, a burst suppression pattern (171). Opiates cause changes in alpha, delta and beta power (172). Therefore, it is not possible to directly compare resting EEG spectral power values in critically ill patients that are on

these infusions, as differing levels of sedation and variations in individual pharmacodynamics affect the signal to differing degrees.

There are several methods that can be used to overcome this. One method involves calculation of power relative to the total overall power of the individual EEG, to provide a relative value. Another method is the use of ratios, such as the alpha/delta ratio, to ensure values are comparable. This was one of the rationales behind the use of the ADR in the study described in Chapter 4.

Another limitation of EEG in this patient group is that it is not possible to induce evoked potentials and measure the effects of any intervention on these. However, many studies have now shown that continuous EEG offers a good insight into developing ischaemia after SAH (173). Due to the presence of external ventricular drains (EVDs) and intracranial pressure monitors (ICPs) it is occasionally difficult to apply a full montage of electrodes, reducing the amount of spatial information gained.

6.2.2.2 MRI

As discussed in Chapter 4, acquiring MRI scans acutely in this patient cohort is often challenging. As the patients are fully sedated, intubated and ventilated they require at least one senior anaesthetist to accompany them to the scanner. This service may not be widely available in all centres. The patients are clinically unstable therefore require continuous monitoring of vital signs such as ECG, SpO_2, $PETCO_2$, IABP and fraction of inspired oxygen (FiO_2). To enable this monitoring to continue in the MR scanner, it is necessary to switch to specialist MR compatible monitoring systems, which are expensive and again not widely available.

Ventilation can pose issues in the scanner, as most intensive care ventilators are not MR compatible. It is therefore necessary to have ventilators that are safe to use in the scanner. Patients who are on high levels of respiratory support may not be suitable for transfer, as switching ventilators involves disconnecting the patient briefly, running the risk of a drop in oxygen levels. The patients are also on several drug infusions, and the infusion pumps are also not MR compatible, necessitating switching to long drug infusion lines. This involves briefly disconnecting the patient from their infusions, which often include powerful vasopressors and ionotropes. Therefore, it is not currently practical to take the very sickest patients to the scan due to the risk posed by cardiovascular instability. This means that any study in this cohort of patients will automatically select for the less unstable and potentially less severely injured patients, possibly introducing a selection bias.

6.2.3 Data analysis challenges

We have already discussed the analysis challenges posed by the MR data obtained in Chapter 5. The EEG data obtained also posed some challenges to accurate analysis. The raw EEG signal suffered from large amounts of 50 Hz interference from other electrical equipment present on the NICU. As we were more interested in the lower power frequencies in this study, this was overcome by passing the data through a linear finite impulse response (FIR) filter from 0.5 – 15 Hz. However, this may pose a problem in future studies when assessing higher frequencies. The recording environment itself was very noisy and not darkened, so the patient was receiving auditory and visual stimulation throughout the recording. However, this remained constant over the duration of the recording.

6.3 Potential for the development of future assessment tools and therapies

The most exciting results from these studies are an indication of potential new methods of non-invasive monitoring of cerebral tissue perfusion and neuronal 'health', enabling identification of patients at risk of deterioration and potentially suggesting a method of risk stratification.

As discussed in Chapter 2, NO donors have been investigated as potential neuroprotective agents after ischaemic brain injury, regardless of the aetiology. Promising results from animal studies include the prevention and reversal of large artery vasospasm (20), decreased infarct sizes after ischaemic stroke (110) and traumatic brain injury (111). These all indicate that repletion of cerebral NO may have a role to play in the prevention of secondary brain injury.

It has been difficult to acutely assess the impact of any new interventions on cerebral function and neuronal health due to lack of availability of suitable imaging and bedside monitoring modalities. Plain computerised tomography (CT) scan is widely available but lacks spatial information and is not particularly sensitive at detecting tissue at risk of ischemia (123). By the time infarct has established on CT it is often too late to initiate any rescue therapies. There is therefore a need for monitoring tools that enable timely and accurate information about the health of cerebral tissue to be obtained. This would also allow for potential new therapies to be assessed on a patient by patient basis, and give useful insights into the potential mechanisms of action of these treatments.

We have shown in Chapter 4 that it is possible to use a combination of EEG and a drug intervention to provide real time information about the changing state of neuronal firing after severe SAH. EEG has been shown to be sensitive at detecting neuronal ischaemia but has traditionally been hampered by the fact that days of recording and expert analysis are needed to gain this information. The advantage of using a drug infusion is that useful information can be gained from only 2 hours recording.

We have also identified a specific qEEG parameter (the ADR) which appears to be directly correlated with the development of ischaemia and outcomes. If this test could be validated in a larger cohort of patients and the analysis automated to enable bedside recording of the ADR this becomes an exciting new technique for monitoring cerebral health and possible risk stratification. Analysis of ADR changes could also be used to assess the development of ischaemia after other brain injuries such as TBI and ischaemic stroke.

In Chapter 5 we demonstrated that it is possible to gain accurate measures of regional tissue perfusion in severe SAH using vessel encoded arterial spin labelling MRI (VEPCASL MRI). This has the potential to not only offer useful insights into the acute changes that happen to cerebral blood flow immediately after SAH, but also as a possible tool to assess the impact of drug and other interventions. This would give a valuable understanding into the likely mechanisms of action of any proposed new agents.

6.4 Conclusions

In conclusion, the work presented in this thesis demonstrates that qEEG is a useful neuromonitoring tool after severe SAH. We have also shown that a cerebral NO donor, sodium nitrite, induces qEEG changes that are indicative of improving neuronal wellbeing in patients that do not develop ischaemia, giving an insight into the possible neuroprotective actions of cerebral NO donors. This represents a step towards translation of the promising work shown in animals to the patient population, and progress towards the development of a novel therapy. It also raises the possibility of using a drug infusion in combination with EEG monitoring to assess the degree of neuronal damage and neurovascular disruption after ischaemic injury. This has the potential to be applicable to all secondary brain injury, e.g. after ischaemic stroke or traumatic brain injury.

We have also shown that we can measure regional cerebral blood flow changes using arterial spin labelling. This is an exciting tool that could also be used to assess the effect of interventions and possibly identify regions of tissue that are at risk of ischaemia. By enabling the arterial supply to these regions to be identified, it may be possible to target the vessel at risk and restore flow. Further work is needed in greater numbers of patients to validate these exciting results, to allow for better outcomes from this severely debilitating condition.

Bibliography

1. Epidemiology of aneurysmal subarachnoid hemorrhage in Australia and New Zealand: incidence and case fatality from the Australasian Cooperative Research on Subarachnoid Hemorrhage Study (ACROSS). Stroke; a journal of cerebral circulation. 2000;31(8):1843-50.
2. van Gijn J, Kerr RS, Rinkel GJ. Subarachnoid haemorrhage. Lancet. 2007;369(9558):306-18.
3. Fisher CM, Kistler JP, Davis JM. Relation of cerebral vasospasm to subarachnoid hemorrhage visualized by computerized tomographic scanning. Neurosurgery. 1980;6(1):1-9.
4. Tewari M, Aggarwal A, Mathuriya S, Gupta V. The outcome after aneurysmal sub arachnoid hemorrhage: a study of various factors. Annals of neurosciences. 2015;22(2):78-80.
5. Molyneux AJ, Birks J, Clarke A, Sneade M, Kerr RS. The durability of endovascular coiling versus neurosurgical clipping of ruptured cerebral aneurysms: 18 year follow-up of the UK cohort of the International Subarachnoid Aneurysm Trial (ISAT). Lancet. 2015;385(9969):691-7.
6. Rowland MJ, Hadjipavlou G, Kelly M, Westbrook J, Pattinson KT. Delayed cerebral ischaemia after subarachnoid haemorrhage: looking beyond vasospasm. Br J Anaesth. 2012;109(3):315-29.
7. Cahill J, Calvert JW, Zhang JH. Mechanisms of early brain injury after subarachnoid hemorrhage. Journal of cerebral blood flow and metabolism : official journal of the International Society of Cerebral Blood Flow and Metabolism. 2006;26(11):1341-53.
8. Fujii M, Yan J, Rolland WB, Soejima Y, Caner B, Zhang JH. Early brain injury, an evolving frontier in subarachnoid hemorrhage research. Transl Stroke Res. 2013;4(4):432-46.
9. Zubkov AY, Ogihara K, Bernanke DH, Parent AD, Zhang J. Apoptosis of endothelial cells in vessels affected by cerebral vasospasm. Surgical neurology. 2000;53(3):260-6.
10. Zhou C, Yamaguchi M, Colohan AR, Zhang JH. Role of p53 and apoptosis in cerebral vasospasm after experimental subarachnoid hemorrhage. Journal of cerebral blood flow and metabolism : official journal of the International Society of Cerebral Blood Flow and Metabolism. 2005;25(5):572-82.
11. Kreiter KT, Copeland D, Bernardini GL, Bates JE, Peery S, Claassen J, et al. Predictors of cognitive dysfunction after subarachnoid hemorrhage. Stroke; a journal of cerebral circulation. 2002;33(1):200-8.
12. Kassell NF, Torner JC, Haley EC, Jr., Jane JA, Adams HP, Kongable GL. The International Cooperative Study on the Timing of Aneurysm Surgery. Part 1: Overall management results. Journal of neurosurgery. 1990;73(1):18-36.
13. Weir B, MacDonald L. Cerebral vasospasm. Clin Neurosurg. 1993;40:40-55.
14. Minhas PS, Menon DK, Smielewski P, Czosnyka M, Kirkpatrick PJ, Clark JC, et al. Positron emission tomographic cerebral perfusion disturbances and transcranial Doppler findings among patients with neurological deterioration after subarachnoid hemorrhage. Neurosurgery. 2003;52(5):1017-22; discussion 22-4.
15. Naidech AM, Drescher J, Tamul P, Shaibani A, Batjer HH, Alberts MJ. Acute physiological derangement is associated with early radiographic cerebral infarction after subarachnoid haemorrhage. Journal of neurology, neurosurgery, and psychiatry. 2006;77(12):1340-4.

16. Macdonald RL, Higashida RT, Keller E, Mayer SA, Molyneux A, Raabe A, et al. Randomised trial of clazosentan, an endothelin receptor antagonist, in patients with aneurysmal subarachnoid hemorrhage undergoing surgical clipping (CONSCIOUS-2). Acta Neurochir Suppl. 2013;115:27-31.
17. Sabri M, Ai J, Lakovic K, D'Abbondanza J, Ilodigwe D, Macdonald RL. Mechanisms of microthrombi formation after experimental subarachnoid hemorrhage. Neuroscience. 2012;224:26-37.
18. Petzold GC, Haack S, von Bohlen Und Halbach O, Priller J, Lehmann TN, Heinemann U, et al. Nitric oxide modulates spreading depolarization threshold in the human and rodent cortex. Stroke. 2008;39(4):1292-9.
19. Sehba FA, Schwartz AY, Chereshnev I, Bederson JB. Acute decrease in cerebral nitric oxide levels after subarachnoid hemorrhage. J Cereb Blood Flow Metab. 2000;20(3):604-11.
20. Fathi AR, Pluta RM, Bakhtian KD, Qi M, Lonser RR. Reversal of cerebral vasospasm via intravenous sodium nitrite after subarachnoid hemorrhage in primates. J Neurosurg. 2011;115(6):1213-20.
21. Furchgott RF, Zawadzki JV. The obligatory role of endothelial cells in the relaxation of arterial smooth muscle by acetylcholine. Nature. 1980;288(5789):373-6.
22. Furchgott RF, Cherry PD, Zawadzki JV, Jothianandan D. Endothelial cells as mediators of vasodilation of arteries. Journal of cardiovascular pharmacology. 1984;6 Suppl 2:S336-43.
23. Palmer RM, Ferrige AG, Moncada S. Nitric oxide release accounts for the biological activity of endothelium-derived relaxing factor. Nature. 1987;327(6122):524-6.
24. Radomski MW, Palmer RM, Moncada S. Endogenous nitric oxide inhibits human platelet adhesion to vascular endothelium. Lancet. 1987;2(8567):1057-8.
25. Moncada S, Higgs EA. Nitric oxide and the vascular endothelium. Handb Exp Pharmacol. 2006(176 Pt 1):213-54.
26. Griffith OW, Stuehr DJ. Nitric oxide synthases: properties and catalytic mechanism. Annual review of physiology. 1995;57:707-36.
27. Toda N, Ayajiki K, Okamura T. Cerebral blood flow regulation by nitric oxide: recent advances. Pharmacol Rev. 2009;61(1):62-97.
28. Gao Y, Raj JU. Regulation of the pulmonary circulation in the fetus and newborn. Physiological reviews. 2010;90(4):1291-335.
29. Stuehr DJ, Griffith OW. Mammalian nitric oxide synthases. Adv Enzymol Relat Areas Mol Biol. 1992;65:287-346.
30. Alderton WK, Cooper CE, Knowles RG. Nitric oxide synthases: structure, function and inhibition. The Biochemical journal. 2001;357(Pt 3):593-615.
31. Huang Z, Huang PL, Ma J, Meng W, Ayata C, Fishman MC, et al. Enlarged infarcts in endothelial nitric oxide synthase knockout mice are attenuated by nitro-L-arginine. J Cereb Blood Flow Metab. 1996;16(5):981-7.
32. Ko NU, Rajendran P, Kim H, Rutkowski M, Pawlikowska L, Kwok PY, et al. Endothelial nitric oxide synthase polymorphism (-786T->C) and increased risk of angiographic vasospasm after aneurysmal subarachnoid hemorrhage. Stroke; a journal of cerebral circulation. 2008;39(4):1103-8.
33. Bonnin P, Leger PL, Villapol S, Deroide N, Gressens P, Pocard M, et al. Dual action of NO synthases on blood flow and infarct volume consecutive to neonatal focal cerebral ischemia. Experimental neurology. 2012;236(1):50-7.

34. Hudetz AG, Shen H, Kampine JP. Nitric oxide from neuronal NOS plays critical role in cerebral capillary flow response to hypoxia. The American journal of physiology. 1998;274(3 Pt 2):H982-9.
35. Melikian N, Seddon MD, Casadei B, Chowienczyk PJ, Shah AM. Neuronal nitric oxide synthase and human vascular regulation. Trends Cardiovasc Med. 2009;19(8):256-62.
36. Marletta MA. Mammalian synthesis of nitrite, nitrate, nitric oxide, and N-nitrosating agents. Chem Res Toxicol. 1988;1(5):249-57.
37. Pautz A, Art J, Hahn S, Nowag S, Voss C, Kleinert H. Regulation of the expression of inducible nitric oxide synthase. Nitric Oxide. 2010;23(2):75-93.
38. MacMicking J, Xie QW, Nathan C. Nitric oxide and macrophage function. Annu Rev Immunol. 1997;15:323-50.
39. Jones SC, Easley KA, Radinsky CR, Chyatte D, Furlan AJ, Perez-Trepichio AD. Nitric oxide synthase inhibition depresses the height of the cerebral blood flow-pressure autoregulation curve during moderate hypotension. J Cereb Blood Flow Metab. 2003;23(9):1085-95.
40. Attwell D, Buchan AM, Charpak S, Lauritzen M, Macvicar BA, Newman EA. Glial and neuronal control of brain blood flow. Nature. 2010;468(7321):232-43.
41. Girouard H, Iadecola C. Neurovascular coupling in the normal brain and in hypertension, stroke, and Alzheimer disease. J Appl Physiol. 2006;100(1):328-35.
42. Akgoren N, Fabricius M, Lauritzen M. Importance of nitric oxide for local increases of blood flow in rat cerebellar cortex during electrical stimulation. Proc Natl Acad Sci U S A. 1994;91(13):5903-7.
43. Piknova B, Kocharyan A, Schechter AN, Silva AC. The role of nitrite in neurovascular coupling. Brain Res. 2011;1407:62-8.
44. Stefanovic B, Schwindt W, Hoehn M, Silva AC. Functional uncoupling of hemodynamic from neuronal response by inhibition of neuronal nitric oxide synthase. J Cereb Blood Flow Metab. 2007;27(4):741-54.
45. Hamilton NB, Attwell D, Hall CN. Pericyte-mediated regulation of capillary diameter: a component of neurovascular coupling in health and disease. Front Neuroenergetics. 2010;2.
46. Golanov EV, Reis DJ. Nitric oxide and prostanoids participate in cerebral vasodilation elicited by electrical stimulation of the rostral ventrolateral medulla. J Cereb Blood Flow Metab. 1994;14(3):492-502.
47. Peers C, Pearson HA, Boyle JP. Hypoxia and Alzheimer's disease. Essays Biochem. 2007;43:153-64.
48. Mintun MA, Lundstrom BN, Snyder AZ, Vlassenko AG, Shulman GL, Raichle ME. Blood flow and oxygen delivery to human brain during functional activity: theoretical modeling and experimental data. Proc Natl Acad Sci U S A. 2001;98(12):6859-64.
49. Ho JJ, Man HS, Marsden PA. Nitric oxide signaling in hypoxia. J Mol Med (Berl). 2012;90(3):217-31.
50. Takuwa H, Matsuura T, Bakalova R, Obata T, Kanno I. Contribution of nitric oxide to cerebral blood flow regulation under hypoxia in rats. J Physiol Sci. 2010;60(6):399-406.
51. Beall CM, Laskowski D, Erzurum SC. Nitric oxide in adaptation to altitude. Free Radic Biol Med. 2012;52(7):1123-34.
52. Wang Q, Paulson OB, Lassen NA. Effect of nitric oxide blockade by NG-nitro-L-arginine on cerebral blood flow response to changes in carbon dioxide tension. J Cereb Blood Flow Metab. 1992;12(6):947-53.

53. Kirkeby OJ, Kutzsche S, Risoe C, Rise IR. Cerebral nitric oxide concentration and microcirculation during hypercapnia, hypoxia, and high intracranial pressure in pigs. J Clin Neurosci. 2000;7(6):531-8.
54. Zhang F, Sprague SM, Farrokhi F, Henry MN, Son MG, Vollmer DG. Reversal of attenuation of cerebrovascular reactivity to hypercapnia by a nitric oxide donor after controlled cortical impact in a rat model of traumatic brain injury. J Neurosurg. 2002;97(4):963-9.
55. Fathi AR, Yang C, Bakhtian KD, Qi M, Lonser RR, Pluta RM. Carbon dioxide influence on nitric oxide production in endothelial cells and astrocytes: cellular mechanisms. Brain Res. 2011;1386:50-7.
56. Cherian L, Goodman JC, Robertson CS. Brain nitric oxide changes after controlled cortical impact injury in rats. J Neurophysiol. 2000;83(4):2171-8.
57. Tuzgen S, Tanriover N, Uzan M, Tureci E, Tanriverdi T, Gumustas K, et al. Nitric oxide levels in rat cortex, hippocampus, cerebellum, and brainstem after impact acceleration head injury. Neurol Res. 2003;25(1):31-4.
58. Ahn MJ, Sherwood ER, Prough DS, Lin CY, DeWitt DS. The effects of traumatic brain injury on cerebral blood flow and brain tissue nitric oxide levels and cytokine expression. J Neurotrauma. 2004;21(10):1431-42.
59. Hlatky R, Goodman JC, Valadka AB, Robertson CS. Role of nitric oxide in cerebral blood flow abnormalities after traumatic brain injury. J Cereb Blood Flow Metab. 2003;23(5):582-8.
60. Lundblad C, Bentzer P. Effects of L-arginine on cerebral blood flow, microvascular permeability, number of perfused capillaries, and brain water content in the traumatized mouse brain. Microvasc Res. 2007;74(1):1-8.
61. Cherian L, Robertson CS. L-arginine and free radical scavengers increase cerebral blood flow and brain tissue nitric oxide concentrations after controlled cortical impact injury in rats. J Neurotrauma. 2003;20(1):77-85.
62. Pluta RM. Dysfunction of nitric oxide synthases as a cause and therapeutic target in delayed cerebral vasospasm after SAH. Acta neurochirurgica Supplement. 2008;104:139-47.
63. Reiter CD, Wang X, Tanus-Santos JE, Hogg N, Cannon RO, 3rd, Schechter AN, et al. Cell-free hemoglobin limits nitric oxide bioavailability in sickle-cell disease. Nat Med. 2002;8(12):1383-9.
64. Tanishima T. Cerebral vasospasm: contractile activity of hemoglobin in isolated canine basilar arteries. J Neurosurg. 1980;53(6):787-93.
65. Radi R. Peroxynitrite, a stealthy biological oxidant. J Biol Chem. 2013;288(37):26464-72.
66. Moro MA, Almeida A, Bolanos JP, Lizasoain I. Mitochondrial respiratory chain and free radical generation in stroke. Free Radic Biol Med. 2005;39(10):1291-304.
67. Li ST, Pan J, Hua XM, Liu H, Shen S, Liu JF, et al. Endothelial Nitric Oxide Synthase Protects Neurons against Ischemic Injury through Regulation of Brain-Derived Neurotrophic Factor Expression. CNS Neurosci Ther. 2014;20(2):154-64.
68. Ng WH, Moochhala S, Yeo TT, Ong PL, Ng PY. Nitric oxide and subarachnoid hemorrhage: elevated level in cerebrospinal fluid and their implications. Neurosurgery. 2001;49(3):622-6; discussion 6-7.
69. Stein SC, Browne KD, Chen XH, Smith DH, Graham DI. Thromboembolism and delayed cerebral ischemia after subarachnoid hemorrhage: an autopsy study. Neurosurgery. 2006;59(4):781-7; discussion 7-8.

70. Zimmerman GA, Prescott SM, McIntyre TM. Endothelial cell interactions with granulocytes: tethering and signaling molecules. Immunol Today. 1992;13(3):93-100.
71. Davenpeck KL, Gauthier TW, Lefer AM. Inhibition of endothelial-derived nitric oxide promotes P-selectin expression and actions in the rat microcirculation. Gastroenterology. 1994;107(4):1050-8.
72. Leao. Spreading depression of activity in the cerebral cortex. Neurophysiology 1944;7:359-90.
73. Nishizawa S. The roles of early brain injury in cerebral vasospasm following subarachnoid hemorrhage: from clinical and scientific aspects. Acta Neurochir Suppl. 2013;115:207-11.
74. Dreier JP, Woitzik J, Fabricius M, Bhatia R, Major S, Drenckhahn C, et al. Delayed ischaemic neurological deficits after subarachnoid haemorrhage are associated with clusters of spreading depolarizations. Brain. 2006;129(Pt 12):3224-37.
75. Dreier JP. The role of spreading depression, spreading depolarization and spreading ischemia in neurological disease. Nat Med. 2011;17(4):439-47.
76. Dreier JP, Drenckhahn C, Woitzik J, Major S, Offenhauser N, Weber-Carstens S, et al. Spreading ischemia after aneurysmal subarachnoid hemorrhage. Acta Neurochir Suppl. 2013;115:125-9.
77. Scheckenbach KE, Dreier JP, Dirnagl U, Lindauer U. Impaired cerebrovascular reactivity after cortical spreading depression in rats: Restoration by nitric oxide or cGMP. Exp Neurol. 2006;202(2):449-55.
78. Srivastava K, Bath PM, Bayraktutan U. Current therapeutic strategies to mitigate the eNOS dysfunction in ischaemic stroke. Cell Mol Neurobiol. 2012;32(3):319-36.
79. Khurana VG, Besser M. Pathophysiological basis of cerebral vasospasm following aneurysmal subarachnoid haemorrhage. J Clin Neurosci. 1997;4(2):122-31.
80. Vellimana AK, Milner E, Azad TD, Harries MD, Zhou ML, Gidday JM, et al. Endothelial nitric oxide synthase mediates endogenous protection against subarachnoid hemorrhage-induced cerebral vasospasm. Stroke. 2011;42(3):776-82.
81. Khurana VG, Sohni YR, Mangrum WI, McClelland RL, O'Kane DJ, Meyer FB, et al. Endothelial nitric oxide synthase gene polymorphisms predict susceptibility to aneurysmal subarachnoid hemorrhage and cerebral vasospasm. J Cereb Blood Flow Metab. 2004;24(3):291-7.
82. Starke RM, Kim GH, Komotar RJ, Hickman ZL, Black EM, Rosales MB, et al. Endothelial nitric oxide synthase gene single-nucleotide polymorphism predicts cerebral vasospasm after aneurysmal subarachnoid hemorrhage. J Cereb Blood Flow Metab. 2008;28(6):1204-11.
83. Stuehr D, Pou S, Rosen GM. Oxygen reduction by nitric-oxide synthases. J Biol Chem. 2001;276(18):14533-6.
84. Vasquez-Vivar J, Kalyanaraman B, Martasek P, Hogg N, Masters BS, Karoui H, et al. Superoxide generation by endothelial nitric oxide synthase: the influence of cofactors. Proc Natl Acad Sci U S A. 1998;95(16):9220-5.
85. Wink DA, Hanbauer I, Krishna MC, DeGraff W, Gamson J, Mitchell JB. Nitric oxide protects against cellular damage and cytotoxicity from reactive oxygen species. Proc Natl Acad Sci U S A. 1993;90(21):9813-7.
86. Pluta RM, Rak R, Wink DA, Woodward JJ, Khaldi A, Oldfield EH, et al. Effects of nitric oxide on reactive oxygen species production and infarction size after brain reperfusion injury. Neurosurgery. 2001;48(4):884-92; discussion 92-3.

87. Drexler H, Hornig B. Endothelial dysfunction in human disease. J Mol Cell Cardiol. 1999;31(1):51-60.
88. Cai H, Harrison DG. Endothelial dysfunction in cardiovascular diseases: the role of oxidant stress. Circ Res. 2000;87(10):840-4.
89. Sabri M, Ai J, Knight B, Tariq A, Jeon H, Shang X, et al. Uncoupling of endothelial nitric oxide synthase after experimental subarachnoid hemorrhage. J Cereb Blood Flow Metab. 2011;31(1):190-9.
90. Sabri M, Ai J, Marsden PA, Macdonald RL. Simvastatin re-couples dysfunctional endothelial nitric oxide synthase in experimental subarachnoid hemorrhage. PLoS One. 2011;6(2):e17062.
91. Kirkpatrick PJ, Turner CL, Smith C, Hutchinson PJ, Murray GD. Simvastatin in aneurysmal subarachnoid haemorrhage (STASH): a multicentre randomised phase 3 trial. The Lancet Neurology. 2014;13(7):666-75.
92. Sabri M, Ai J, Lass E, D'Abbondanza J, Macdonald RL. Genetic elimination of eNOS reduces secondary complications of experimental subarachnoid hemorrhage. J Cereb Blood Flow Metab. 2013;33(7):1008-14.
93. Shiva S, Sack MN, Greer JJ, Duranski M, Ringwood LA, Burwell L, et al. Nitrite augments tolerance to ischemia/reperfusion injury via the modulation of mitochondrial electron transfer. J Exp Med. 2007;204(9):2089-102.
94. Willmot M, Gray L, Gibson C, Murphy S, Bath PM. A systematic review of nitric oxide donors and L-arginine in experimental stroke; effects on infarct size and cerebral blood flow. Nitric Oxide. 2005;12(3):141-9.
95. Roberts BW, Mitchell J, Kilgannon JH, Chansky ME, Trzeciak S. Nitric oxide donor agents for the treatment of ischemia/reperfusion injury in human subjects: a systematic review. Shock. 2013;39(3):229-39.
96. Ichinose F. Improving outcomes after cardiac arrest using NO inhalation. Trends Cardiovasc Med. 2013;23(2):52-8.
97. Dezfulian C, Alekseyenko A, Dave KR, Raval AP, Do R, Kim F, et al. Nitrite therapy is neuroprotective and safe in cardiac arrest survivors. Nitric Oxide. 2012;26(4):241-50.
98. Kida K, Shirozu K, Yu B, Mandeville JB, Bloch KD, Ichinose F. Beneficial effects of nitric oxide on outcomes after cardiac arrest and cardiopulmonary resuscitation in hypothermia-treated mice. Anesthesiology. 2014;120(4):880-9.
99. Iadecola C, Zhang F, Casey R, Nagayama M, Ross ME. Delayed reduction of ischemic brain injury and neurological deficits in mice lacking the inducible nitric oxide synthase gene. J Neurosci. 1997;17(23):9157-64.
100. Iadecola C, Zhang F, Xu X. Inhibition of inducible nitric oxide synthase ameliorates cerebral ischemic damage. Am J Physiol. 1995;268(1 Pt 2):R286-92.
101. Wada K, Chatzipanteli K, Kraydieh S, Busto R, Dietrich WD. Inducible nitric oxide synthase expression after traumatic brain injury and neuroprotection with aminoguanidine treatment in rats. Neurosurgery. 1998;43(6):1427-36.
102. Clark RS, Kochanek PM, Schwarz MA, Schiding JK, Turner DS, Chen M, et al. Inducible nitric oxide synthase expression in cerebrovascular smooth muscle and neutrophils after traumatic brain injury in immature rats. Pediatric research. 1996;39(5):784-90.
103. Tisdall MM, Rejdak K, Kitchen ND, Smith M, Petzold A. The prognostic value of brain extracellular fluid nitric oxide metabolites after traumatic brain injury. Neurocrit Care. 2013;19(1):65-8.
104. Terpolilli NA, Zweckberger K, Trabold R, Schilling L, Schinzel R, Tegtmeier F, et al. The novel nitric oxide synthase inhibitor 4-amino-tetrahydro-L-biopterine

prevents brain edema formation and intracranial hypertension following traumatic brain injury in mice. J Neurotrauma. 2009;26(11):1963-75.
105. Stover JF, Belli A, Boret H, Bulters D, Sahuquillo J, Schmutzhard E, et al. Nitric oxide synthase inhibition with the antipterin VAS203 improves outcome in moderate and severe traumatic brain injury: a placebo-controlled randomized Phase IIa trial (NOSTRA). Journal of neurotrauma. 2014;31(19):1599-606.
106. Foley LM, Hitchens TK, Melick JA, Bayir H, Ho C, Kochanek PM. Effect of inducible nitric oxide synthase on cerebral blood flow after experimental traumatic brain injury in mice. J Neurotrauma. 2008;25(4):299-310.
107. Sinz EH, Kochanek PM, Dixon CE, Clark RS, Carcillo JA, Schiding JK, et al. Inducible nitric oxide synthase is an endogenous neuroprotectant after traumatic brain injury in rats and mice. J Clin Invest. 1999;104(5):647-56.
108. Bayir H, Kagan VE, Borisenko GG, Tyurina YY, Janesko KL, Vagni VA, et al. Enhanced oxidative stress in iNOS-deficient mice after traumatic brain injury: support for a neuroprotective role of iNOS. J Cereb Blood Flow Metab. 2005;25(6):673-84.
109. Shiva S. Nitrite: A Physiological Store of Nitric Oxide and Modulator of Mitochondrial Function. Redox Biol. 2013;1(1):40-4.
110. Terpolilli NA, Kim SW, Thal SC, Kataoka H, Zeisig V, Nitzsche B, et al. Inhalation of nitric oxide prevents ischemic brain damage in experimental stroke by selective dilatation of collateral arterioles. Circ Res. 2012;110(5):727-38.
111. Terpolilli NA, Kim SW, Thal SC, Kuebler WM, Plesnila N. Inhaled nitric oxide reduces secondary brain damage after traumatic brain injury in mice. J Cereb Blood Flow Metab. 2013;33(2):311-8.
112. Li YS, Shemmer B, Stone E, M AN, Jonas S, Quartermain D. Neuroprotection by inhaled nitric oxide in a murine stroke model is concentration and duration dependent. Brain Res. 2013;1507:134-45.
113. Pluta RM, Oldfield EH, Bakhtian KD, Fathi AR, Smith RK, Devroom HL, et al. Safety and feasibility of long-term intravenous sodium nitrite infusion in healthy volunteers. PLoS One. 2011;6(1):e14504.
114. Oldfield EH, Loomba JJ, Monteith SJ, Crowley RW, Medel R, Gress DR, et al. Safety and pharmacokinetics of sodium nitrite in patients with subarachnoid hemorrhage: a Phase IIA study. J Neurosurg. 2013;119(3):634-41.
115. van Faassen EE, Bahrami S, Feelisch M, Hogg N, Kelm M, Kim-Shapiro DB, et al. Nitrite as regulator of hypoxic signaling in mammalian physiology. Med Res Rev. 2009;29(5):683-741.
116. Pluta RM, Dejam A, Grimes G, Gladwin MT, Oldfield EH. Nitrite infusions to prevent delayed cerebral vasospasm in a primate model of subarachnoid hemorrhage. JAMA. 2005;293(12):1477-84.
117. Edlow JA. Diagnosis of subarachnoid hemorrhage. Neurocritical care. 2005;2(2):99-109.
118. Bryan RN, Levy LM, Whitlow WD, Killian JM, Preziosi TJ, Rosario JA. Diagnosis of acute cerebral infarction: comparison of CT and MR imaging. AJNR American journal of neuroradiology. 1991;12(4):611-20.
119. Dankbaar JW, de Rooij NK, Velthuis BK, Frijns CJ, Rinkel GJ, van der Schaaf IC. Diagnosing delayed cerebral ischemia with different CT modalities in patients with subarachnoid hemorrhage with clinical deterioration. Stroke; a journal of cerebral circulation. 2009;40(11):3493-8.

120. de Oliveira Manoel AL, Mansur A, Murphy A, Turkel-Parrella D, Macdonald M, Macdonald RL, et al. Aneurysmal subarachnoid haemorrhage from a neuroimaging perspective. Critical care (London, England). 2014;18(6):557.
121. Dhar R, Scalfani MT, Zazulia AR, Videen TO, Derdeyn CP, Diringer MN. Comparison of induced hypertension, fluid bolus, and blood transfusion to augment cerebral oxygen delivery after subarachnoid hemorrhage. Journal of neurosurgery. 2012;116(3):648-56.
122. Mutoh T, Ishikawa T, Suzuki A, Yasui N. Continuous cardiac output and near-infrared spectroscopy monitoring to assist in management of symptomatic cerebral vasospasm after subarachnoid hemorrhage. Neurocritical care. 2010;13(3):331-8.
123. Kistka H, Dewan MC, Mocco J. Evidence-based cerebral vasospasm surveillance. Neurology research international. 2013;2013:256713.
124. Foreman B, Claassen J. Quantitative EEG for the detection of brain ischemia. Crit Care. 2012;16(2):216.
125. Labar DR, Fisch BJ, Pedley TA, Fink ME, Solomon RA. Quantitative EEG monitoring for patients with subarachnoid hemorrhage. Electroencephalogr Clin Neurophysiol. 1991;78(5):325-32.
126. Baron JC. Perfusion thresholds in human cerebral ischemia: historical perspective and therapeutic implications. Cerebrovascular diseases (Basel, Switzerland). 2001;11 Suppl 1:2-8.
127. Tolonen U, Sulg IA. Comparison of quantitative EEG parameters from four different analysis techniques in evaluation of relationships between EEG and CBF in brain infarction. Electroencephalography and clinical neurophysiology. 1981;51(2):177-85.
128. Babadi B, Brown EN. A review of multitaper spectral analysis. IEEE transactions on bio-medical engineering. 2014;61(5):1555-64.
129. Rivierez M, Landau-Ferey J, Grob R, Grosskopf D, Philippon J. Value of electroencephalogram in prediction and diagnosis of vasospasm after intracranial aneurysm rupture. Acta neurochirurgica. 1991;110(1-2):17-23.
130. Vespa PM, Nuwer MR, Juhasz C, Alexander M, Nenov V, Martin N, et al. Early detection of vasospasm after acute subarachnoid hemorrhage using continuous EEG ICU monitoring. Electroencephalogr Clin Neurophysiol. 1997;103(6):607-15.
131. Claassen J, Hirsch LJ, Kreiter KT, Du EY, Connolly ES, Emerson RG, et al. Quantitative continuous EEG for detecting delayed cerebral ischemia in patients with poor-grade subarachnoid hemorrhage. Clin Neurophysiol. 2004;115(12):2699-710.
132. Rathakrishnan R, Gotman J, Dubeau F, Angle M. Using continuous electroencephalography in the management of delayed cerebral ischemia following subarachnoid hemorrhage. Neurocrit Care. 2011;14(2):152-61.
133. Gollwitzer S, Groemer T, Rampp S, Hagge M, Olmes D, Huttner HB, et al. Early prediction of delayed cerebral ischemia in subarachnoid hemorrhage based on quantitative EEG: A prospective study in adults. Clin Neurophysiol. 2014.
134. Okell TW, Chappell MA, Kelly ME, Jezzard P. Cerebral blood flow quantification using vessel-encoded arterial spin labeling. Journal of cerebral blood flow and metabolism : official journal of the International Society of Cerebral Blood Flow and Metabolism. 2013;33(11):1716-24.
135. Alsop DC, Detre JA, Golay X, Gunther M, Hendrikse J, Hernandez-Garcia L, et al. Recommended implementation of arterial spin-labeled perfusion MRI for clinical applications: A consensus of the ISMRM perfusion study group and the European consortium for ASL in dementia. Magnetic resonance in medicine. 2015;73(1):102-16.

136. Kaufmann TJ, Huston J, 3rd, Mandrekar JN, Schleck CD, Thielen KR, Kallmes DF. Complications of diagnostic cerebral angiography: evaluation of 19,826 consecutive patients. Radiology. 2007;243(3):812-9.
137. Wong EC. Vessel-encoded arterial spin-labeling using pseudocontinuous tagging. Magnetic resonance in medicine. 2007;58(6):1086-91.
138. Garry PS, Ezra M, Rowland MJ, Westbrook J, Pattinson KT. The role of the nitric oxide pathway in brain injury and its treatment--from bench to bedside. Experimental neurology. 2015;263:235-43.
139. Ostergaard L, Aamand R, Karabegovic S, Tietze A, Blicher JU, Mikkelsen IK, et al. The role of the microcirculation in delayed cerebral ischemia and chronic degenerative changes after subarachnoid hemorrhage. J Cereb Blood Flow Metab. 2013;33(12):1825-37.
140. Jung KH, Chu K, Ko SY, Lee ST, Sinn DI, Park DK, et al. Early intravenous infusion of sodium nitrite protects brain against in vivo ischemia-reperfusion injury. Stroke. 2006;37(11):2744-50.
141. O'Gorman RL, Poil SS, Brandeis D, Klaver P, Bollmann S, Ghisleni C, et al. Coupling between resting cerebral perfusion and EEG. Brain Topogr. 2013;26(3):442-57.
142. Vergouwen MD, Vermeulen M, van Gijn J, Rinkel GJ, Wijdicks EF, Muizelaar JP, et al. Definition of delayed cerebral ischemia after aneurysmal subarachnoid hemorrhage as an outcome event in clinical trials and observational studies: proposal of a multidisciplinary research group. Stroke. 2010;41(10):2391-5.
143. Maher AR, Milsom AB, Gunaruwan P, Abozguia K, Ahmed I, Weaver RA, et al. Hypoxic modulation of exogenous nitrite-induced vasodilation in humans. Circulation. 2008;117(5):670-7.
144. Siddiqi N, Neil C, Bruce M, MacLennan G, Cotton S, Papadopoulou S, et al. Intravenous sodium nitrite in acute ST-elevation myocardial infarction: a randomized controlled trial (NIAMI). Eur Heart J. 2014;35(19):1255-62.
145. Weisscher N, Vermeulen M, Roos YB, de Haan RJ. What should be defined as good outcome in stroke trials; a modified Rankin score of 0-1 or 0-2? J Neurol. 2008;255(6):867-74.
146. Delorme A, Makeig S. EEGLAB: an open source toolbox for analysis of single-trial EEG dynamics including independent component analysis. J Neurosci Methods. 2004;134(1):9-21.
147. Oostenveld R, Fries P, Maris E, Schoffelen JM. FieldTrip: Open source software for advanced analysis of MEG, EEG, and invasive electrophysiological data. Comput Intell Neurosci. 2011;2011:156869.
148. Team RC. R: A language and environment for statistical computing. R Foundation for Statistical Computing, Vienna, Austria. 2015.
149. Pinheiro J BD, DebRoy S, Sarkar D, {R Core Team}. R package version 31-122. 2015.
150. Crobeddu E, Mittal MK, Dupont S, Wijdicks EF, Lanzino G, Rabinstein AA. Predicting the lack of development of delayed cerebral ischemia after aneurysmal subarachnoid hemorrhage. Stroke. 2012;43(3):697-701.
151. Finnigan S, van Putten MJ. EEG in ischaemic stroke: quantitative EEG can uniquely inform (sub-)acute prognoses and clinical management. Clin Neurophysiol. 2013;124(1):10-9.
152. Hinzman JM, Andaluz N, Shutter LA, Okonkwo DO, Pahl C, Strong AJ, et al. Inverse neurovascular coupling to cortical spreading depolarizations in severe brain trauma. Brain. 2014;137(Pt 11):2960-72.

153. Pacher P, Beckman JS, Liaudet L. Nitric oxide and peroxynitrite in health and disease. Physiological reviews. 2007;87(1):315-424.
154. Schwartz AY, Sehba FA, Bederson JB. Decreased nitric oxide availability contributes to acute cerebral ischemia after subarachnoid hemorrhage. Neurosurgery. 2000;47(1):208-14; discussion 14-5.
155. Kondziella D, Friberg CK, Wellwood I, Reiffurth C, Fabricius M, Dreier JP. Continuous EEG Monitoring in Aneurysmal Subarachnoid Hemorrhage: A Systematic Review. Neurocrit Care. 2014.
156. Dorsch NW, King MT. A review of cerebral vasospasm in aneurysmal subarachnoid haemorrhage Part I: Incidence and effects. J Clin Neurosci. 1994;1(1):19-26.
157. Kelly ME, Rowland MJ, Okell TW, Chappell MA, Corkill R, Kerr RS, et al. Pseudo-continuous arterial spin labelling MRI for non-invasive, whole-brain, serial quantification of cerebral blood flow following aneurysmal subarachnoid haemorrhage. Translational stroke research. 2013;4(6):710-8.
158. Hanggi D, Turowski B, Beseoglu K, Yong M, Steiger HJ. Intra-arterial nimodipine for severe cerebral vasospasm after aneurysmal subarachnoid hemorrhage: influence on clinical course and cerebral perfusion. AJNR American journal of neuroradiology. 2008;29(6):1053-60.
159. Budohoski KP, Czosnyka M, Kirkpatrick PJ, Smielewski P, Steiner LA, Pickard JD. Clinical relevance of cerebral autoregulation following subarachnoid haemorrhage. Nat Rev Neurol. 2013;9(3):152-63.
160. Jenkinson M, Bannister P, Brady M, Smith S. Improved optimization for the robust and accurate linear registration and motion correction of brain images. NeuroImage. 2002;17(2):825-41.
161. Buxton RB, Frank LR, Wong EC, Siewert B, Warach S, Edelman RR. A general kinetic model for quantitative perfusion imaging with arterial spin labeling. Magnetic resonance in medicine. 1998;40(3):383-96.
162. Chappell MA, Okell TW, Jezzard P, Woolrich MW. A general framework for the analysis of vessel encoded arterial spin labeling for vascular territory mapping. Magnetic resonance in medicine. 2010;64(5):1529-39.
163. Zhang Y, Brady M, Smith S. Segmentation of brain MR images through a hidden Markov random field model and the expectation-maximization algorithm. IEEE transactions on medical imaging. 2001;20(1):45-57.
164. Mazziotta J, Toga A, Evans A, Fox P, Lancaster J, Zilles K, et al. A probabilistic atlas and reference system for the human brain: International Consortium for Brain Mapping (ICBM). Philosophical transactions of the Royal Society of London Series B, Biological sciences. 2001;356(1412):1293-322.
165. Andersson JLR JM, Smith S. Non-linear registration, aka spatial normalisation. FMRIB technical report TR07JA2. 2010.
166. Vergouwen MD. Vasospasm versus delayed cerebral ischemia as an outcome event in clinical trials and observational studies. Neurocrit Care. 2011;15(2):308-11.
167. Frontera JA, Ahmed W, Zach V, Jovine M, Tanenbaum L, Sehba F, et al. Acute ischaemia after subarachnoid haemorrhage, relationship with early brain injury and impact on outcome: a prospective quantitative MRI study. Journal of neurology, neurosurgery, and psychiatry. 2015;86(1):71-8.
168. Budohoski KP, Czosnyka M, Kirkpatrick PJ, Reinhard M, Varsos GV, Kasprowicz M, et al. Bilateral failure of cerebral autoregulation is related to unfavorable outcome after subarachnoid hemorrhage. Neurocritical care. 2015;22(1):65-73.

169. Kirkman MA, Smith M. Intracranial pressure monitoring, cerebral perfusion pressure estimation, and ICP/CPP-guided therapy: a standard of care or optional extra after brain injury? British journal of anaesthesia. 2014;112(1):35-46.
170. Hop JW, Rinkel GJ, Algra A, van Gijn J. Case-fatality rates and functional outcome after subarachnoid hemorrhage: a systematic review. Stroke; a journal of cerebral circulation. 1997;28(3):660-4.
171. San-juan D, Chiappa KH, Cole AJ. Propofol and the electroencephalogram. Clinical neurophysiology : official journal of the International Federation of Clinical Neurophysiology. 2010;121(7):998-1006.
172. Phillips RL, Herning R, London ED. Morphine effects on the spontaneous electroencephalogram in polydrug abusers: correlations with subjective self-reports. Neuropsychopharmacology : official publication of the American College of Neuropsychopharmacology. 1994;10(3):171-81.
173. Hanggi D. Monitoring and detection of vasospasm II: EEG and invasive monitoring. Neurocritical care. 2011;15(2):318-23.

Appendix A